NAVAL POSTGRADUATE SCHOOL

MONTEREY, CALIFORNIA

THESIS

AN ANALYSIS OF A DUST STORM IMPACTING OPERATION IRAQI FREEDOM, 25-27 MARCH 2003

by

John W. Anderson

December 2004

Thesis Advisor: Carlyle H. Wash
Second Reader: Tom Murphree

THIS PAGE INTENTIONALLY LEFT BLANK

REPORT DOCUMENTATION PAGE	*Form Approved OMB No. 0704-0188*

1. AGENCY USE ONLY *(Leave blank)*	2. REPORT DATE	3. REPORT TYPE AND DATES COVERED
	December 2004	Master's Thesis

4. TITLE AND SUBTITLE: An Analysis of a Dust Storm Impacting Operation IRAQI FREEDOM, 25-27 March 2003	5. FUNDING NUMBERS
6. AUTHOR(S) John W. Anderson	
7. PERFORMING ORGANIZATION NAME(S) AND ADDRESS(ES) Naval Postgraduate School Monterey, CA 93943-5000	8. PERFORMING ORGANIZATION REPORT NUMBER
9. SPONSORING /MONITORING AGENCY NAME(S) AND ADDRESS(ES) N/A	10. SPONSORING/MONITORING AGENCY REPORT NUMBER

11. SUPPLEMENTARY NOTES The views expressed in this thesis are those of the author and do not reflect the official policy or position of the Department of Defense or the U.S. Government.

Approved for public release; Distribution is unlimited.	12b. DISTRIBUTION CODE

13. ABSTRACT (maximum 200 words)

On day five of combat operations during Operation IRAQI FREEDOM, advances by coalition forces were nearly halted by a dust storm, initiated by the passage of a synoptically driven cold front. This storm impacted ground and air operations across the entire Area of Responsibility, and delayed an impending ground attack on the Iraqi capital. Military meteorologists were able to assist military planners in mitigating at least some of the effects of this storm. This thesis examines the synoptic conditions leading to the severe dust storm, evaluates the numerical weather prediction model performance in predicting the event, and reviews metrics pertaining to the overall impacts on the Operation IRAQI FREEDOM combined air campaign. In general, the numerical model guidance correctly predicted the location and onset of the dust storms on 25 March, 2003. As a result of this forecast guidance, mission planners were able to front load Air Tasking Orders with extra sorties prior to the onset of the dust storm, and were able to make changes to planned weapons loads, favoring GPS-guided munitions.

14. SUBJECT TERMS Operation IRAQI FREEDOM, Southwest Asia, Iraq, Middle East, Case Study, Analysis, Dust Storm, Sand Storm, Shamal, Synoptic Cold Front, Extra-tropical Cyclone, Numerical Weather Prediction Models, NOGAPS, COAMPS, GFS,	15. NUMBER OF PAGES 123
	16. PRICE CODE

17. SECURITY CLASSIFICATION OF REPORT	18. SECURITY CLASSIFICATION OF THIS PAGE	19. SECURITY CLASSIFICATION OF ABSTRACT	20. LIMITATION OF ABSTRACT
Unclassified	Unclassified	Unclassified	UL

NSN 7540-01-280-5500 Standard Form 298 (Rev. 2-89)
Prescribed by ANSI Std. 239-18

THIS PAGE INTENTIONALLY LEFT BLANK

Approved for public release; distribution is unlimited.

AN ANALYSIS OF A DUST STORM IMPACTING
OPERATION IRAQI FREEDOM, 25-27 MARCH 2003

John W. Anderson
Captain, United States Air Force
B.S., University of Colorado, 1994

Submitted in partial fulfillment of the
requirements for the degree of

MASTER OF SCIENCE IN METEOROLOGY

from the

NAVAL POSTGRADUATE SCHOOL
December 2004

Author: John W. Anderson

Approved by: Carlyle H. Wash
Thesis Advisor

Tom Murphree
Second Reader

Philip A. Durkee
Chairman, Department of Meteorology

THIS PAGE INTENTIONALLY LEFT BLANK

ABSTRACT

On day five of combat operations during Operation IRAQI FREEDOM, advances by coalition forces were nearly halted by a dust storm, initiated by the passage of a synoptically driven cold front. This storm impacted ground and air operations across the entire Area of Responsibility, and delayed an impending ground attack on the Iraqi capital. Military meteorologists were able to assist military planners in mitigating at least some of the effects of this storm. This thesis examines the synoptic conditions leading to the severe dust storm, evaluates the numerical weather prediction model performance in predicting the event, and reviews metrics pertaining to the overall impacts on the Operation IRAQI FREEDOM combined air campaign. In general, the numerical model guidance correctly predicted the location and onset of the dust storms on 25 March, 2003. As a result of this forecast guidance, mission planners were able to front load Air Tasking Orders with extra sorties prior to the onset of the dust storm, and were able to make changes to planned weapons loads, favoring GPS-guided munitions.

THIS PAGE INTENTIONALLY LEFT BLANK

TABLE OF CONTENTS

LIST OF FIGURES

THIS PAGE INTENTIONALLY LEFT BLANK

LIST OF TABLES

THIS PAGE INTENTIONALLY LEFT BLANK

ACKNOWLEDGMENTS

The author would like to acknowledge and thank Professor Wash and Professor Murphree for their patient mentoring and guidance in the completion of this thesis. It was indeed an honor and privilege to work with these gentlemen.

The author also appreciates the support provided by his professors and peers. The knowledge and experience base provided by Captain Jeff Jarry, USAF, Captain John Sandifer, USAF, Captain Darren Sokol, USAF, and Captain Clay Baskin, USAF, proved extremely valuable in analyzing the upper atmospheric charts presented here. This thesis would not have been possible without the support of Major Christopher Finta, USAF, and the excellent forecasters at the 28th Operational Weather Squadron, nor would it have been possible without LCDR Jacob Hinz, USN, and the dedicated professionals at the Fleet Numerical Meteorology and Oceanography Center.

The author also wishes to extend his heartfelt gratitude to Lieutenant Colonel Philip Lanman, USAF, who is an exemplary Air Force officer, and mentor. His tireless efforts in support of the author and the lessons on leadership taught by his example will never be forgotten.

Finally, to my beloved wife, Christin, I would like to express my sincere gratitude and undying love. Her patience and love made it possible for me to stick to the project when frustration was high and morale low. She and my daughter, Rachel, are the reason I serve this nation, so that they and others may live free in peace.

THIS PAGE INTENTIONALLY LEFT BLANK

I. INTRODUCTION

A. EARLY TIMELINE OF OPERATIONS

On 20 March, 2003, at 05:34 local time in Baghdad, Operation IRAQI FREEDOM commenced with a "decapitation attack" on leadership targets around the Iraqi capital (CNN.com 2004). The attack was carried out by Tomahawk Land Attack Missiles (TLAM's) fired from various ships operating in the North Arabian Gulf, as well as F-117's and other coalition aircraft (Lee 2003). By 15:57L on the same day, the ground war was under way as lead elements of the 1st Marine Division (1 MARDIV) engaged and destroyed 2 Iraqi armored personnel carriers south of the Iraq-Kuwait border (Pike 2004). Less than an hour later, the 1 MARDIV was well inside the Iraqi border and en-route to Basra, a major city north of the critical port of Umm Qasr. By late in the evening on 20 March, U.S. and British forces had captured the port and much of southeastern Iraq (Pike 2004).

The crushing air strikes and rapid advance of coalition ground forces continued for the next 4 days (21-24 March), relatively unaffected by weather considerations. As of the 24th, coalition ground forces had pressed to within 100 miles of Baghdad, and more than 6000 sorties had been flown in the air campaign, with more than 1500 sorties coming on day 5 alone (Pike 2004). The combined effect was a pace of combat operations so rapid as to be unprecedented in the annals of military history.

However, on 25 March, the environmental situation changed. A severe dust storm blanketed most of the region, blackening the skies and dramatically slowing or halting

altogether military operations. This storm made it difficult for both land-based vehicles and helicopters to operate, and severely impacted naval air operations in the North Arabian Gulf (Pike 2004). The blowing dust intensified on the 26th, with an even greater impact on the coalition air campaign, before beginning to clear on the 27th (Pike 2004). The effects of this storm, combined with an over-stretched supply line, resulted in a 5-day delay in the impending ground-attack on Baghdad (Grossman 2003).

B. DUST STORM SIGNIFICANCE

In spite of the impact this storm had on operations in the early stages of Operation IRAQI FREEDOM, there was actually ample warning of its severity. This storm was relatively well forecast out to approximately 5 days (Revkin 2003). Unlike the early 1990's and Operation DESERT STORM, when storms of this type hit with little or no warning, military meteorologists this time were able to provide coalition commanders with enough information to enable them to tailor battle plans, and implement force protection measures to better exploit the weather conditions for battle. Lt Col Thomas B. Frooninckx (pronounced FRAWNIX), the commander of the 28th Operational Weather Squadron, the Air Force organization responsible for forecasting for the Middle East, said, "It's one thing to say there's going to be a big storm, but another thing to say where and when it's going to be sand or a thunderstorm or where there'll be cloud cover and rain. We hit this one pretty darn well" (Revkin 2003). According to Revkin (2003), in many cases, the mission planners incorporated the forecast conditions by shifting aircraft weapons load-outs from laser-guided weapons to GPS-guided

munitions, and by fitting surface guns with heat-detecting gun sights that were able to, in effect, "see through the dust."

C. OBJECTIVES

The objectives for this thesis are three-fold. First, this thesis will conduct a complete and thorough case study of the meteorological conditions that led to the dust storm. The case study will include an analysis of upper air charts at the 500 and 300 millibar (mb) levels and low level charts at 850 mb and the surface. The upper level analysis will track the synoptic trough that tracked southward from Europe, across the Eastern Mediterranean, and northeastward toward the Caspian Basin. The lower level analysis will be used to asses the placement and timing of the surface cold front and the associated strong winds which lifted the dust. These analyses will be compared to satellite imagery.

Second, an evaluation of the numerical weather prediction (NWP) models which forecast this event will be conducted. The models of comparison will be the National Centers for Environmental Prediction (NCEP) Global Forecasting System (GFS) Model, the Navy Operational Global Atmospheric Prediction System (NOGAPS) and Naval Research Laboratory's Coupled Ocean/Atmosphere Mesoscale Prediction System (COAMPS). Each model will be compared against its own analysis and surface observations at a few key locations to assess their performance in predicting the necessary conditions for the dust event.

Finally, an intensive review of mission metrics from Major Christopher Finta, USAF, (2004) of the 28th

Operational Weather Squadron, and a case study done by Lieutenant Commander Jacob Hinz, USN (2004) will be conducted. The impacts of this storm on combined air operations, as highlighted in their work, will show the important role forecasters played in the development of Air Tasking Orders (ATOs) for Operation IRAQI FREEDOM.

II. BACKGROUND

A. DEFINITIONS

Dust events, such as the one described in this thesis, are common in Southwest Asia, particularly in the winter, spring, and summer. They are typically associated with "shamal winds," or seasonal northwesterly winds occurring throughout the region. The name "shamal" comes from the Arabic word for "north" (FNMOC 2004). These winds can generate tremendous amounts of atmospheric dust as they travel across the northern Arabian Peninsula, Iraq and Kuwait. Shamal winds can be further defined in terms of the seasons in which they occur, namely summer and winter (Wilkerson 1991).

1. Summer Shamal

The summer shamal is also known locally as the "wind of 120 days" (Wilkerson 1991). It occurs usually between May and July. The synoptic pattern which creates these winds is a high surface pressure over northern Saudi Arabia, a low surface pressure over Afghanistan, and a thermal low/monsoon trough over southern Saudi Arabia (COMET 2003). Figure 2.1 shows the circulations around the high to the west and the low to the east that combine to enhance the northwesterly winds along the Iraq/Iran border leading to the Northern Arabian Gulf (NAG). When compared to the winter shamal, this wind event is more persistent and has greater vertical motion over a larger horizontal area, primarily as a result of the higher surface temperatures and stronger associated upper level convective currents (Higdon 2002). These winds can carry dust from the surface to approximately 5000 feet, and wind strength

generally decreases after sunset, due to the radiative cooling of the surface (COMET 2003).

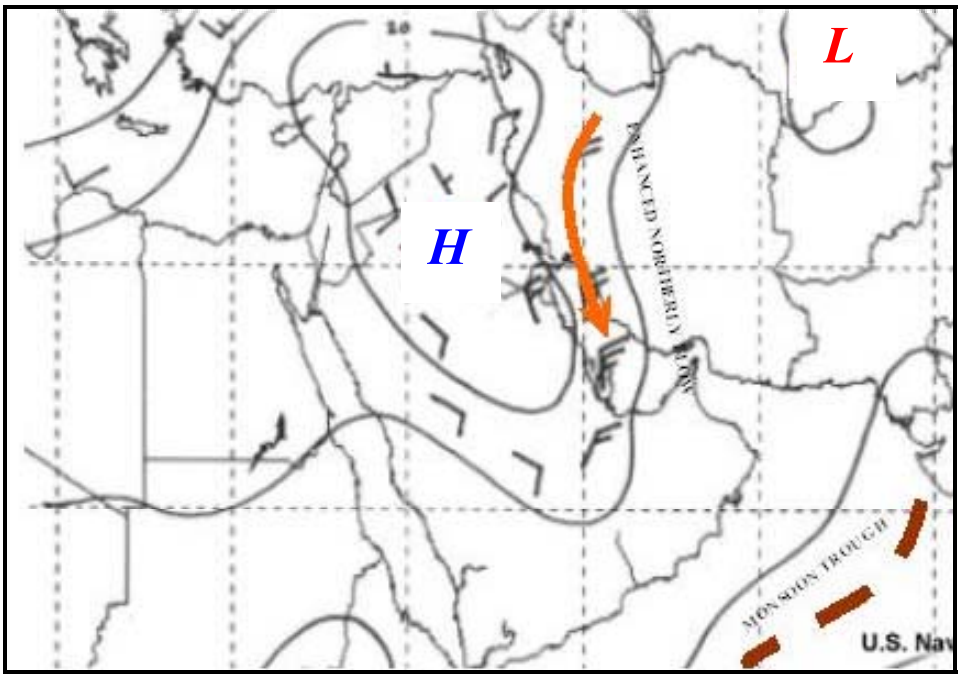

Figure 2.1. Typical synoptic pattern for summer shamals. (After: COMET, 2003)

2. Winter Shamal

The winter shamal is a northwesterly wind driven by the passage of a strong synoptically forced cold front, as shown in Figure 2.2. The dust storms which arise from winter shamals are also referred to as post-frontal dust storms (Wilkerson 1991). This type of event generally contains the most wide-spread and hazardous weather associated with the region (COMET 2003). Strong thunderstorms generally precede the front, accompanied by strong southerly winds, which initially lift the dust particles. Winter shamal events generally come in two different types. The first typically lasts a total of 24-36 hours as a frontal system moves in and through the area

rather quickly. The second type occurs when the frontal system stalls over the Arabian Peninsula, and usually lasts about 3-5 days (Wilkerson 1991). Both cases can result in greater than 50 knot surface winds and 10-13 foot seas far out in the Arabian Gulf (COMET 2003). The deep vertical mixing occurring as the front passes through helps keep the dust kicked up by pre-frontal southerly winds suspended, while the northwesterly winds behind the front carry the aerosol particles across the entire region. Dust storms of this type are generally more severe for the first 1-3 frontal passages of the season (COMET 2003). For the particular case being studied, the winter shamal is the most accurate description of the event. Hence, for the rest of this thesis, the term "shamal" will generally refer to the winter shamal.

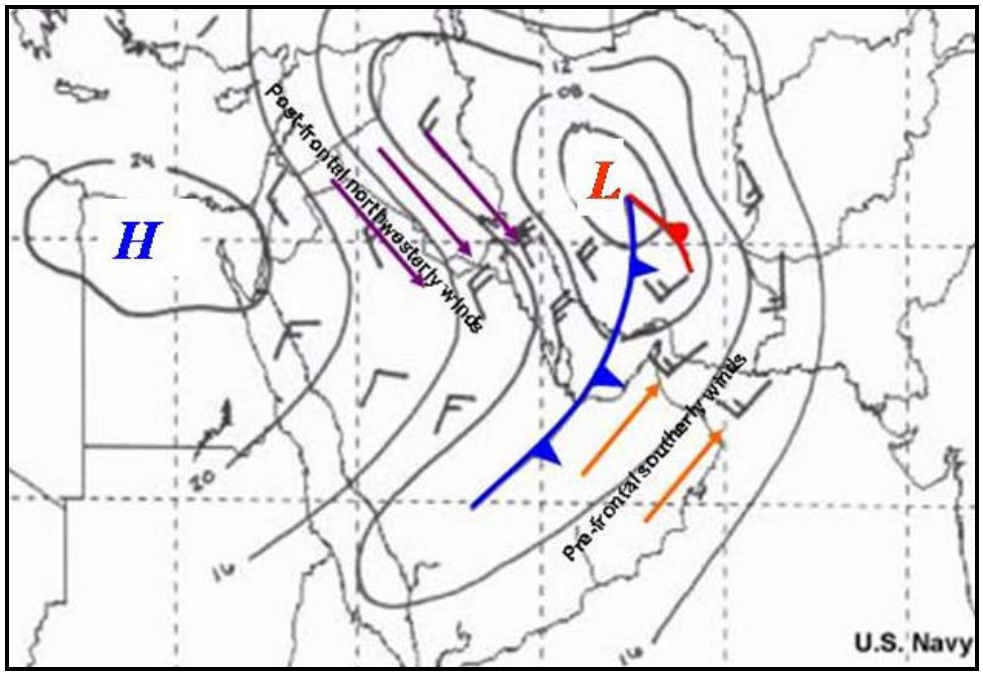

Figure 2.2. Typical synoptic pattern for winter shamals. (After: COMET, 2003)

B. KEY ELEMENTS OF FORECASTING DUST STORMS IN SWA

In forecasting dust storms for any given region, it is crucial to answer several important questions: What is the distribution of dust particle sizes? What are the critical wind speeds for the given distribution of particle sizes? Factors such as topography and surface conditions play a crucial role in determining source regions. Once these factors are analyzed, the physical processes for the transport of dust can be evaluated.

1. SWA Source Regions

Southwest Asia is surrounded by relatively rugged topography, which in turn, lends itself to large source regions for dust. The region is considered largely semi-arid, even though it is bordered on the north by the Caspian and Black Seas, on the west by the Mediterranean and Red Seas, on the east and south by the Persian Gulf and Arabian Sea (Evans et. al. 2001). The Taurus and Zagros mountains cut into the region through southern Turkey and western Iran. For the Saudi Arabian region, the Jordanian and Syrian mountains lie to the northwest, the Al Hijaz and Asir ranges to the southwest, while the Hadramaunt Mountains lie to the southeast. These mountain ranges effectively block precipitation from transiting extra-tropical cyclones. The lack of precipitation in the far inland regions of the Arabian Peninsula provide a suitably dry surface region comprised of sand, clay and fine silt, ideal for the formation of dust storms (Bartlett 2004). According to Bartlett (2004), the primary source regions for dust in this area are shown in Figure 2.3 and described as follows:

- Region 1: the Fertile Crescent region between the Tigris and Euphrates river deltas and flood plains,

- Region 2: the An Nafud desert, in northern Saudi Arabia, which is an extension of the high Syrian desert,

- Region 3: the Ad Dhana desert in central-eastern Saudi Arabia, and

- Region 4: the Rub al-Khali desert in the south eastern part of the Arabian Peninsula.

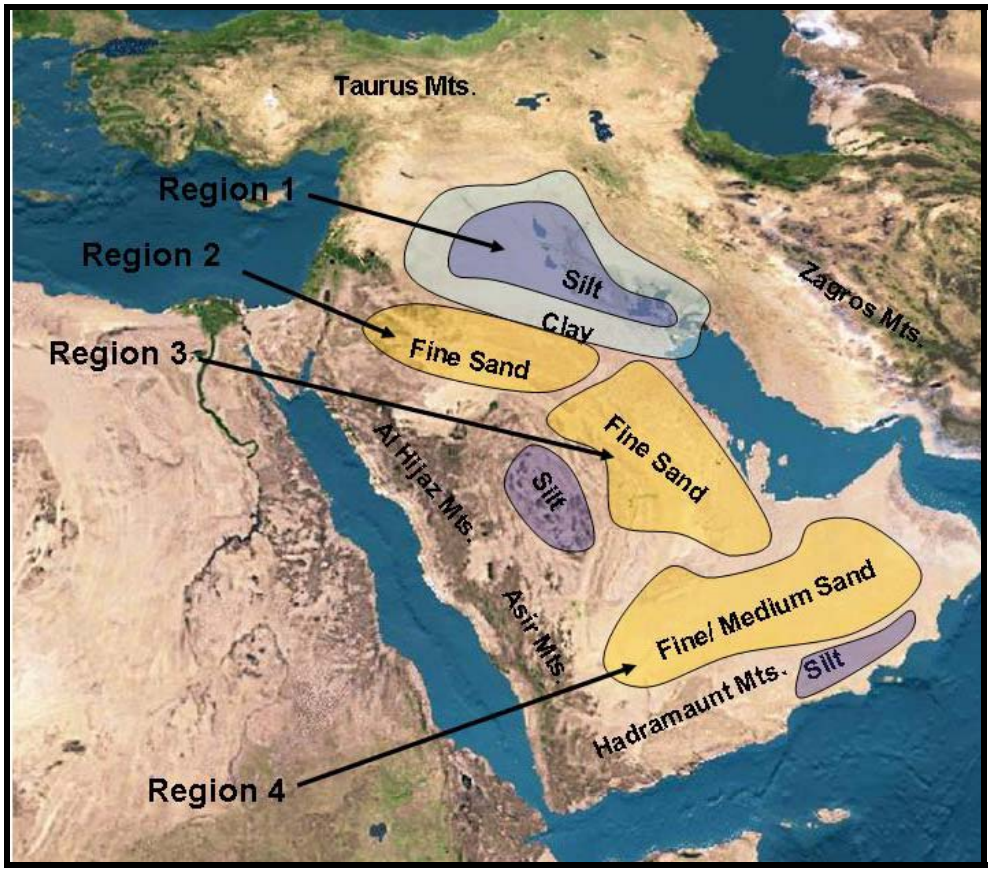

Figure 2.3. SWA dust source region. (Image: Israeli Science and Technology Directory 2004; Graphical overlays of source regions adapted from COMET 2003)

As Figure 2.3 shows, the Fertile Crescent is a source region comprised of alluvial fans and dry flood plains containing a mixture of clay particles, which have a typical size of less than 2 micrometers, and silt particles, which range in size between 2-50 micrometers. The other source regions are generally comprised of fine to medium sand, ranging in particle sizes from 50-1000 micrometers, with only a few small areas of silt (COMET 2003). Once the composition of the source regions is known, it is possible to look at the physical processes by which the dust is transported through the atmosphere.

2. Physical Processes of Dust Transport

The transport of dust can be described in three processes depending on particle size and wind strength. These processes are creep, saltation, and suspension, as shown in Figure 2.4. Creep refers to a process by which particles slide or roll over the surface, generally without breaking contact with the surface. This process is favored by large particles or lower wind speeds and will not usually result in large-scale dust storms (COMET 2003). Saltation is a process by which the particles may get airborne for short distances before falling back to earth. Although the particles do not travel far from their source regions in this process, they can contribute to much larger scale dust transport by disrupting the surface at each impact, thus kicking up much finer particles which are then more susceptible to the third process, suspension. Suspension occurs when the particles are held aloft by the air currents and can result in the dust plume being carried far away from the source region if the lofted particles are small enough for the air currents to keep them airborne (COMET 2003).

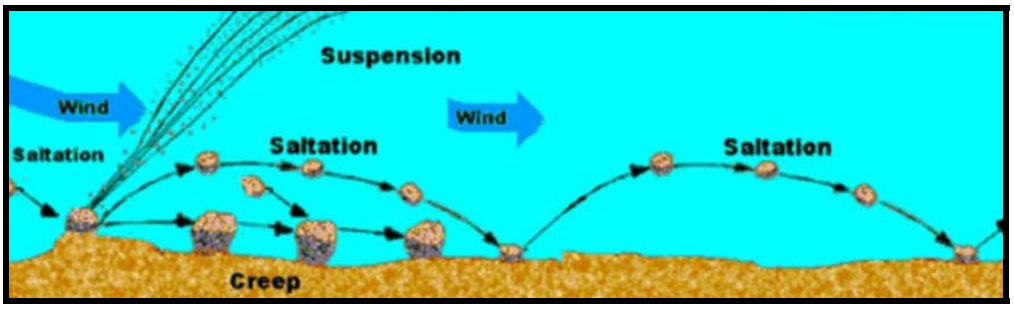

Figure 2.4. Dust transport processes. (From: Heidorn 2003)

Generally the wind speeds required to activate particle movement, and thus initiate the three processes summarized above will depend on the size of the particles. This relationship between particle size and wind speed was extensively studied by Clements et al (1963). They found that as wind speeds increase, larger particles are transported and suspended more easily (Bartlett 2004). In general, the critical threshold wind speeds for mobilization of particles are summarized in Table 2.1.

Soil Type	Wind Threshold
Fine to Medium Sand Dunes	10-15 mph (8.7- 13 kts)
Sandy Areas, Poorly developed desert pavement	20 mph (17.4 kts)
Fine Materials, Desert Flats	20-25 mph (17.4-21.7 kts)
Alluvial Fans, Crusted Salt Flats	30-35 mph (26.1-30.4 kts)
Well-Developed Desert Pavement	40 mph (36.8 kts)

Table 2.1. Critical wind speeds for dust mobilization. (After: COMET, 2003)

In addition to achieving a critical wind speed, the lofting of dust also requires turbulence in the boundary layer. Wind shear aloft can create the necessary turbulent eddies that loft the dust particles from a thin layer near

the bottom of the boundary layer. As a general rule of thumb, surface winds of 15 knots require a wind at 1000 ft that is greater than 30 knots to create this turbulent mixing (COMET 2003). Additionally, instability as a result of day-time heating further contributes to the favorable conditions for lofting dust.

A convenient parameter for dust forecasting which accounts for the effects of wind speed, boundary layer turbulence, and low-level stability is friction velocity (u^*). It is defined in the American Meteorological Society's Glossary of Meteorology (Glickman 2000) as a reference wind velocity that is the square root of the Reynolds stress (τ) divided by air density (ρ).

$$u^* = (|\tau / \rho|)^{1/2}$$

In simple terms, it represents the momentum flux into the surface by the mean wind.

Following Westphal et al (1988), the friction velocity can also be defined (in cm/sec) as:

$$u^* = V_s \kappa / [\ln(Z_s/Z_o) - \psi_m(Z_s/L)]$$

where:

V_s = the wind speed at the mid-point(Z_s) of surface layer
κ = the Von Karmann constant
Z_o = the surface roughness (usually 0.01 for deserts)
ψ_m = the stability parameter for momentum
L = the Monin-Obukhov length.

From the research of Westphal et al. (1988), it has been determined that on average a friction velocity of greater than 60 cm/s is required for the lifting of dust.

Finally, the last key process of dust storms to look at is the dissipation process. Eventually, dust is removed from the atmosphere by four processes: dispersion, advection, settling, and entrainment in precipitation. Dispersion is the process by which the dust plume fans out and becomes dilute as a result of the winds. The speed with which this process occurs is mainly governed by the wind strength and turbulence, both mechanical and thermal. Atmospheric stability works counter to turbulent mixing to inhibit the dispersion of dust (COMET 2003). Advection is simply the transport of dust out of the area by the winds. However, winds aloft can often differ in direction from surface winds; therefore it is not uncommon for dust in the upper regions of the plume to be advected in a different direction than in the near surface regions (COMET 2003).

Settling of dust is governed by the dust particle size. Typically, particles in the 10-50 micrometer size range tend to fall out of the atmosphere at approximately 1000 feet per hour (COMET 2003). The total amount of dust in the air, its particle size distribution, and the height of the dust determine the length of time for this process to clear the air. For post-frontal dust storms, the process of settling normally will clear the air of dust within a few hours of the frontal passage. Entrainment of dust in precipitation refers to the process by which the particles serve as condensation nuclei for cloud droplets. As the droplets activate, they grow in size to the point at which they fall out as precipitation, thus carrying the dust particles with them.

C. REGIONAL CLIMATOLOGY AND LITERATURE REVIEW

The weather in Iraq from December to March generally consists of fair skies and reasonably temperate weather. However, migratory lows and troughs tend to pass through the region every 3-5 days, bringing with them short periods of precipitation and occasional dust storms (Franklin 2004). The large-scale dust storms associated with the 24-36 hour winter shamals occur typically 2-3 times per month during December–March, and it is not uncommon to have the 3-5 day shamals occur 1-3 times during the entire season (COMET 2003). These storms appear to occur slightly more frequently during El Niño years (Franklin 2004). As a general rule, in spite of the almost continuous presence of dust haze during the winter, the overall visibility in between dust storms is better than during the summer. (Franklin 2004). The strongest of the dust storms can result in visibilities dropping to zero meters in a matter of a few hours, as was the case in the storm being studied.

The Fleet Numerical Meteorology and Oceanography Center (FNMOC) paper, "Operation IRAQI FREEDOM (OIF) Numerical Model Validation," (FNMOC 2004) reviewed three different cases of 24-36 hour shamal events in February, March and April of 2003, including the event from 25-27 March. The paper broke down the case studies into objective and subjective analyses for the purpose of evaluating various numerical weather prediction model tendencies. The prime focus was on the performance of NOGAPS and COAMPS relative to GFS. This thesis will conduct a similar qualitative analysis, but for a more focused look at the specific case occurring in late March of 2003.

III. SYNOPTIC DUST STORM ANALYSIS

A. METHODOLOGY

In the analysis of this storm, it is important to first look 2 to 3 days ahead of the onset of blowing dust and analyze the synoptic situation leading up to the event. According to Perrone (1979), the initial indication of a synoptically forced shamal event is the presence of an "upper level trough with a corresponding surface low moving over Syria from the eastern Mediterranean." He describes a southerly flow ahead of the advancing cold front, which gradually increases in intensity with time, as the cold front approaches. These winds activate dust particles in the source regions described above and commence the dust storm process. The winds do not actually shift to a more northerly component until after the passage of the cold front. With this conceptual model of a classical synoptic shamal in mind, the case study will step through the development of the storm by looking at numerical model analysis representing the "best-estimate" of the state of the atmosphere at the time. Also, the model analyses will be compared with satellite imagery. The storm development analysis begins 22 March at 0000 GMT, and steps through the event in 12 hour increments until 27 March at 0000 GMT, when the system moves northeastward toward the Caspian basin.

B. 22 MARCH 2003

On 22 March, 2003, the synoptic pattern indicates the presence of the conditions described above, which Perrone (1979) calls the "pre-shamal period". At 0000 GMT, GFS

model analysis shows a 5-wave long-wave pattern in the 500 mb height field with a closed low over the southern and central Ukraine (Figure 3.1). An enlargement of the NOGAPS analysis 500 mb height field (Figure 3.2) agrees very well with the GFS analysis, and shows in finer detail a building ridge centered over the North Sea and a strong vorticity maximum along the trough axis extending from the Ukraine, across the Black Sea into northwestern Turkey. The 300 mb height field (Figure 3.3) shows a closed upper-level low centered slightly northwest of the 500 mb trough axis with a relatively strong upper-level jet entering the upwind side of the trough, wrapping around the base, and indicating the upper-level trough will dig southwestward. A strong subtropical jet cuts across northern Africa and turns northward over southeastern Iraq.

At 850 mb, the height field indicates a 1360 meter (m) closed low over the Sea of Azov, just south of the Ukraine, with a trough forming over central Turkey east of the 500 mb and 300 mb troughs. A region of tight thermal packing cuts across Turkey diagonally from the northeast to southwest, across the Aegean Sea, Greece, and eastern Italy, indicating the presence of a long stationary front, as shown by the magenta line in Figure 3.4, and significant cold air advection under the 500 mb trough.

Moving to 1200 GMT, 22 March, there is little change in the overall system with the long-wave troughs remaining relatively stationary over the previous 12 hours. The major exception is that the upper level jet entering the upwind side of the 300 mb trough intensifies, further aiding the trough in digging southwestward over northern Italy. The jet on the downwind side of the trough,

separates from its upwind counterpart, and connects to the sub-tropical jet. The net effect of all of this is seen in Figure 3.5, where the 500 mb pattern shows a secondary vorticity maximum forming in the western base of the trough, over the central Balkans. At 850 mb, the trough forming over central Turkey becomes a 1440 m closed low just north of the Turkey/Syria border, and the stationary front pushes southward towards the southern coast of Turkey (Figure 3.6).

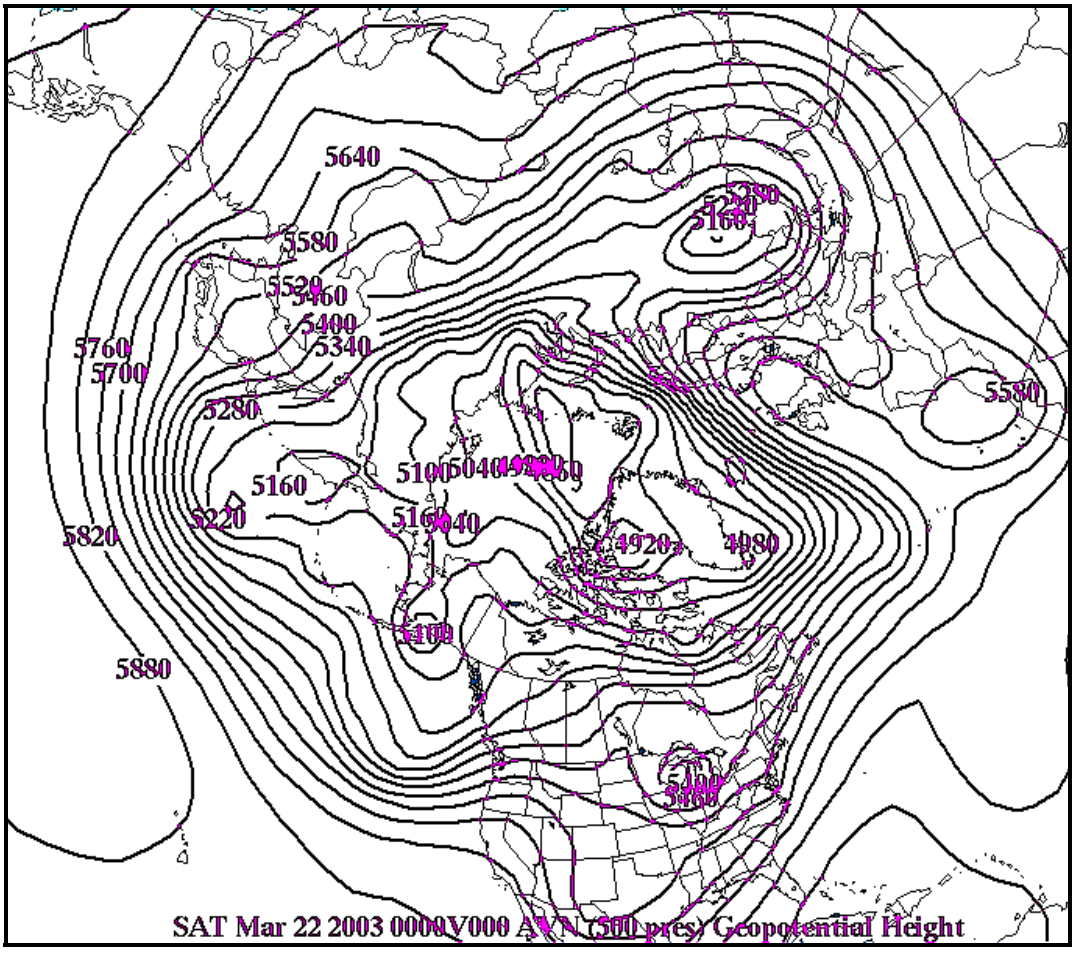

Figure 3.1. 500 mb Long wave Height Pattern (m): 0000 GMT, 22 March 2003.

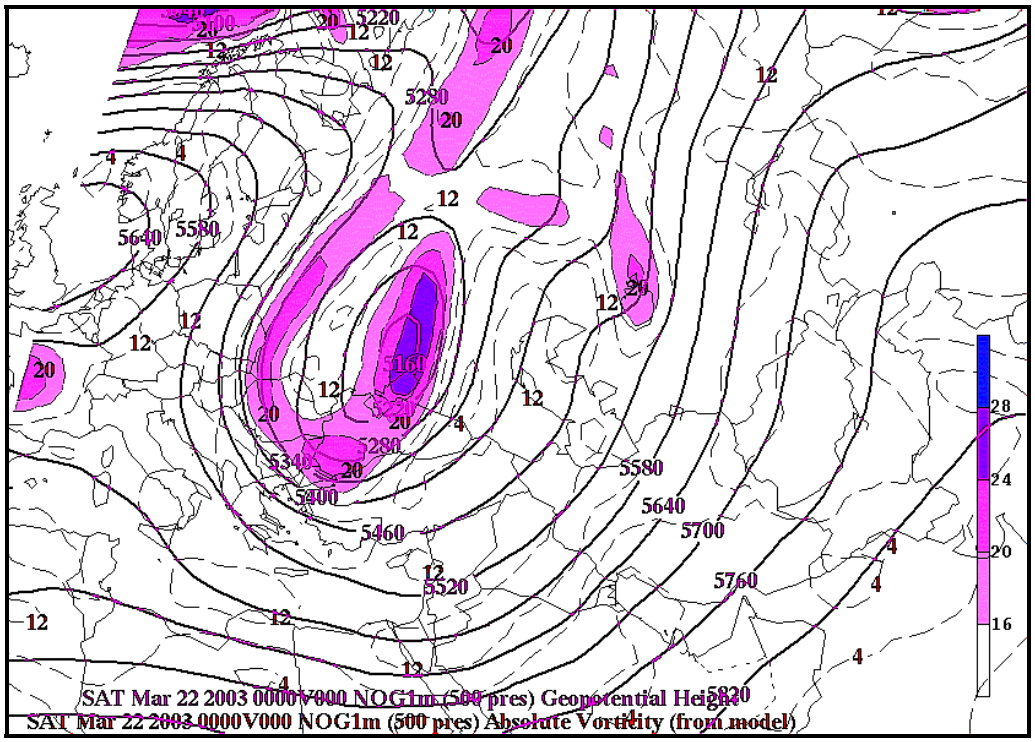

Figure 3.2. 500 mb Height (m) & Absolute Vorticity (10^{-5}/sec): 0000 GMT, 22 March 2003.

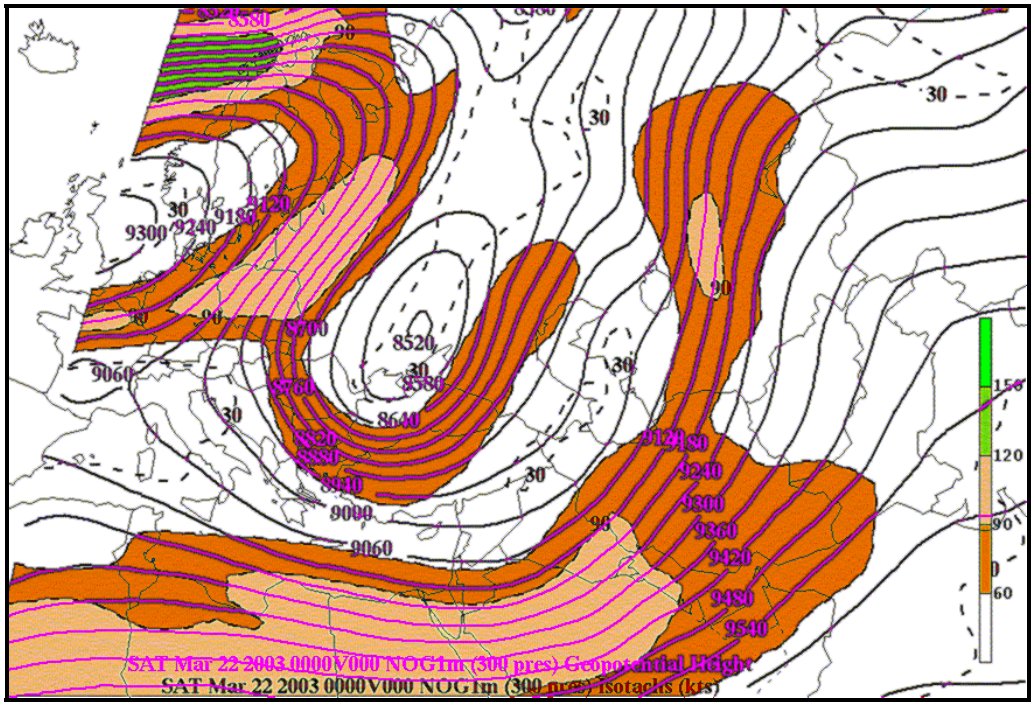

Figure 3.3. 300 mb Height (m) & Winds (kts): 0000 GMT, 22 March 2003.

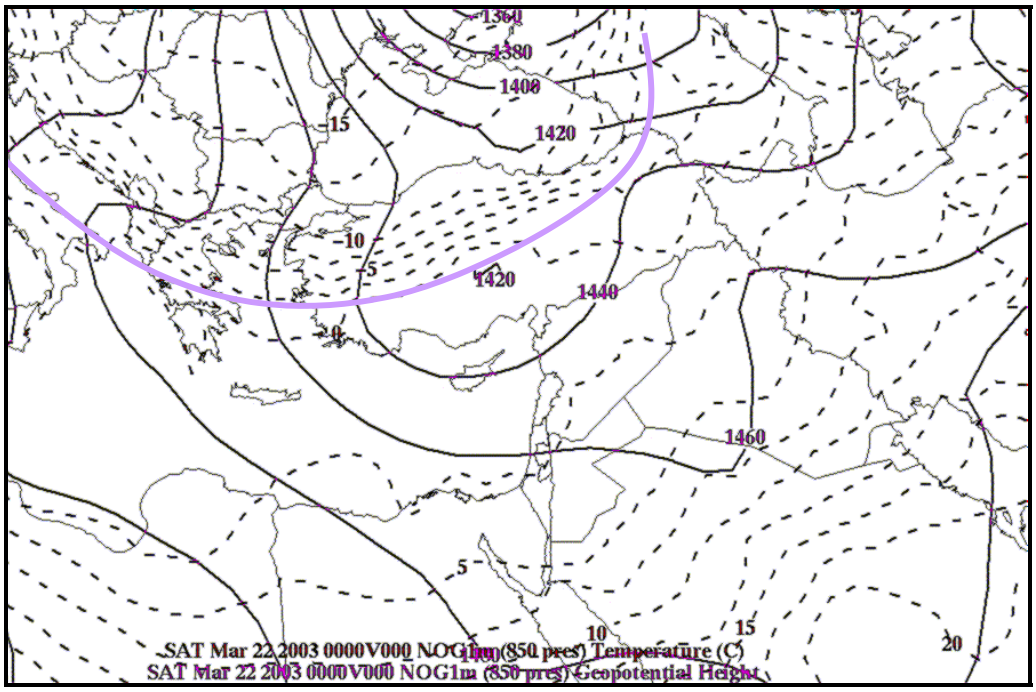

Figure 3.4. 850 mb Height (m) & Temperature (°C): 0000 GMT, 22 March 2003. Magenta line represents a stationary front.

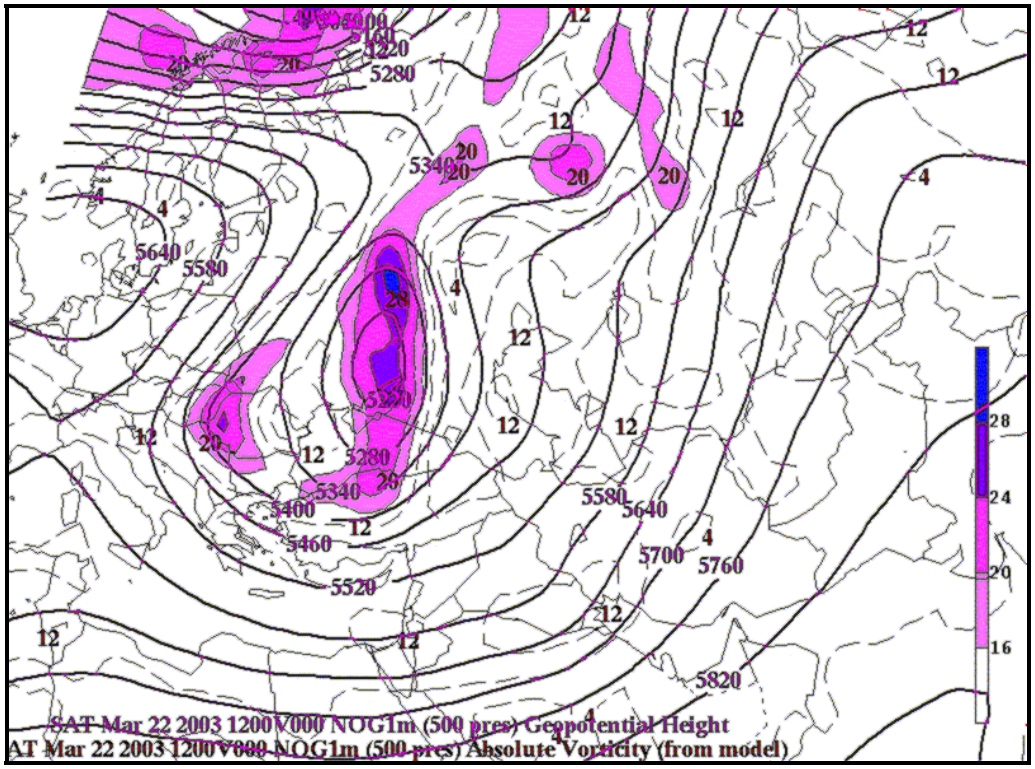

Figure 3.5. 500 mb Height (m) & Absolute Vorticity (10^{-5}/sec): 1200 GMT, 22 March 2003.

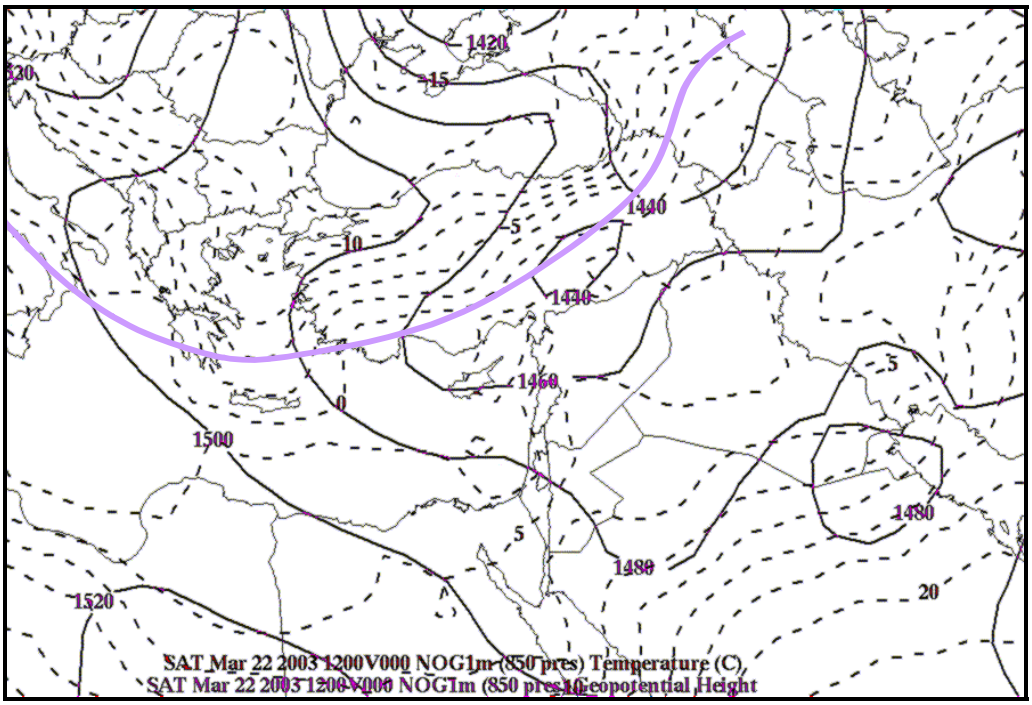

Figure 3.6. 850 mb Height (m) & Temperature (°C): 1200 GMT, 22 March 2003. Magenta line represents a stationary front.

C. 23 MARCH 2003

By 0000 GMT on 23 March, the 500 mb ridge over the North Sea shifts eastward over the coast of Germany and the Baltic States, building to 5700 m. Figure 3.7 shows this development along with the developing vorticity maximum in the southwestern side of the trough. As the trough deepens, the elongated lobe of maximum vorticity along the trough axis in the previous time period, as shown in Figure 3.5, wraps around the northern end of the closed low and becomes more concentrated (Figure 3.7). This development is assisted by the continual strengthening of the jet at 300 mb, which creates a strong region of upper-level cyclonic shear in the trough axis (Figure 3.8).

At 850 mb, there is now a long trough extending from northern Syria and Iraq, across Turkey, to the island of

Crete (Figure 3.9). Cyclonic flow around this broad region of low pressure continues to advect cold air from the Aegean Sea around the western side, which begins to deform the stationary front as shown in Figure 3.9.

By 1200 GMT, 23 March, the 500 mb trough begins to extend farther southward, with the central low pressure reaching the middle of the Black Sea at its southernmost end. The 500 mb vorticity maximum, previously at the north end of the closed low, rotates down the upwind side of the trough, elongating again, joining up with the developing maximum in the southwest base of the trough as depicted in Figure 3.10.

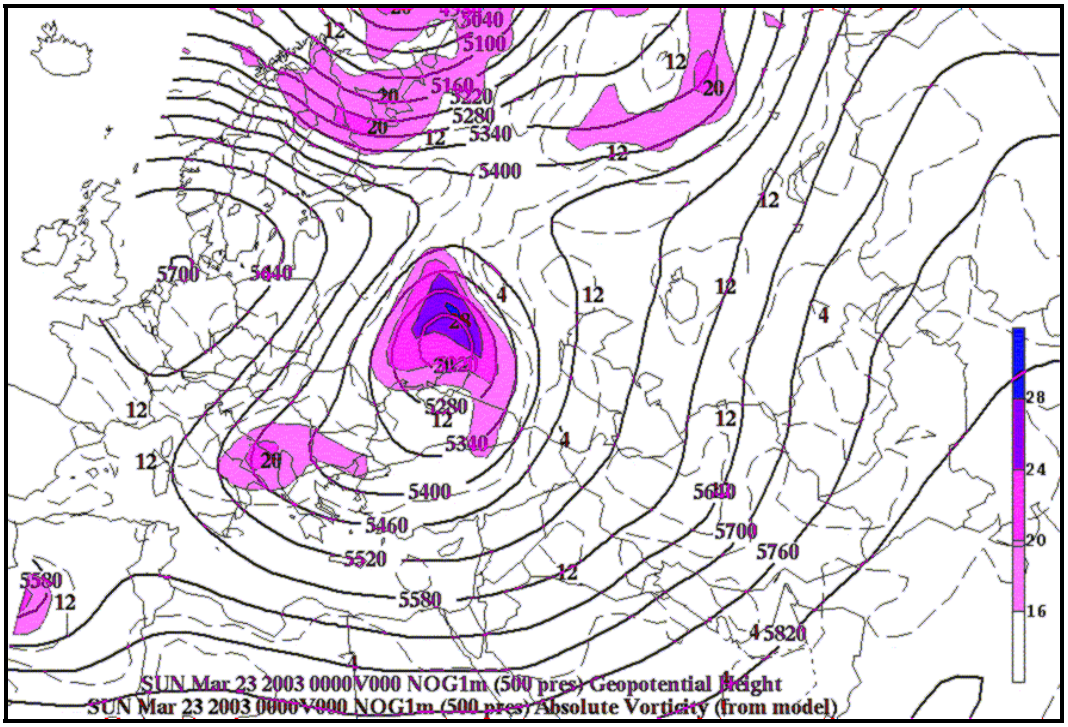

Figure 3.7. 500 mb Height (m) & Absolute Vorticity (10^{-5} /sec): 0000 GMT, 23 March 2003.

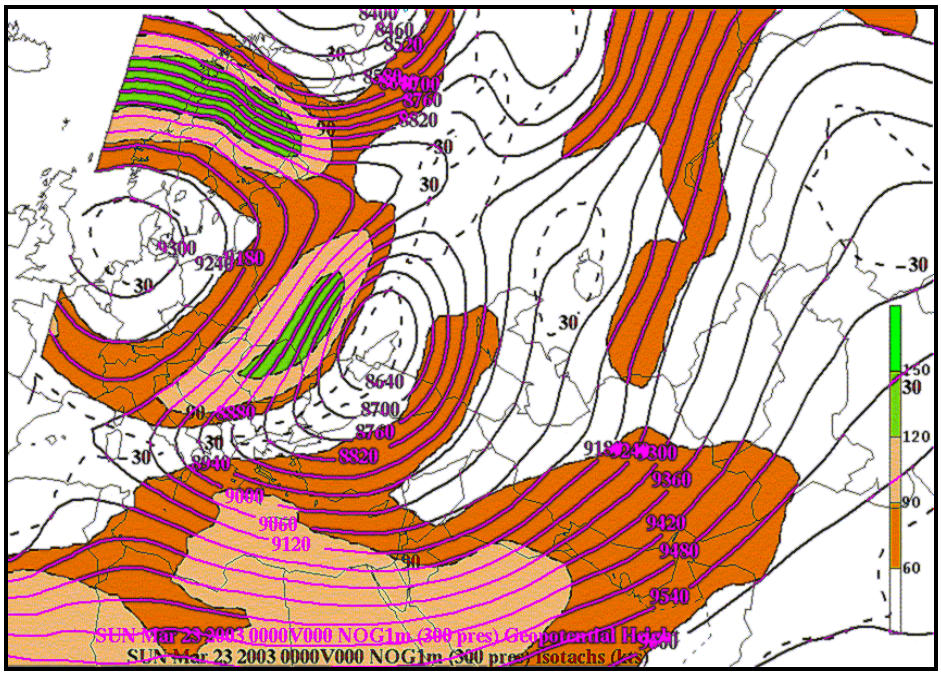

Figure 3.8. 300 mb Height (m) & Winds (kts): 0000 GMT, 23 March 2003.

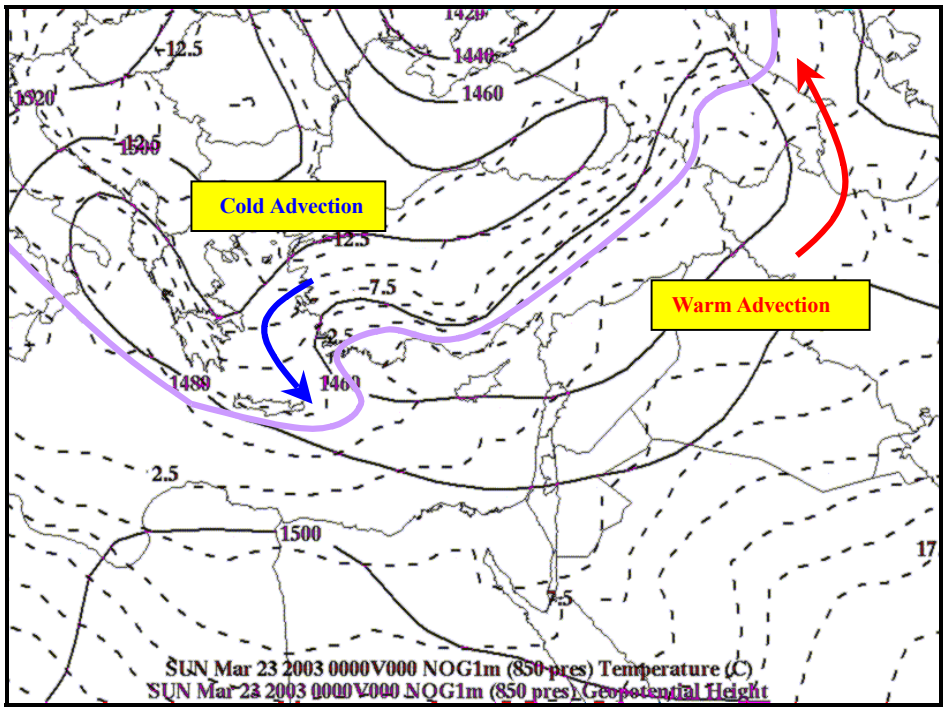

Figure 3.9. 850 mb Height (m) & Temperature (°C): 0000 GMT, 23 March 2003. Magenta line shows the deformation of the stationary front by the cold and warm air advections around the elongated low pressure region.

At 850 mb, the cyclonic flow around the broad region of low pressure continues to strengthen the cold air advection on the west side, leading to the beginning stages of a weak cold front extending from the southern coast of Turkey, and bending back across the central Mediterranean, south of the island of Crete. Meanwhile on the northeastern side of the low pressure area, a weak warm front starts to form along the border between Iran and Azerbaijan (Figure 3.11). Figure 3.12 shows the METEOSAT water vapor (WV) image from 1200 GMT, 23 March. This image verifies the position of the stationary front across Turkey shown in Figure 3.11, with a band of clouds diagonally bisecting the country in approximately the same location as the thermal gradient in the model analysis.

Interestingly, Figure 3.12 also shows a high altitude cloud formation over the coast of Egypt and Libya. The formation is due to a transiting short-wave disturbance related to the 1440 m closed low approaching the region in the southwest corner of Figure 3.11. This disturbance will move eastward along the associated baroclinic zone extending over northern Libya and Egypt and help amplify the rapid cyclogenesis in the main low pressure feature over the next 24 hours. As depicted in Figure 3.11, the flow around eastern side of the low in the southwest corner of the image meets up with the flow around the western edge of the main low, which strengthens the baroclinicity in the region, resulting in the cloud formation shown in Figure 3.12.

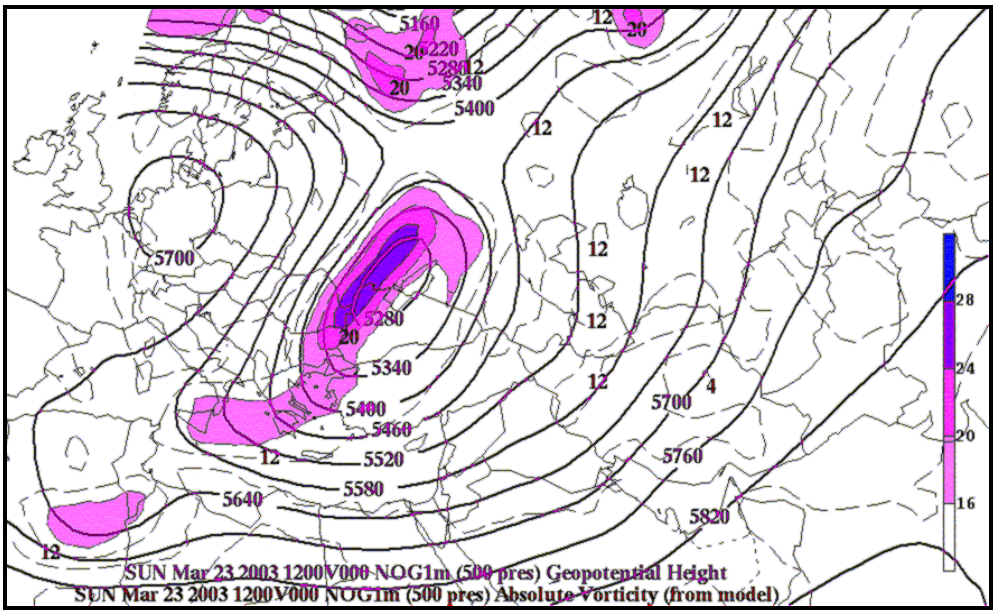

Figure 3.10. 500 mb Height (m) & Absolute Vorticity (10^{-5} /sec): 1200 GMT, 23 March 2003.

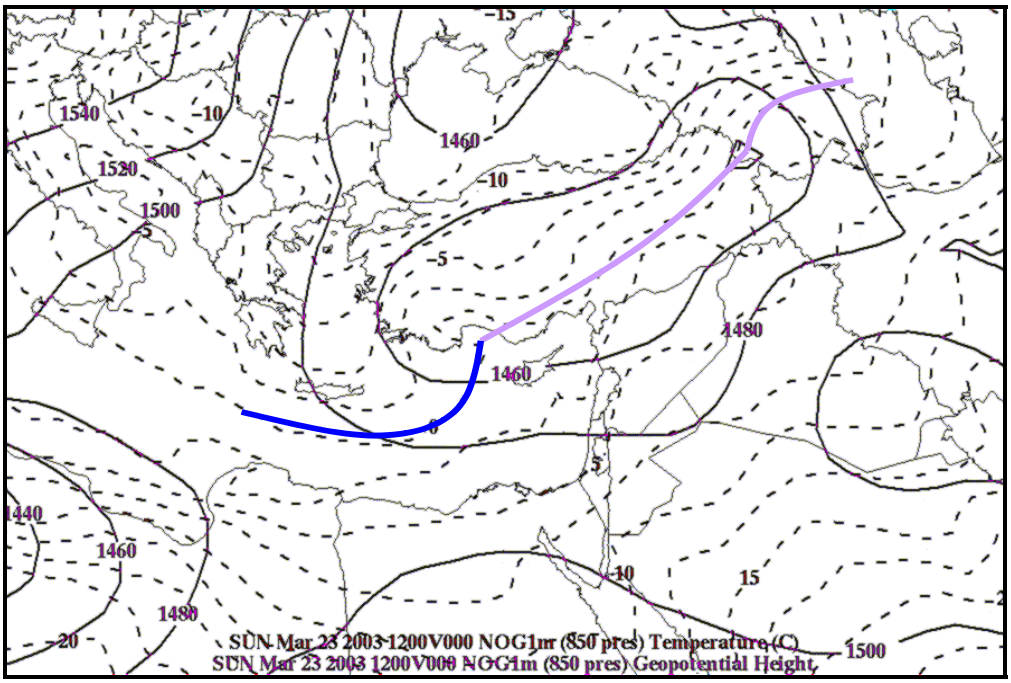

Figure 3.11. 850 mb Height (m) & Temperature (°C): 1200 GMT, 23 March 2003. Magenta line shows a relatively stationary frontal boundary with slight deformation on the northeastern end; blue lines represents a developing cold front.

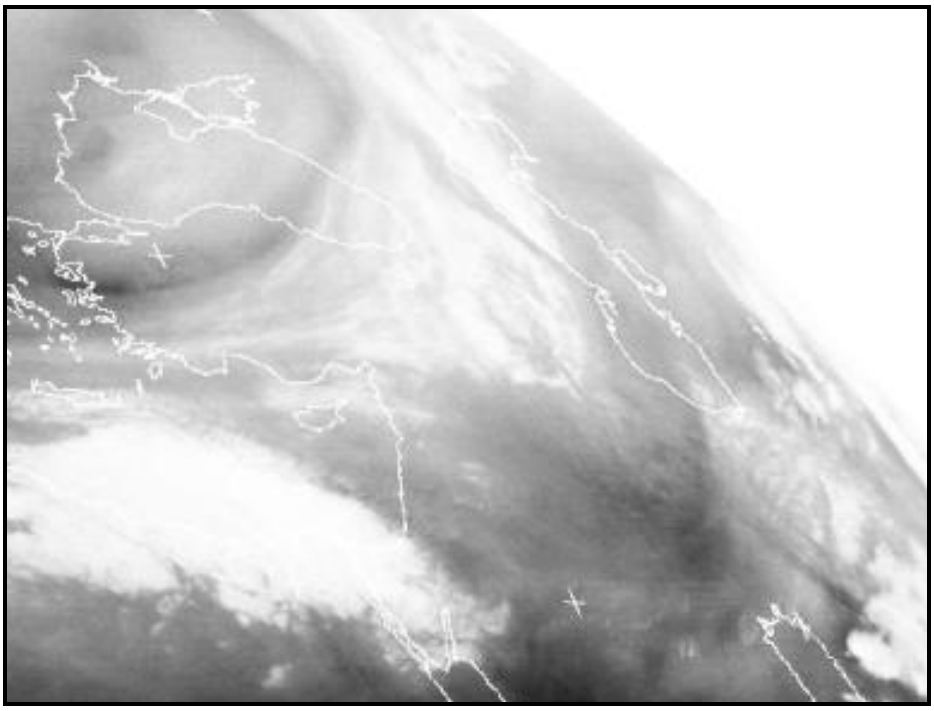

Figure 3.12. METEOSAT Water Vapor Image: 1200 GMT, 23 March 2003. (From: NERC Satellite Receiving Station, Dundee University, Scotland: http://www.sat.dundee.ac.uk/, courtesy of EUMETSAT: http://www.eumetsat.de/)

D. 24 MARCH 2003

By 0000 GMT, the 500 mb trough axis is now stretched across the Black Sea and southwestern Turkey, with the base reaching the northern Mediterranean (Figure 3.13). The ridge over Europe continues its progression eastward maintaining a magnitude of approximately 5700 m. The 300 mb jet continues to contribute to the overall amplification of the system, with the northeastward branch of the sub-tropical jet at the southeastern end of the trough intensifying to 120 knots.

At 850 mb, the large area of low pressure deepens to 1420 m, with central low pressure centering over southern/central Turkey, just north of Cyprus, as shown in

Figure 3.14. The circulation around the low intensifies the warm air advection to the northeast and cold air advection over the Mediterranean, thus strengthening respectively the warm and cold fronts developing in those regions. In particular, the cold front starts to advance eastward just west of Cyprus, before trailing off to the west across the southern Mediterranean. The frontal movement to the east is aided by the merging short-wave over the coast of Egypt.

This analysis again compares well with the METEOSAT IR image from 0000 GMT (Figure 3.15). Figure 3.15 once again shows the previously mentioned short-wave moving eastward along the zonally oriented cold front depicted in Figure 3.14. The cloud feature associated with this short-wave begins to join into the baroclinic leaf cloud structure

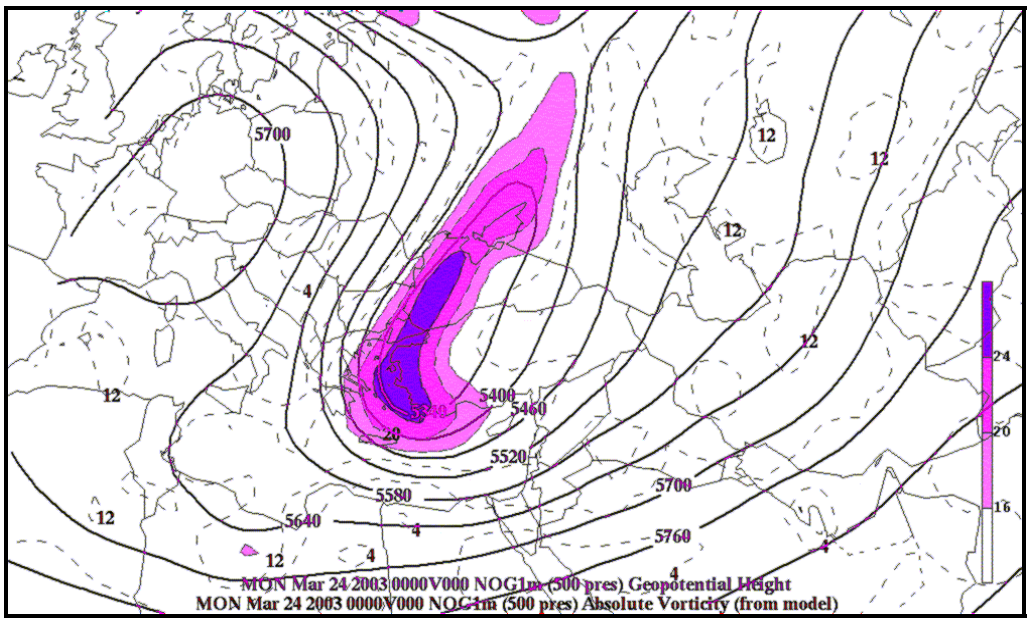

Figure 3.13. 500 mb Height (m) & Absolute Vorticity (10^{-5} /sec): 0000 GMT, 24 March 2003.

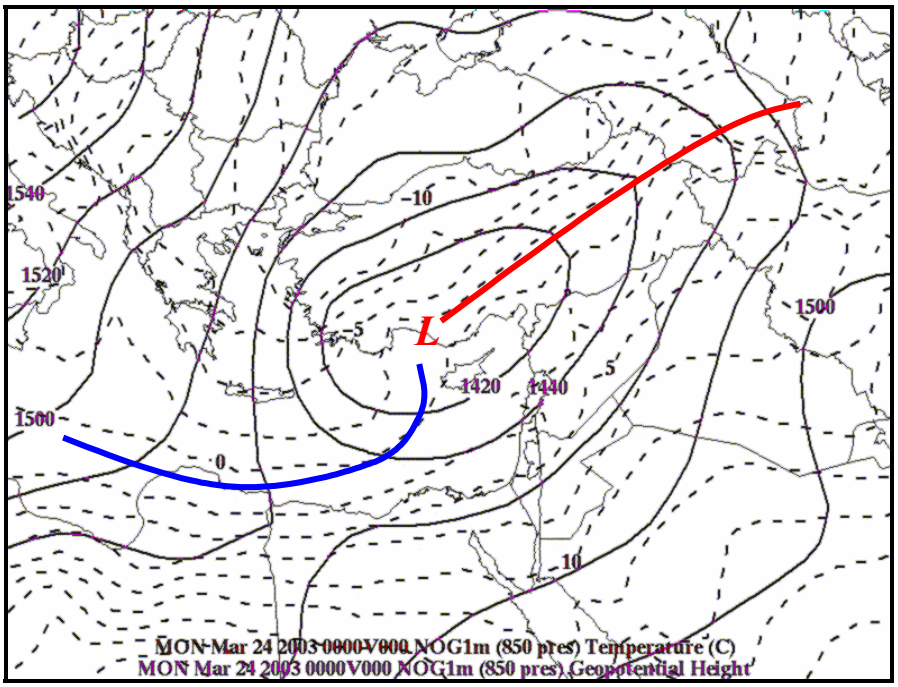

Figure 3.14. 850 mb Height (m) & Temperature (°C): 0000 GMT, 24 March 2003. Blue and red lines indicate cold and warm fronts respectively.

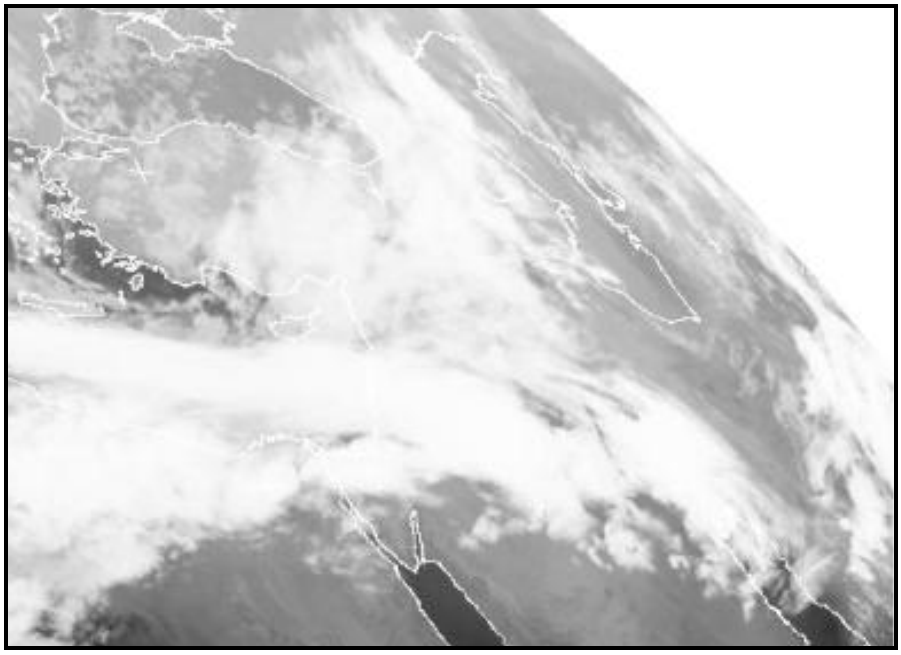

Figure 3.15. METEOSAT IR: 0000 GMT. 24 March 2003. (From: NERC Satellite Receiving Station, Dundee University, Scotland: http://www.sat.dundee.ac.uk/, courtesy of EUMETSAT: http://www.eumetsat.de/)

extending from the eastern Mediterranean, across Israel and into southwestern Iraq. This cloud formation gives a strong indication of a rapidly developing cyclone.

The surface low pressure feature associated with the short-wave disturbance is shown in Figure 3.16. At 0000 GMT, 24 March, the center of this disturbance is located in southern/central Libya. Over the next 24 hours, the short-wave will sweep rapidly eastward into northwestern Saudi Arabia, just ahead of the cold front associated with the main low pressure system over Cyprus. Figure 3.17 shows this development, which will lead to the overall strengthening of the pressure gradient ahead of the cold front. The main result will be an increase in pre-frontal southerly winds, thereby amplifying the severity of the dust storm that will eventually strike the area of responsibility (AOR), encompassing Iraq, the Arabian Peninsula, and the NAG.

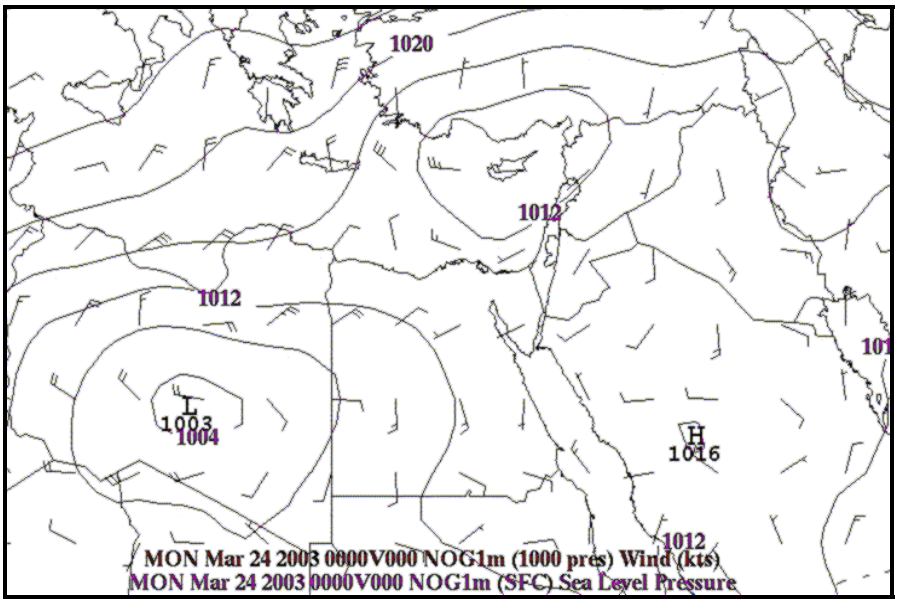

Figure 3.16. Sea-Level Pressure (mb) & 1000 mb Winds (kts): 0000 GMT, 24 March 2003.

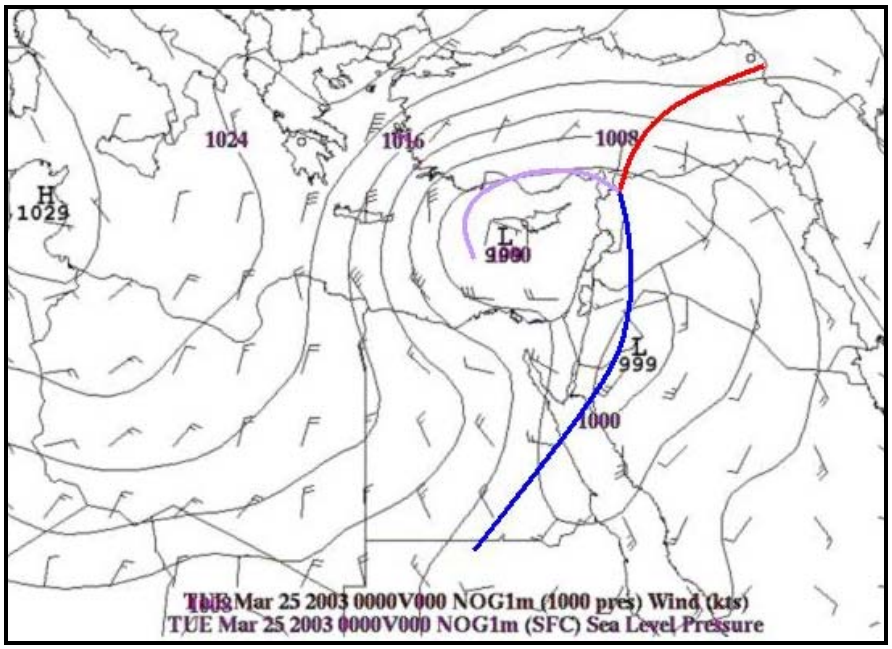

Figure 3.17. Sea-Level Pressure (mb) & 1000 mb Winds (kts): 0000 GMT, 25 March 2003. Magenta line represents an occluded front; blue and red lines represent cold and warm fronts respectively.

In the mean time, by 1200 GMT, 24 March, the 500 mb vorticity maximum at the base of the trough intensifies significantly and strong frontogenesis continues to occur over the eastern Mediterranean. The 300 mb jet strongly supports lower-level system development with the jet entering the upwind side of the highly meridional trough and the northeastward branch of the subtropical jet on the downwind side working together to intensify the region of upper-level cyclonic shear (Figure 3.18).

At 850 mb, the low pressure center deepens further to 1350 m, and shifts southward over the region just to the west of Cyprus as the short-wave has now fully merged with the main low pressure system. As shown in Figure 3.19, the cold front continues to rotate cyclonically, and extend across eastern and central Egypt.

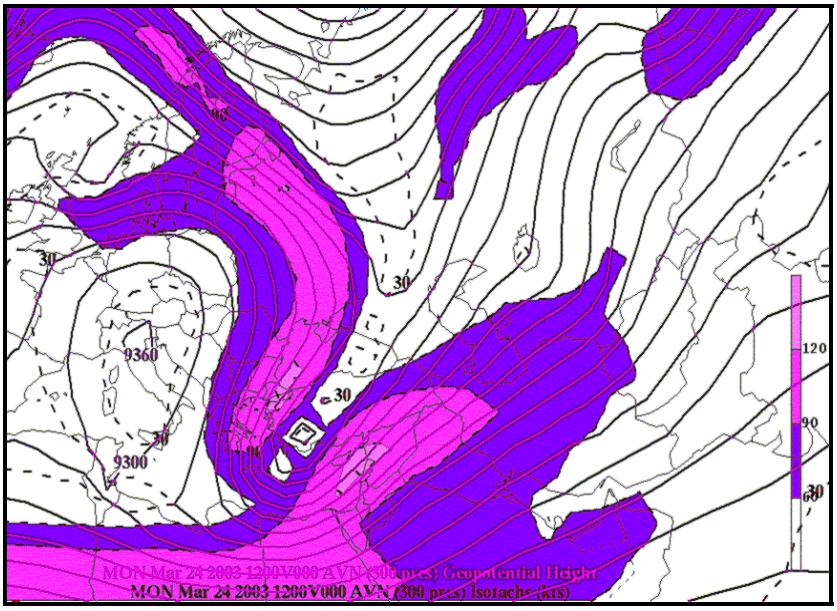

Figure 3.18. 300 mb Height (m) & Winds (kts): 1200 GMT, 24 March 2003.

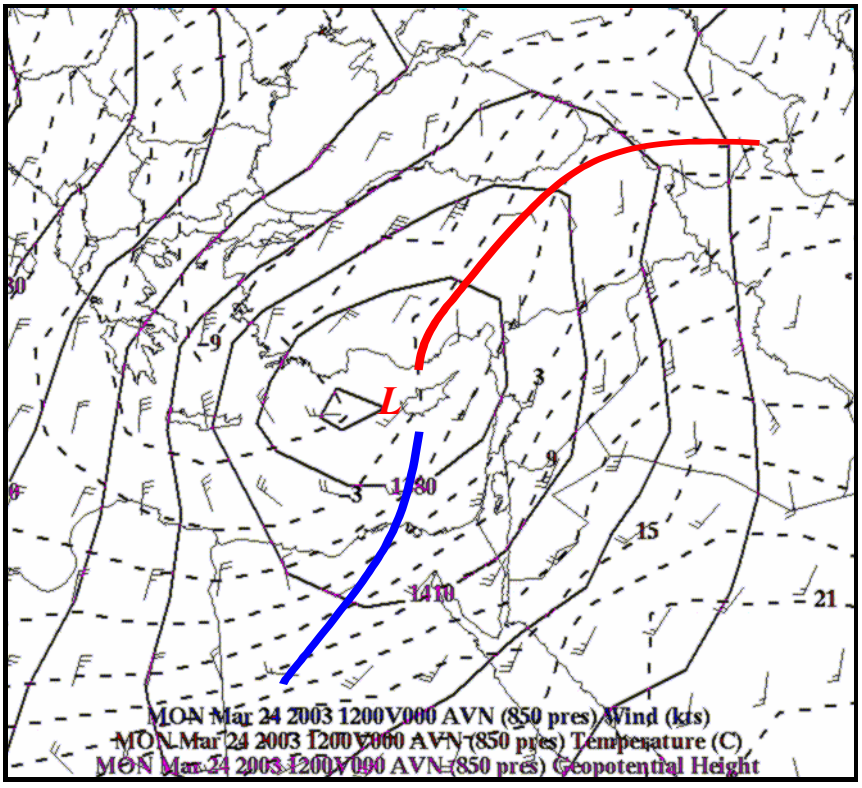

Figure 3.19. 850 mb Height (m), Temperature (°C) & Winds (kts): 1200 GMT, 24 March 2003. Blue and red lines represent cold and warm fronts respectively.

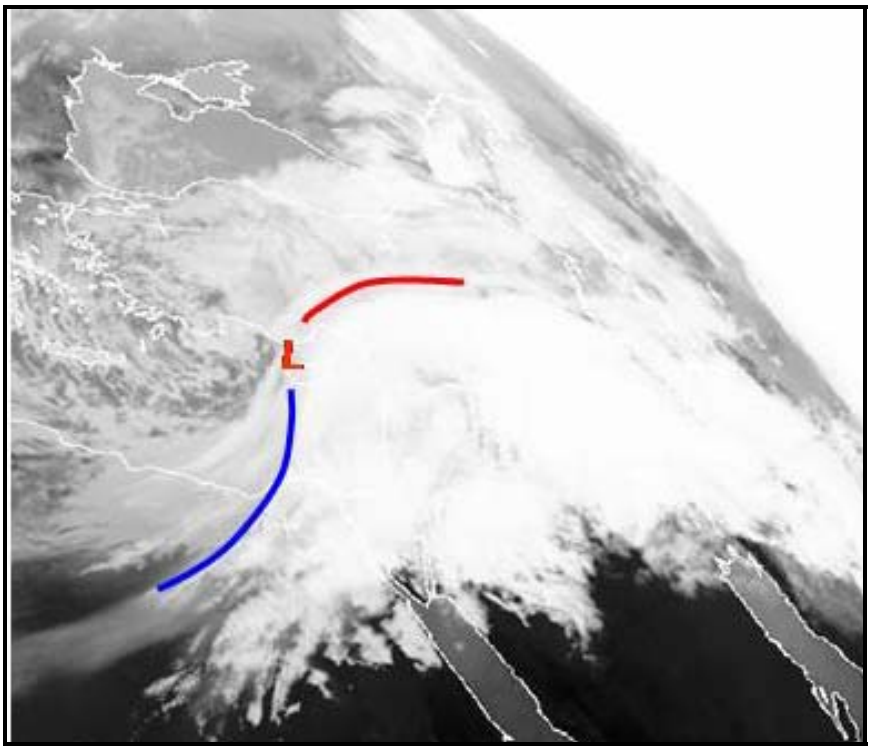

Figure 3.20. METEOSAT IR Image: 1200 GMT. 24 March 2003. Blue and red lines represent cold and warm fronts respectively. (After: NERC Satellite Receiving Station, Dundee University, Scotland: http://www.sat.dundee.ac.uk/, courtesy of EUMETSAT, http://www.eumetsat.de/)

This development once again compares extremely well to Figure 3.20, the 1200 GMT, 24 March METEOSAT IR image. The previously mentioned baroclinic leaf rotates cyclonically to a more meridional orientation as the system develops. Figure 3.20 also shows the intense region of convective clouds in the warm sector of the developing cyclone. This type of activity is common ahead of a synoptically forced shamal event.

At this point, the short-wave feature has completely merged with the cyclone and is strengthening the southerly flow ahead of the cold front. Also noteworthy in Figure 3.19, the 850 mb southerly winds, intensified by the short-

wave, are sweeping into Iraq across the Saudi Arabian border at an approximate average of 15-25 knots. At that time, stations in the region, such as Kuwait International Airport, Camp Doha, Kuwait, and Prince Sultan Airbase report light southeasterly surface winds, and "CAVOK" (Ceiling and Visibility OK) conditions, with no significant weather (Finta 2004a).

E. 25 MARCH 2003

Over the next 12 hours, the intensifying cyclone remains mostly stationary, shifting eastward only slightly. By 0000 GMT on 25 March, the center of the system at 500 mb is located in the northeastern Mediterranean, just off the west coast of Cyprus. The downwind side of the trough at 500 mb shows a short-wave ridge building over Iraq and eastern Turkey, indicating further system amplification (Figure 3.21). The 300 mb jet again continues to aid in cyclone development, while the center of the upper level trough slopes back to the west of Cyprus leading to a strong baroclinic zone in the upper levels (Figure 3.22).

The 850 mb central low is at approximately 1320 m, and situated over the western coastline of Cyprus. The system starts to show signs of an occluding process, with a triple point situated over northwestern Syria as displayed in Figures 3.17 and 3.23. This analysis is again verified by the 24 March, 2330 GMT METSAT IR image (Figure 3.24) in the typical "comma" cloud formation blanketing the region.

As shown in Figure 3.23, the southerly winds at 850 mb ahead of the cold front nearly double to an approximate average of 30-40 knots over the 12 hour period. At the

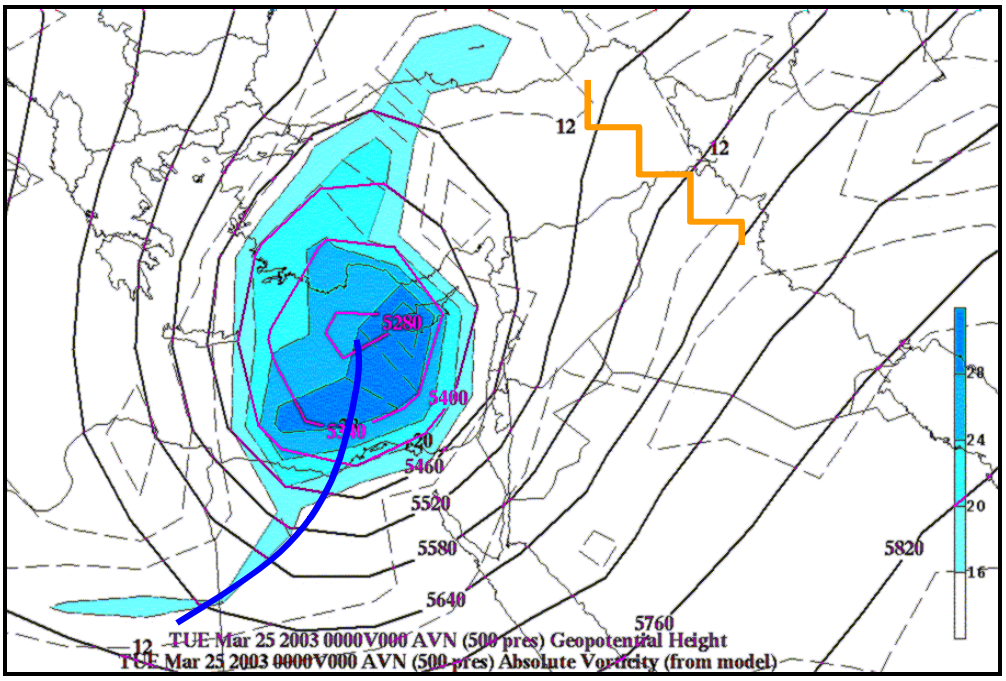

Figure 3.21. 500 mb Height (m) & Absolute Vorticity (10^{-5} /sec): 0000 GMT, 25 March 2003.

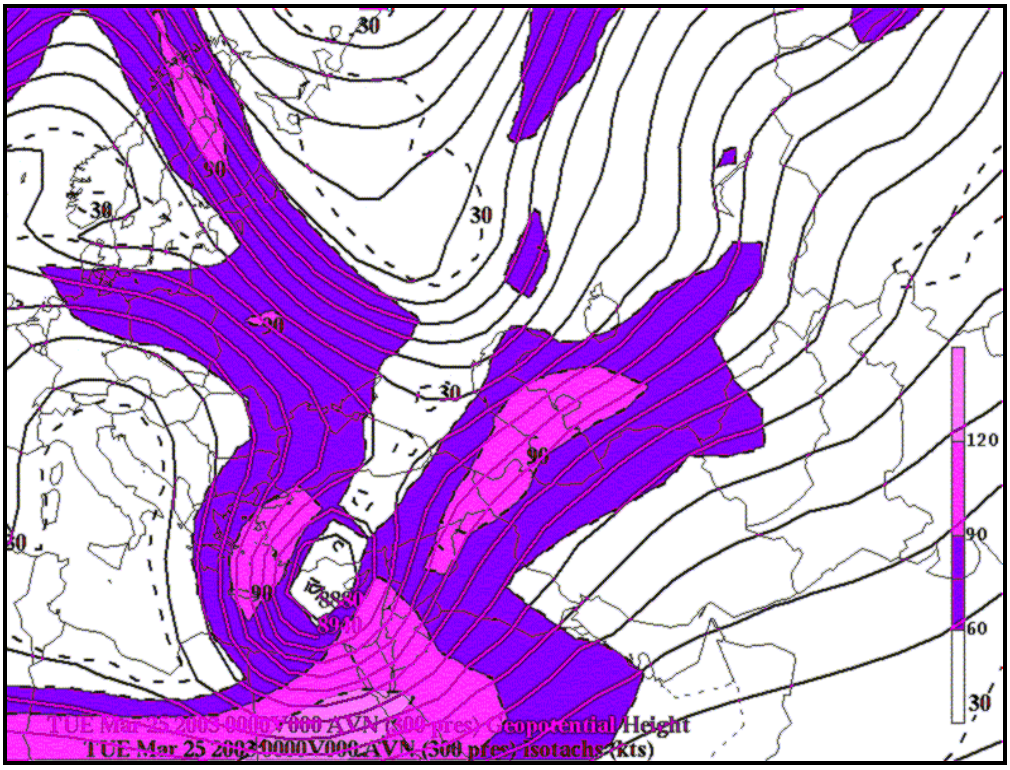

Figure 3.22. 300 mb Height (m) & Winds (kts): 0000 GMT, 25 March 2003.

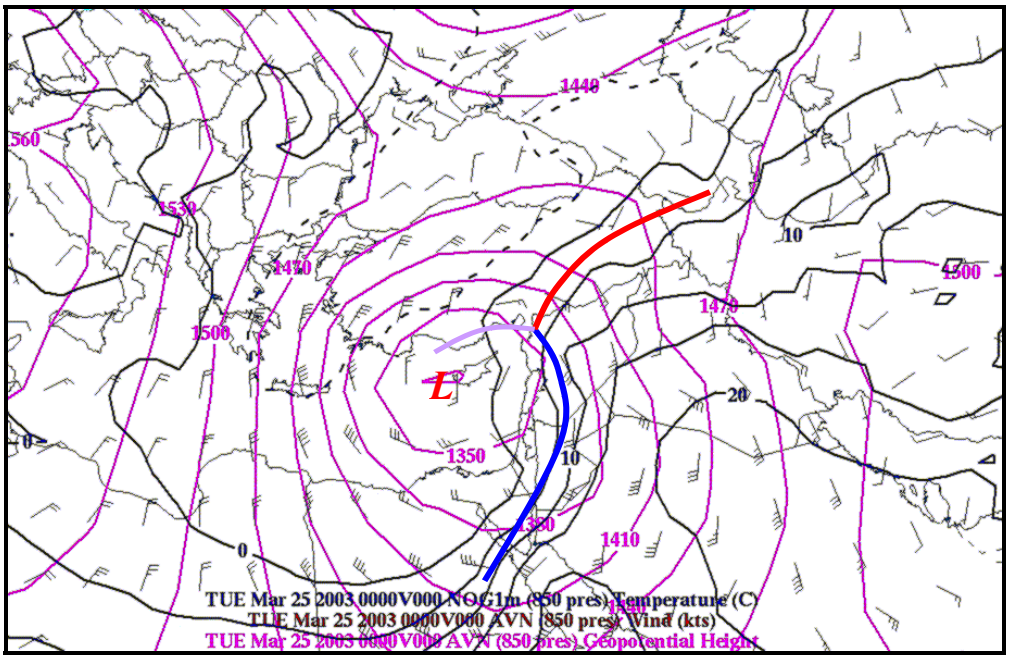

Figure 3.23. 850 mb Height (m), Temperature (°C) & Winds (kts): 0000 GMT, 25 March 2003. Magenta line represents an occluded front; blue and red lines represent cold and warm fronts respectively.

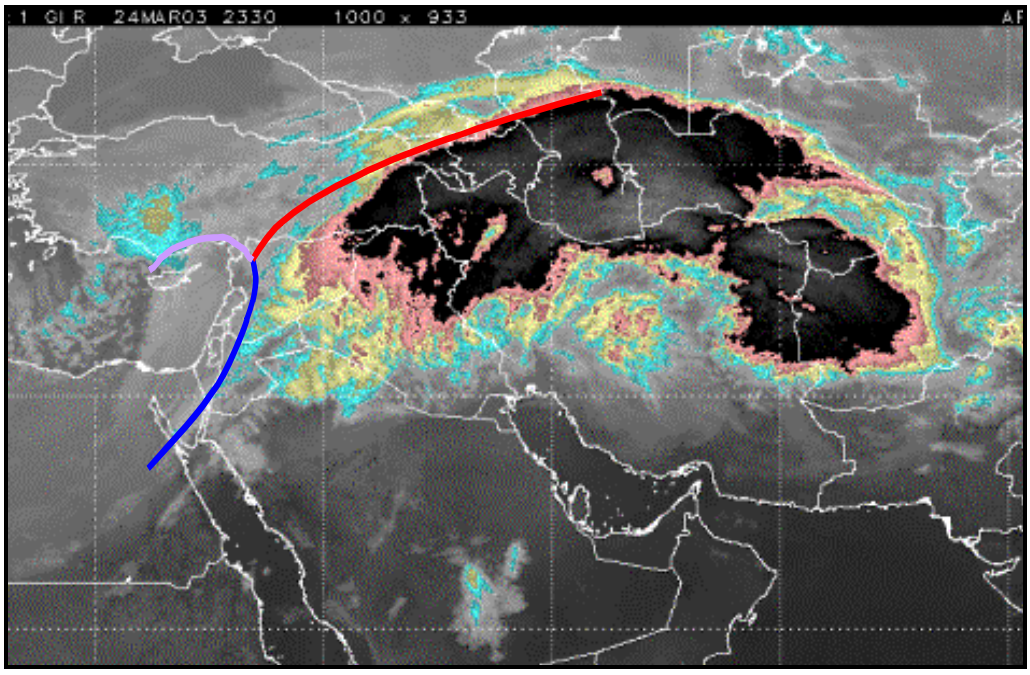

Figure 3.24. METSAT IR Image: 2330 GMT, 24 March 2003. Magenta line represents an occluded front; blue and red lines represent cold and warm fronts respectively. (After: Finta 2004a)

same time, the sea-level pressure chart (Figure 3.25) shows southerly surface winds south of the Iraq/Saudi Arabia border at an approximate average of 20 knots. The difference in surface winds and 850 mb winds indicates strong boundary layer mixing.

Once again Kuwait International Airport and Camp Doha, Kuwait report light southeasterly winds at 5 knots, and clear sky conditions. Prince Sultan Airbase, near Riyadh in central Saudi Arabia notes an increase in surface winds to 16 knots but also no blowing dust as of 0000 GMT. This situation changes at 0255 GMT when Prince Sultan AB first notes the presence of blowing dust in its hourly METAR report. At that time, they report southeasterly winds at

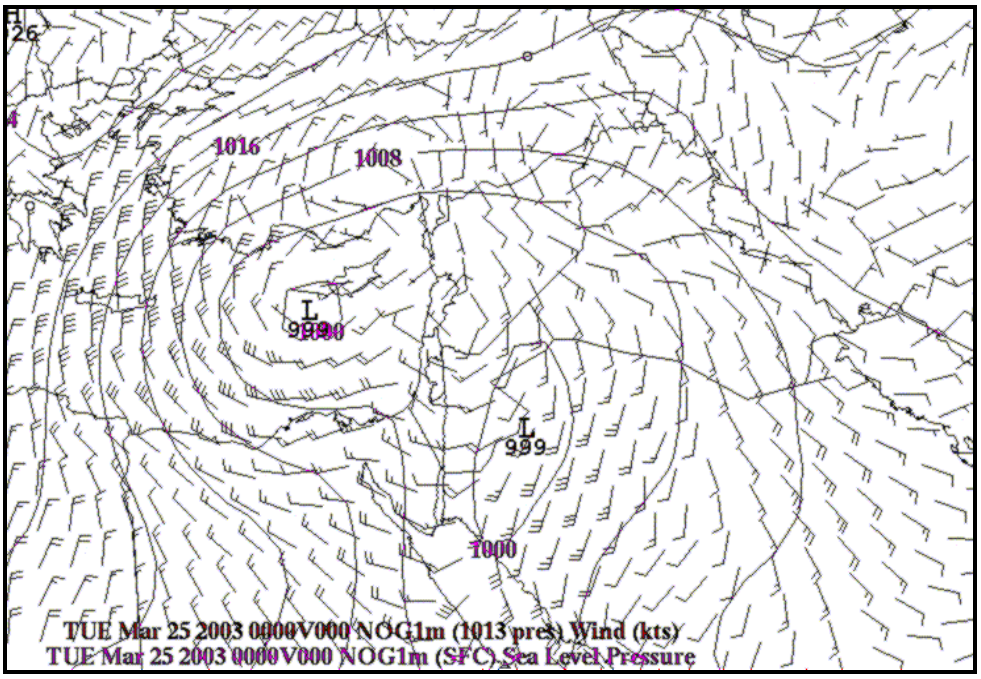

Figure 3.25. Sea-Level Pressure (mb) & Winds (kts): 0000 GMT, 25 March 2003.

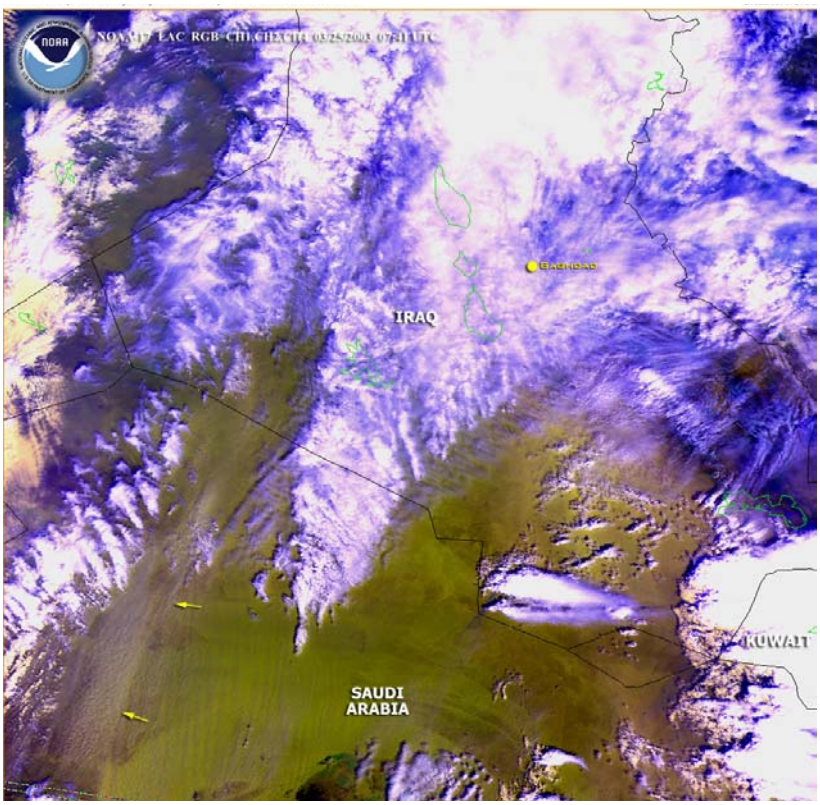

Figure 3.26. NOAA-17 RGB composite image: 0730 GMT, 25 March 2003. Yellow arrows point to activated dust source regions. (From: National Oceanic and Atmospheric Administration: http://www.osei.noaa.gov/Events/Iraq/2003/)

17 knots, gusting to 21 knots, but no significant restrictions to visibility (Finta 2004a).

The NOAA-17 polar orbiting satellite pass at 0730 GMT, 25 March, clearly shows the surface winds activating the dust source regions in northern Saudi Arabia, as indicated by the yellow arrows in Figure 3.26. With the intensification of the pre-frontal southerly winds, the dust storm, now casually referred to as the "Mother of All Fronts" (Finta 2004a), is under way.

By 1200 GMT, 25 March, the 500 mb low center migrates into the southeastern Mediterranean, (Figure 3.27) with the downwind short-wave ridge building over eastern Turkey.

The jet on the upwind side of the 300 mb trough weakens to 90 knots, but the sub-tropical jet continues to support the upper-level cyclonic rotation, as it wraps northeastward around the base (Figure 3.28).

At 850 mb, the low center moves eastward into northwestern Syria, with the triple point also shifting into the northeastern corner of the country. As shown in Figure 3.29, the cold front continues to rotate counter-clockwise, and pushes into western Iraq. Once again model analysis frontal positions verify well in the METSAT water vapor and METSAT IR images from 25 March, 1200 GMT (Figure 3.30).

At the surface, the winds vary in intensity from approximately 45 knots over the central An-Nafud desert, in northwestern Saudi Arabia to 15 knots along the coast of the Northern Arabian Gulf (Figure 3.31). The intensity of the surface winds increases greatly close to the front, and drops off further ahead of the approaching front. Comparing the surface winds with the values for dust particle activation from Table 2.1, the surface winds over a wide spread area are clearly strong enough for the activation of dust and sand from the source regions in the area.

At 1155 GMT, 25 March, observations at Prince Sultan AB report winds at 170 degrees and 25 knots, with gusts to 33 knots. A dust storm is also included in the report, which drops the visibility to 800 meters, or approximately

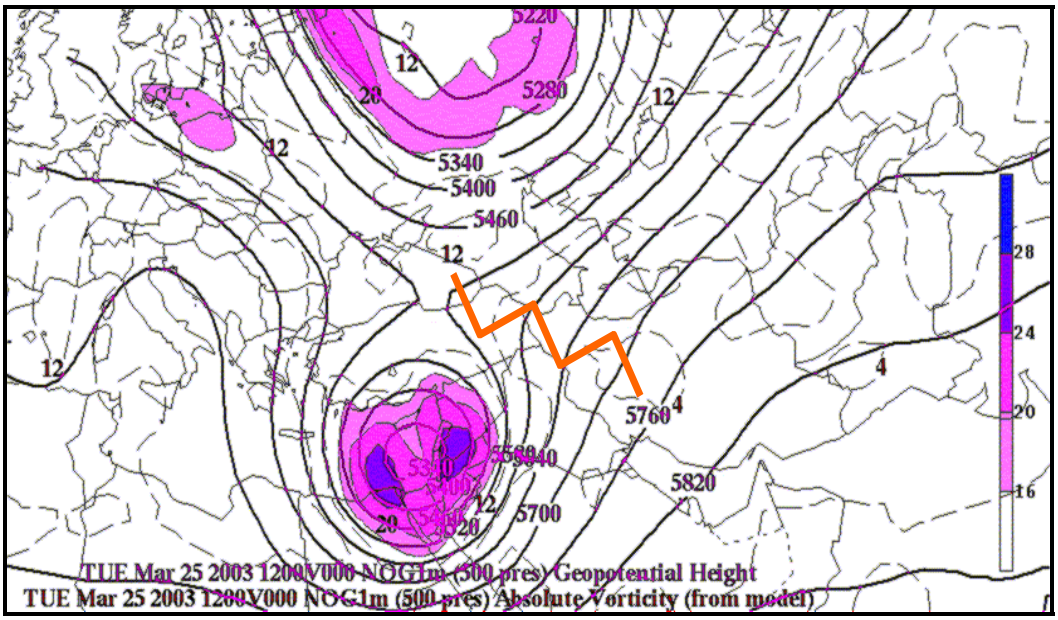

Figure 3.27. 500mb Height (m) & Absolute Vorticity (10^{-5} /sec): 1200 GMT, 25 March 2003.

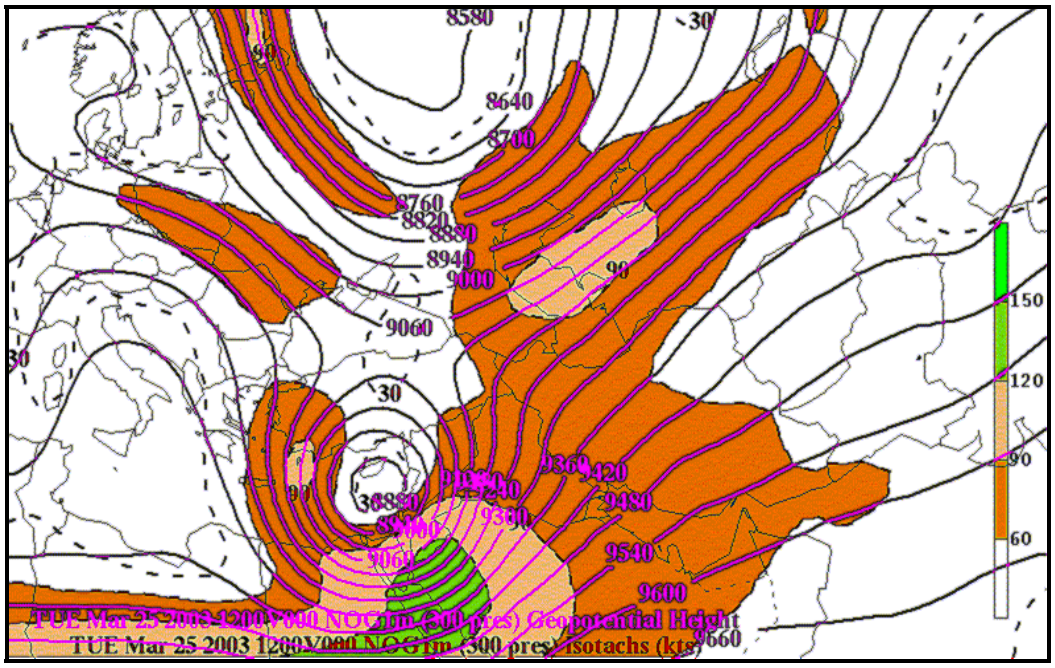

Figure 3.28. 300 mb Height (m) & Winds (kts): 1200 GMT, 25 March 2003.

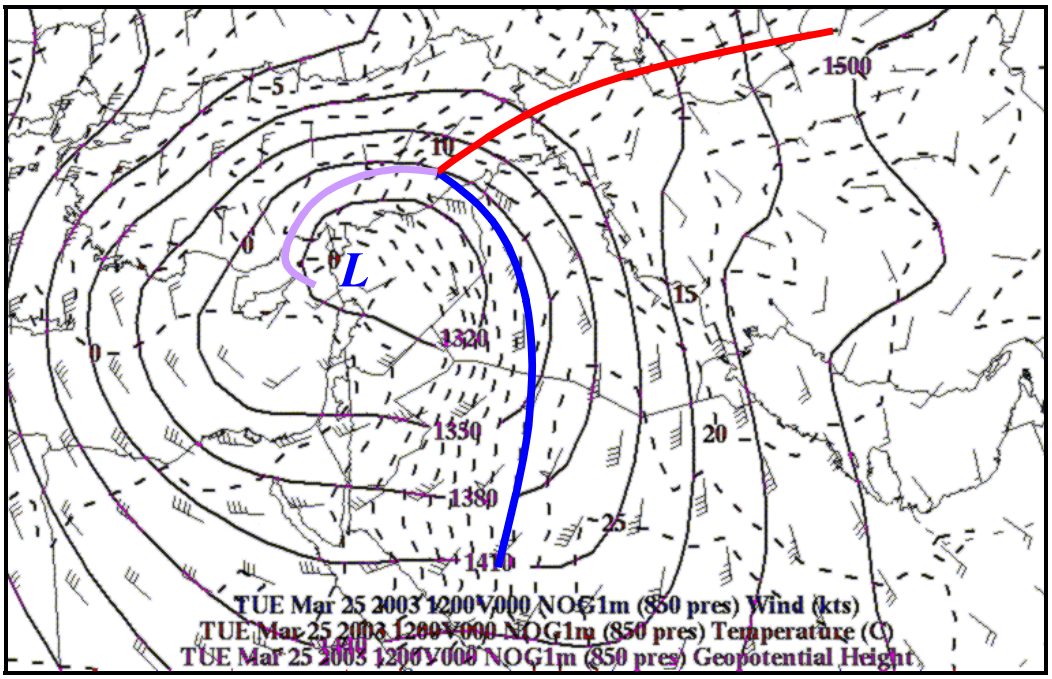

Figure 3.29. 850 mb Height (m), Temperature (°C) & Winds (kts): 1200 GMT, 25 March 2003. Magenta line represents an occluded front; blue and red lines represent cold and warm fronts respectively.

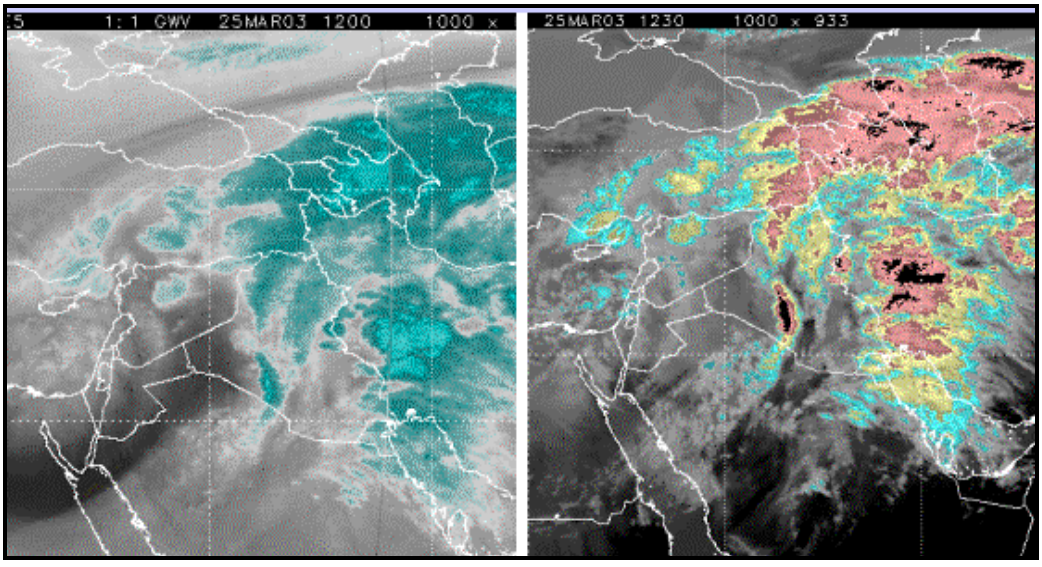

Figure 3.30. METSAT Water Vapor (left) & IR images (right): 1200 GMT, 25 March 2003. (From: Finta 2004a)

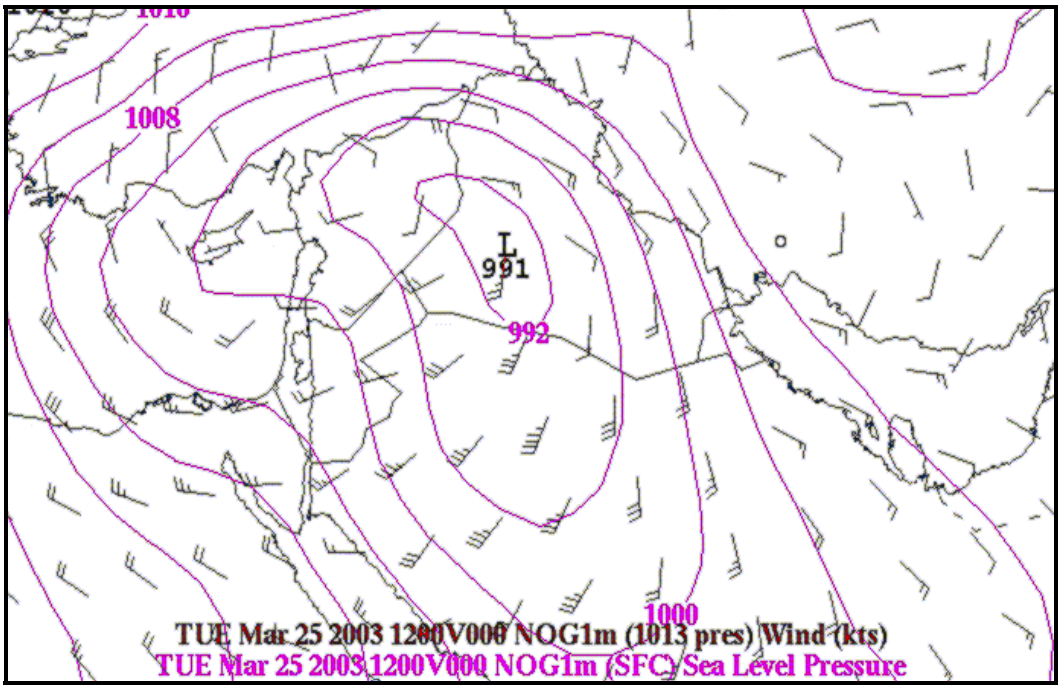

Figure 3.31. Sea-Level Pressure (mb) & Winds (kts): 1200 GMT, 25 March 2003.

one-half statute mile. At the same time, however, Kuwait International Airport only reports southeasterly winds at 9 knots and light thunderstorm activity (Finta 2004a).

F. 26 MARCH 2003

From 1200 GMT on the 25th to 0000 GMT on the 26th, the 500 mb low center shifts rapidly northeastward, crossing inland and centering over central Syria. The 300 mb pattern shows little change other than shifting inland and aligning vertically with the 500 mb pattern. The 850 mb low center deepens to 1280 m, but remains relatively stationary over northwestern Syria, just slightly to the northwest of the upper level low centers. This slight southeastward stacking of the system, shown in Figure 3.32, becomes the first indication of system decay.

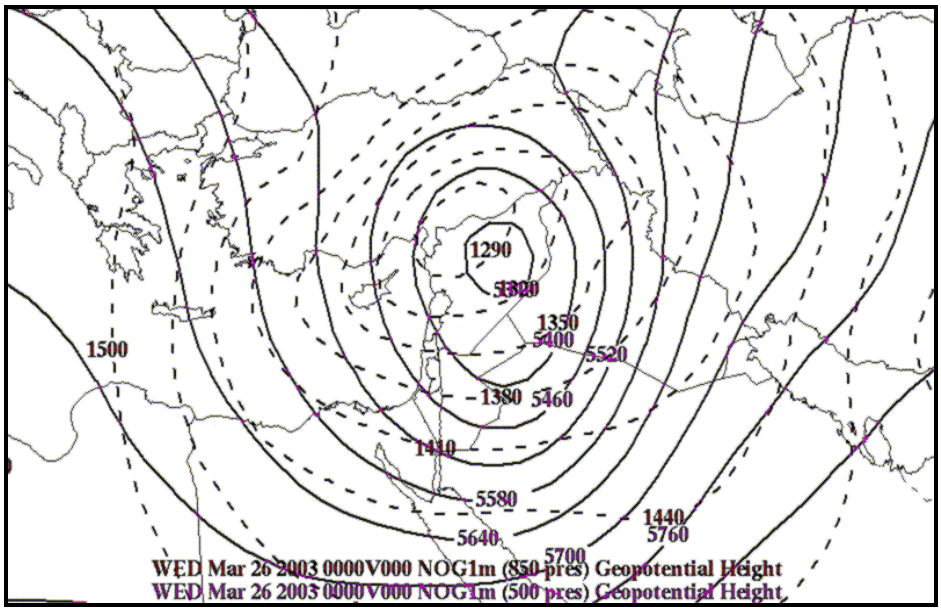

Figure 3.32. 500 mb Height (m) (Solid Lines) & 850 mb height (m) (Dashed lines): 0000 GMT, 26 March 2003.

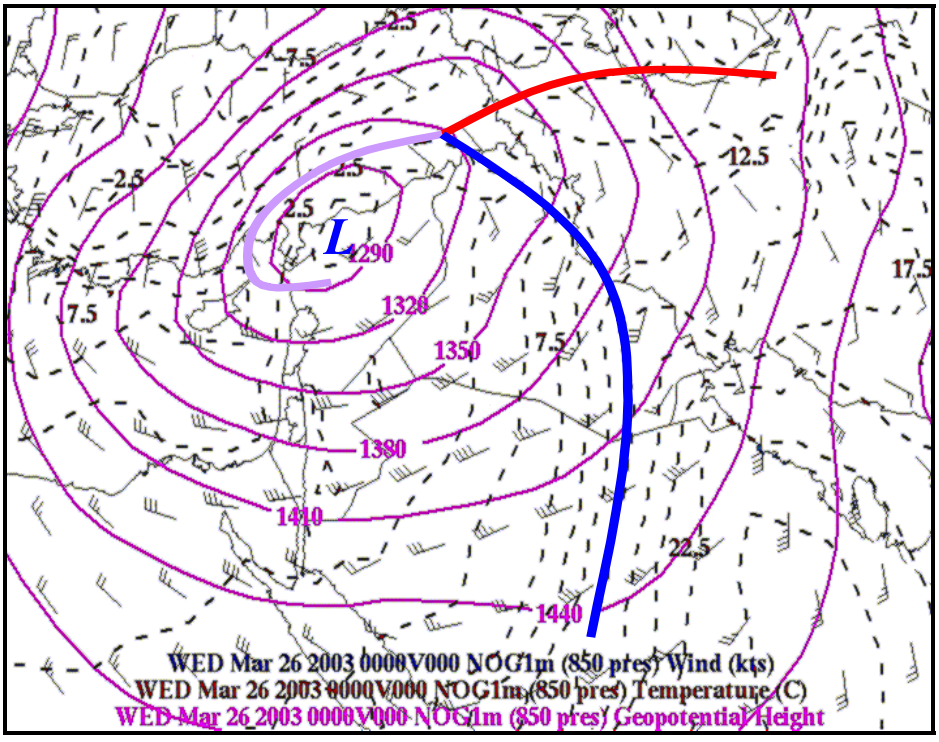

Figure 3.33. 850 mb Height (m), Temperature (°C) & Winds (kts): 0000 GMT, 26 March 2003. Magenta line represents an occluded front; blue and red lines represent cold and warm fronts respectively.

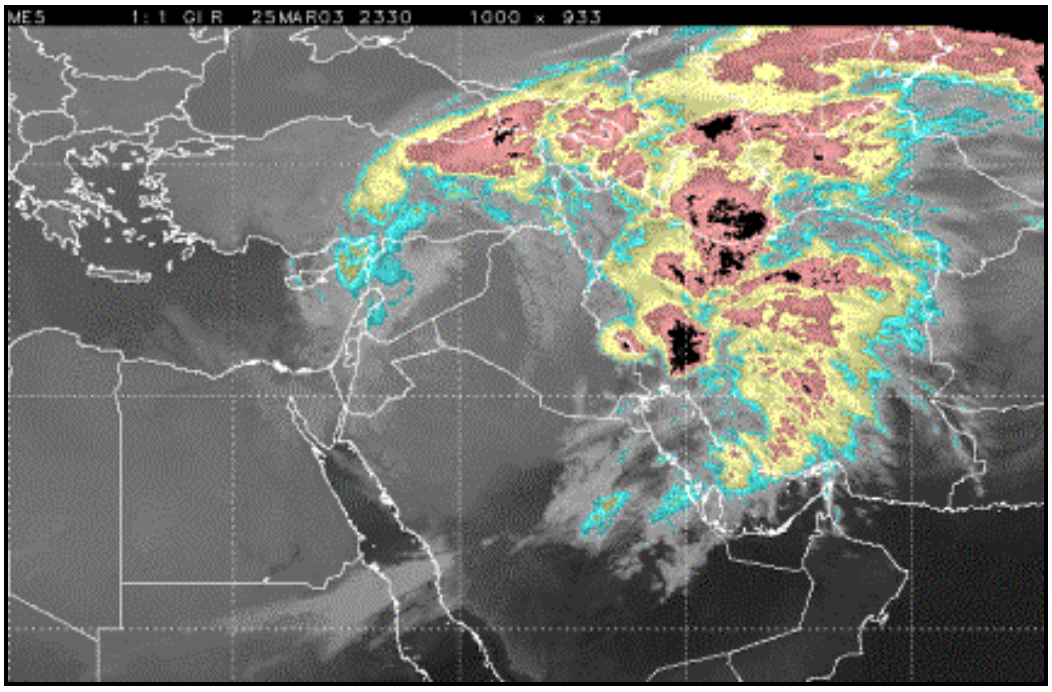

Figure 3.34. METSAT IR Image: 0000 GMT, 26 March 2003 (From: Finta 2004a)

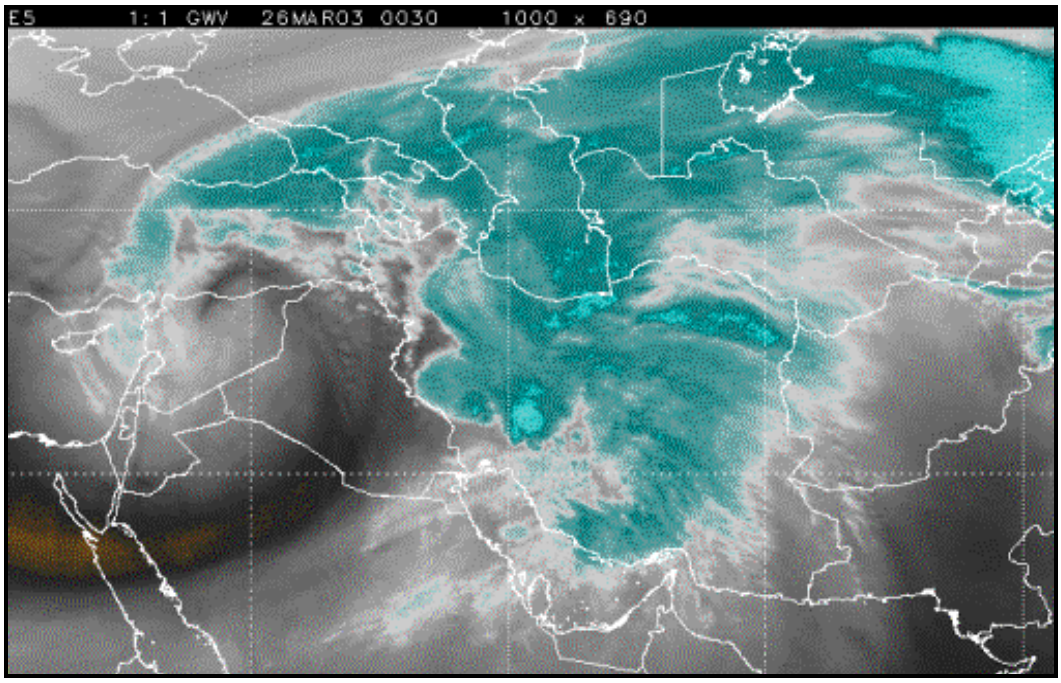

Figure 3.35. METSAT Water Vapor Image: 0000 GMT, 26 March 2003. (From: Finta 2004a)

As shown in Figure 3.33, the cold front passes almost completely through Iraq, with only the eastern most portion of the country under the thermal ridge ahead of the front. Post-frontal winds at 850 mb shift to a west/southwest direction in the northern regions of Saudi Arabia, with wind speeds averaging approximately 40 knots.

This analysis once again verifies very well in the 0000 GMT METSAT IR imagery (Figure 3.34). The lighter shade of gray in the post-frontal region across northern Saudi Arabia and central Iraq, shown in Figure 3.34 indicates the strong presence of atmospheric dust, having been lifted from the surface and cooled, relative to the warmer dark gray/black regions in southern Saudi Arabia. Figure 3.35, the water vapor image from the same time, confirms this analysis, showing the post-frontal "dry tongue" stretching across the same region.

The surface chart for 0000 GMT, 26 March (Figure 3.36) shows a large region of 15-20 knot westerly winds in northern Saudi Arabia, and southern Iraq. When compared to the approximately 40 knot winds at 850 mb, continues to suggests the presence of significant boundary layer mixing, which contributes to the overall lofting and suspension of dust and sand in that region.

At 0000 GMT, 26 March, Prince Sultan AB reports southwesterly winds at 12 knots gusting to 22 knots, with no mention of dust or restrictions to visibility. At the same time, Kuwait International Airport reports southeasterly winds at 20 knots, with light blowing dust limiting visibility only to 7000 meters.

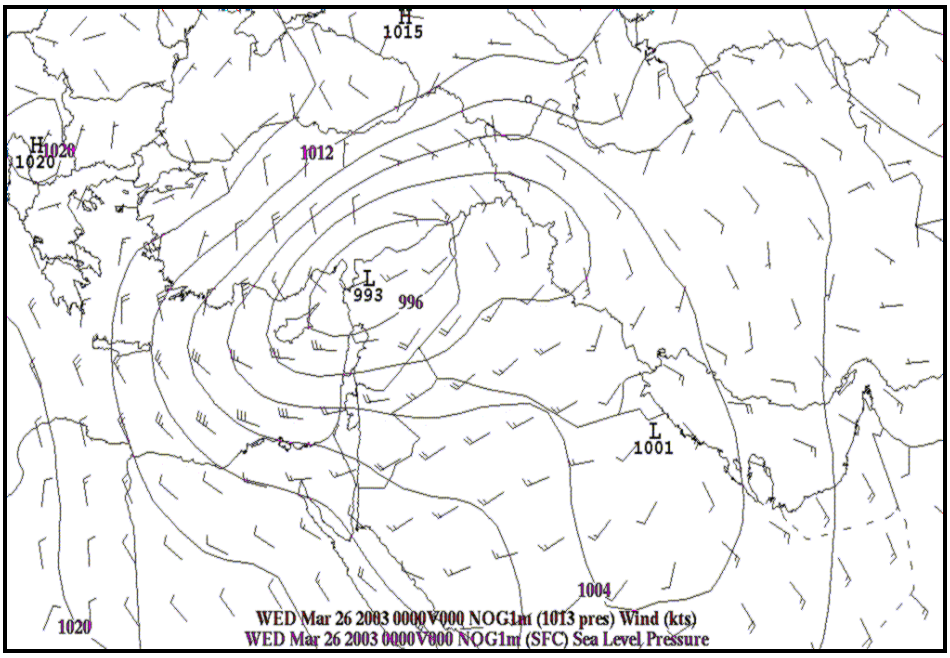

Figure 3.36. Sea-Level Pressure (mb) & Winds (kts): 0000 GMT, 26 March 2003.

By 1200 GMT on the 26th, the 500 mb trough continues to march eastward into northern Iraq, and begins to fill in. At 300 mb, the subtropical jet shows a sign of shifting to a more zonal flow pattern once again as it weakens to 90 knots. The upper-level trough begins to lift out towards the Caspian basin northeast of the AOR (Figure 3.37).

During the 12 hour period prior to 1200 GMT, a secondary low at 850 mb forms over northern Iran, and the low that was previously the transiting cyclone shifts northeast and fills in to 1380 m (Figure 3.38). At that particular time, the cold front passes into the central Arabian Gulf and a ridge of relative high pressure, typical following a cold frontal passage, builds over most of Iraq. The southwesterly winds across northern Saudi Arabia begin to weaken once again, averaging approximately 30 knots.

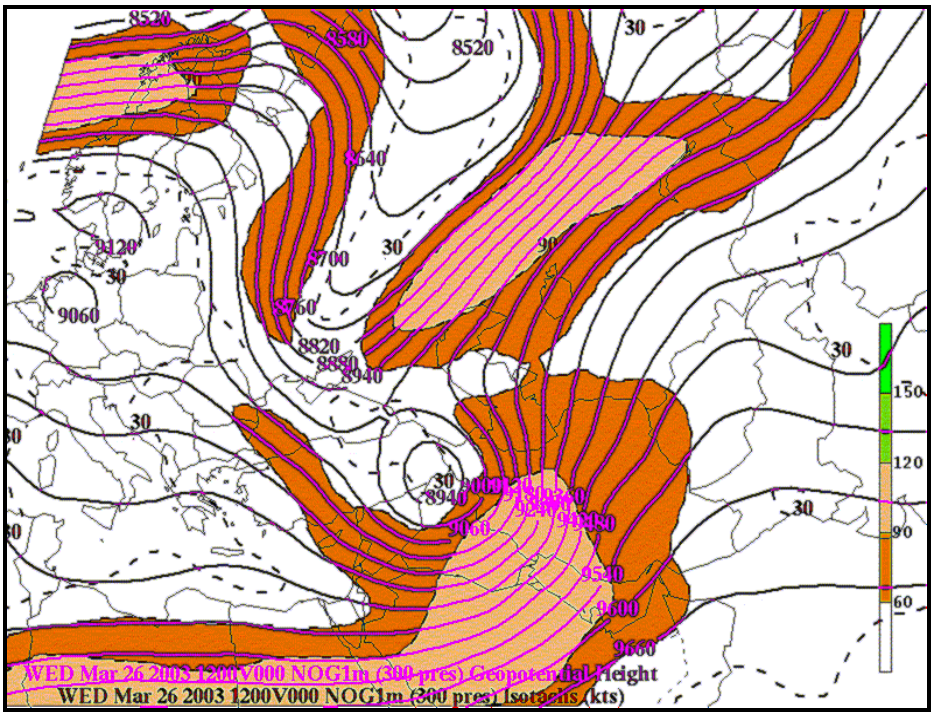

Figure 3.37. 300 mb Height (m) & Winds (kts): 1200 GMT, 26 March 2003.

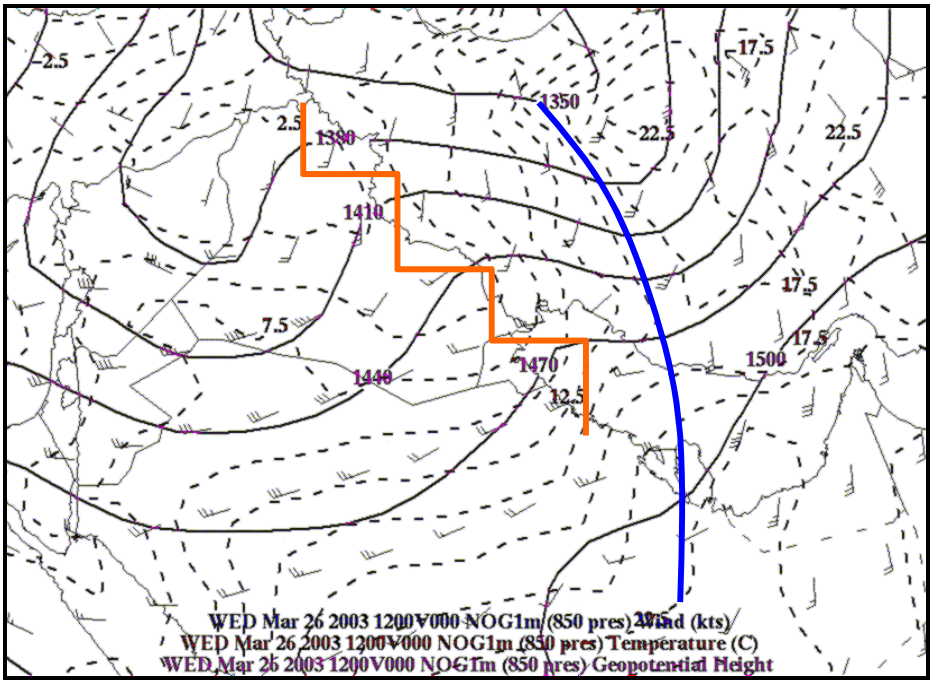

Figure 3.38. 850 mb Height (m), Temperature (°C) & Winds (kts): 1200 GMT, 26 March 2003. Orange zig-zag represents the low level ridging behind the cold front represented by the blue line.

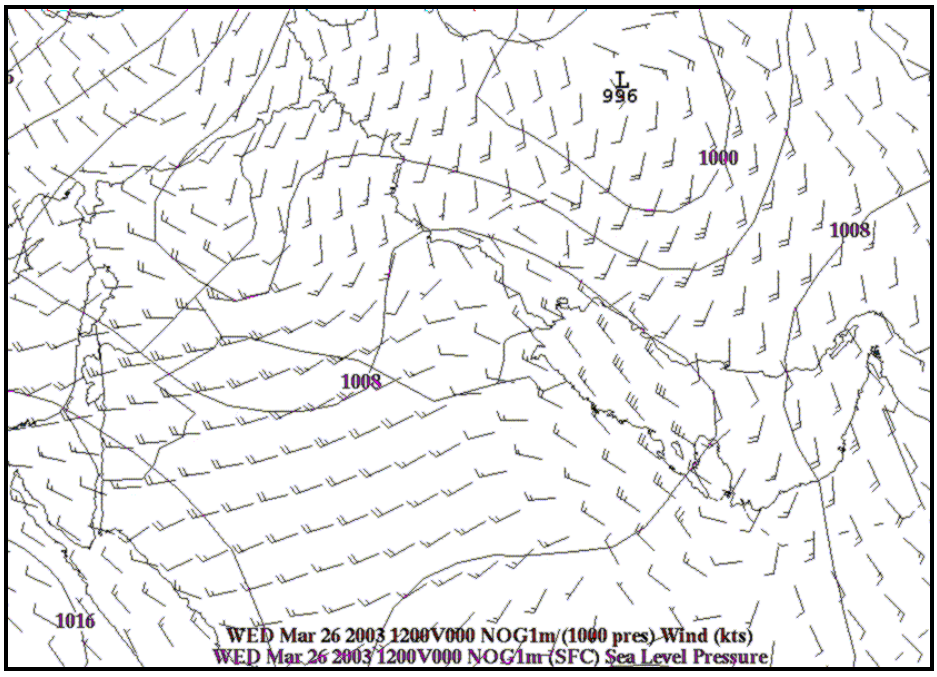

Figure 3.39. Sea-Level Pressure (mb) & Winds (kts): 1200 GMT, 26 March 2003.

At the surface, the winds sweep westerly across northern Saudi Arabia and into Iraq at an approximate average of 20 knots. Figure 3.39 shows the relative high pressure system that builds over Kuwait in the wake of the passing cold front. The winds at 850 mb are still strong enough to advect the airborne dust into central Iraq. However, the increase in surface winds, coupled with relatively strong winds at the 850 mb level lead to a decrease in boundary layer mixing. This effect combined with the subsidence created by the high pressure in the front's wake aid in the settling of dust south of the Iraq/Saudi Arabia border.

This analysis is confirmed in the 1200 GMT, 26 March METSAT IR image shown in Figure 3.40. The image shows a large dark region of relatively warm temperatures south of the Iraq/Saudi Arabian border. To the north, the lighter

gray shaded region encompassing almost all of Iraq suggests the presence of a significant amount of atmospheric dust, still suspended in the atmosphere, obscuring most of the surface features. Figure 3.40 also confirms the presence of the trough over the Iraq/Syria border, as shown in Figure 3.39, which is the remnant of the cyclone that is now lifting out of the AOR. However, while the cyclone itself is lifting out of the region, the post-frontal dust storm is reaching its maximum intensity.

Prince Sultan AB, located in the tail end of the comma cloud in Figure 3.40, reports northerly winds at 21 knots, gusting to 26 knots. The visibility is reported as 100 meters in heavy blowing dust. Strong winds aloft in this region are able to carry the dust far out into the NAG.

At Kuwait International Airport, the situation is a little different. The winds there are reported as northwesterly at 14 knots. The visibility is better at 800 meters and the obscuring phenomenon is listed as haze, rather than dust (Finta 2004a).

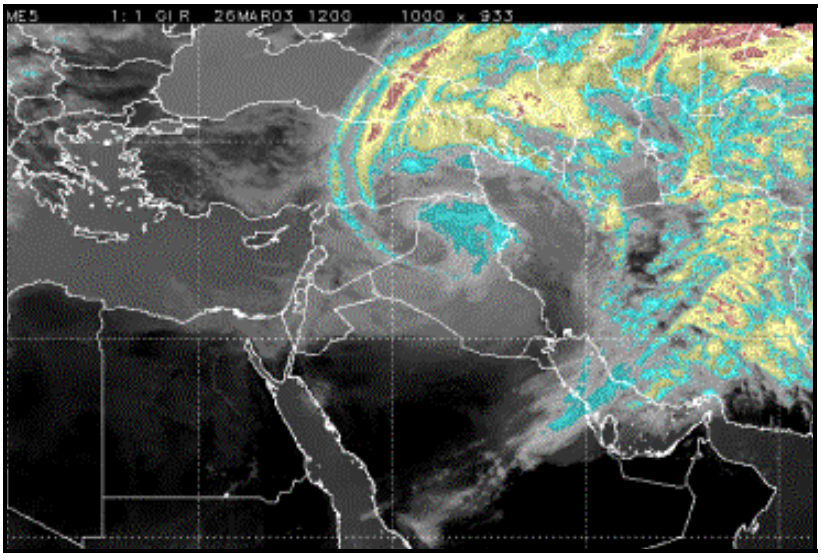

Figure 3.40. METSAT IR Image: 1200 GMT, 26 March 2003. (From: Finta 2004a)

G. 27 MARCH 2003

By 0000 GMT on 27 March, the 500 mb trough finally lifts out to the Caspian basin. The upper-level flow at 300 mb returns to mostly zonal across the AOR, before turning northeastward over the Arabian Gulf (Figure 3.41). The 850 mb analysis field places the remnant low pressure system over the Caspian Sea, with a weak trough axis extending through northern Iran, Iraq, reaching to Israel (Figure 3.42). The 0000 GMT METEOSAT IR image, shown in Figure 3.43, shows significant clearing behind the remnant of the cold front, which still extends across the central Arabian Gulf.

As of 0000 GMT, Prince Sultan AB still reports northeasterly winds at 11 knots and dust, but the visibility has improved to 4000 meters. Kuwait International Airport reports light winds and sky clear conditions, with 3000 meters visibility in light haze (Finta 2004a).

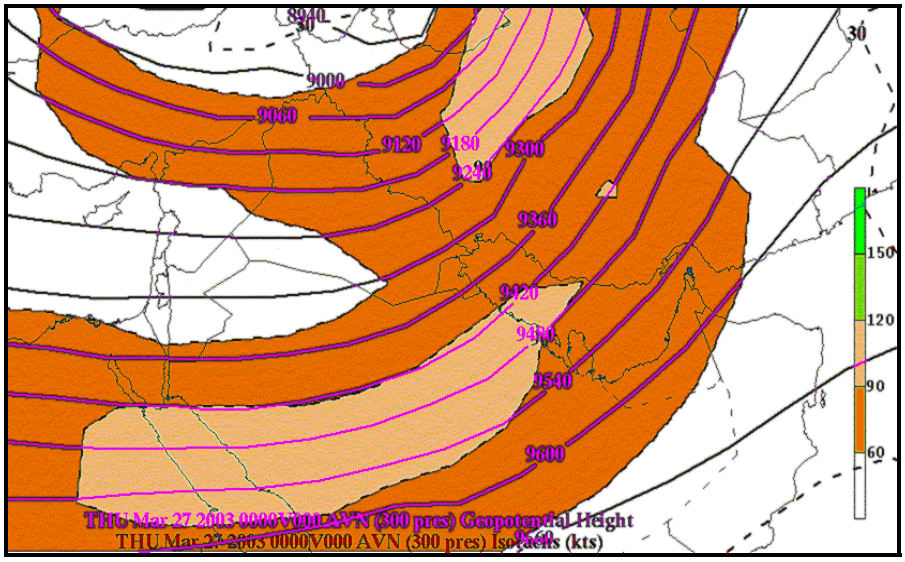

Figure 3.41. 300 mb Heights (m) & Winds (kts):0000 GMT, 27 March 2003.

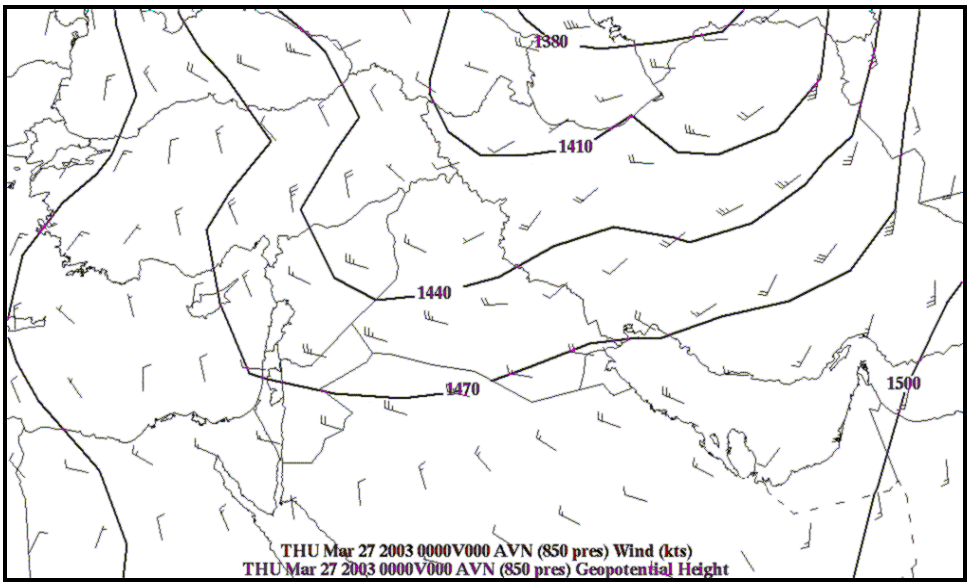

Figure 3.42. 850 mb Heights (m) & Winds (kts): 0000 GMT, 27 March 2003.

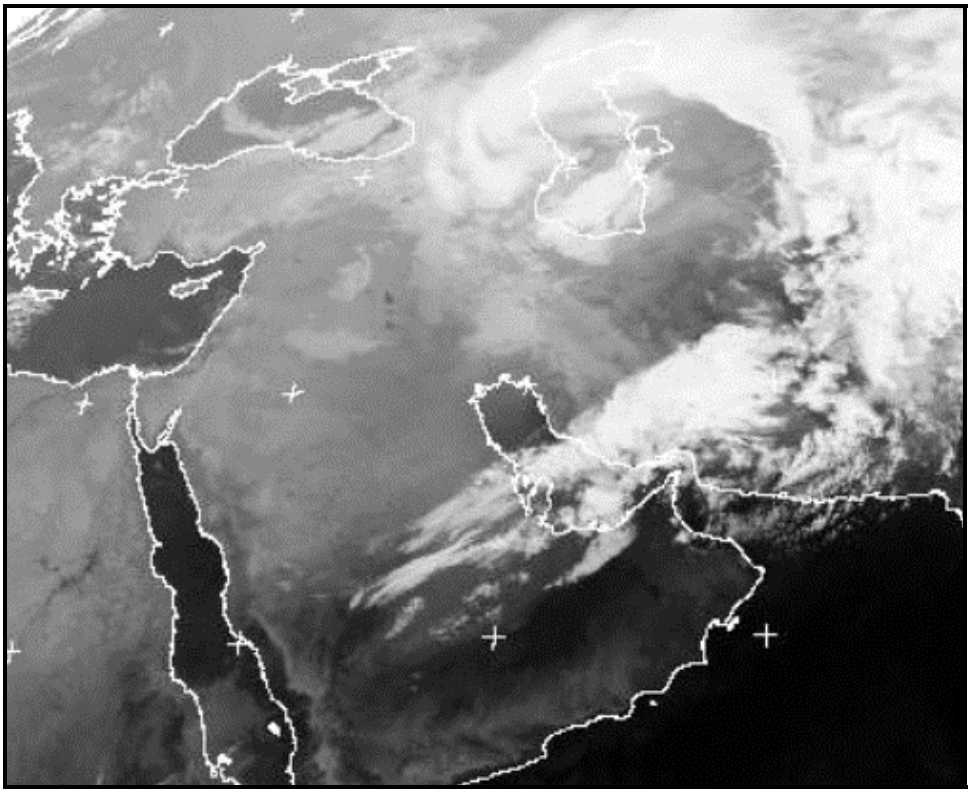

Figure 3.43. METEOSAT IR Image: 0000 GMT, 27 March 2003. (From: Finta 2004, courtesy of EUMETSAT: http://www.eumetsat.de/)

On 27 March, conditions across the AOR continue to improve throughout the day. The dust continues to advect out of the region or settle out of the air as the frontal system kicks out to the northeast of the Caspian Sea. And with that, the "Mother of All Fronts" (Finta 2004a) is over.

H. STORM SUMMARY AND CONCLUSIONS

In summary, this particular case could be considered a textbook example of a well defined winter shamal event. A large scale synoptic trough, develops over Turkey and the Black Sea on 22 March, 2003. The trough deepens, and digs into the eastern Mediterranean, intensifying in the process. Over the course of the next 5 days, it sweeps across the Southwest Asia AOR. In its wake, it initiates a major dust storm that severely impacts the theater of operations in the critical fist days of Operation IRAQI FREEDOM.

However, there is major difference in this case. Clearly the short-wave feature that works its way across the northern regions of Africa and ties in with the main surface low pressure system strengthens the overall effect of the system. Without this additional disturbance, a dust storm would still likely develop in the other existing environmental conditions. The short-wave disturbance however is an important component of the strong intensification of the storm observed in the AOR. The models and satellite imagery performed well in capturing this feature. In the next section, an overall analysis of model performance in providing forecasters with guidance will be conducted.

IV. MODEL PERFORMANCE

A. IN-DEPTH LOOK AT THE FNMOC STUDY

In conducting a study of model performance with respect to the forecasting of this particular dust event, it is appropriate to start with a summary of the work already accomplished by the FNMOC Model Verification team (FNMOC 2004). In March of 2004, FNMOC released the only comprehensive study found at the time of this writing that deals with shamal events in SWA for the period encompassing the time domain immediately prior to, during, and immediately following the commencement of Operation IRAQI FREEDOM. For purposes of their case study, the FNMOC model validation team (FNMOC 2004) defines a shamal wind as a wind with a northerly component greater than 20 knots in magnitude.

The FNMOC (2004) paper conducts a validation study of GFS, NOGAPS, and COAMPS for a time period from February to April of 2003. During this period, three large scale shamal events passing through the region are recorded and used in the validation. In general, the FNMOC study breaks the verification into objective and subjective analyses. The objective part applies quantitative biases and root means square (RMS) errors to score the overall model performance. The subjective part is a qualitative analysis of the gridded model output fields to determine trends, errors, and tendencies (FNMOC 2004).

For the FNMOC (2004) study, the meteorological data for the entire period is analyzed to determine individual model tendencies relative to the model's own analysis and observations. 12-hour forecast cycles are used, starting

at the 0000 and 1200 GMT model runs. The analysis fields represent the initial conditions of the atmosphere at the start of the following model run while the observations represent a benchmark of the true atmospheric state (FNMOC 2004).

The three shamal events studied in the paper are 20-25 February 2003, 25-27 March 2003 and 02-08 April 2003. In all cases, the three models identify strong post-frontal northwesterly winds that match the applied shamal criteria, i.e., 20 knots with a northerly component. The objective verification is carried out by comparing the model forecast winds to surface observations from civilian airports, stations and surface ships, received by FNMOC every 6 hours (FNMOC 2004). Quality screening of the data allows for the rejection of reports containing erroneous or unrealistic data. Both NOGAPS and GFS are run at approximately 50 km grid-spacing, and the data is bilinearly interpolated to the station observation location to create a basis for comparison at the 12-hourly output forecast times (FNMOC 2004). According to FNMOC (2004), the COAMPS Southwest Asia regional model uses a nest-2 grid with 18 km resolution extending out to the 80 hour forecast, and a nest-3 grid with 6 km resolution carried out to 30 hours. COAMPS forecast winds are also interpolated to the observation points every 6 hours in the verification process (FNMOC 2004).

1. Objective Verification

The objective part of the FNMOC (2004) evaluation of model performance begins with a look at forecast-minus-analysis mean tendencies for NOGAPS in the Eurasian continent (20°-60° N, 0°-130° E). Table 4.1, taken from the

FNMOC (2004) report, shows values for NOGAPS biases and RMS errors in the 500 and 1000 mb wind speeds, geopotential heights, and temperatures all averaged over the entire time domain.

Their results reveal that the NOGAPS 500 mb wind speed, height and temperature biases are negative, as is the 1000 mb wind speed and temperature biases. Only the 1000 mb height bias is positive. The wind speed biases hold relatively constant at all forecast lengths at both 500 and 1000 mb, as does the 1000 mb height bias (FNMOC 2004). The 500 mb height bias and the temperature biases at both 500 and 1000 mb exhibit a slight increasing trend with forecast length (FNMOC 2004). At both 500 and 1000 mb levels, all forecast fields exhibit RMS errors that generally increase approximately linearly with forecast length. The slope of the linearity varies with the forecast field being considered.

Tau	24	48	72	120
Wind Speed (ms^{-1})				
500 mb BIAS	-0.10	-0.18	-0.15	-0.19
500 mb RMSE	2.23	3.57	4.67	6.36
1000 mb BIAS	-0.22	-0.24	-0.24	-0.24
1000 mb RMSE	1.52	1.83	2.08	2.44
Geopotential Height (m)				
500 mb BIAS	-3.15	-6.96	-9.81	-11.56
500 mb RMSE	11.86	21.21	30.05	49.97
1000 mb BIAS	1.73	1.55	1.15	1.83
1000 mb RMSE	13.60	20.75	26.48	38.53
Air Temperature (K)				
500 mb BIAS	-0.26	-0.41	-0.50	-0.58
500 mb RMSE	0.79	1.34	1.81	2.65
1000 mb BIAS	-0.24	-0.37	-0.49	-0.64
1000 mb RMSE	2.31	2.95	3.31	3.83

Table 4.1. NOGAPS forecast minus analysis differences for Eurasian continent. Data from 3 case studies between 1 February, 2003 and 30 April, 2003. (From: FNMOC 2004).

For comparison, COAMPS Southwest Asia bias and RMS errors relative to the model's own analysis are tabulated in Table 4.2 (FNMOC 2004). Like NOGAPS, the temperature biases at both 500 mb and close to the surface are negative. However, the COAMPS temperature bias at 48 hours is approximately two times greater in magnitude at 500 mb than NOGAPS. FNMOC's results also generally reveal that COAMPS tends to forecast low pressure systems too deep, but without necessarily translating that anomalous low into higher than observed wind speeds (FNMOC 2004).

Table 4.2 shows that the COAMPS wind speed bias scores obtained by FNMOC (2004) are fairly small and vary in sign, depending on whether over land or sea. RMS errors in wind speeds remain relatively constant with forecast length, independent of surface type. The other forecast fields exhibit some degree of increase in RMS error with increasing forecast tau. According to FNMOC (2004), the tendency for COAMPS to be too deep with mid-latitude

Tau	24		48	
Wind Speed (ms^{-1})	Bias	RMS	Bias	RMS
Sfc land $ff_{10\,m}$	0.97	3.39	1.09	3.55
Ship $ff_{10\,m}$	-0.78	3.67	-0.74	3.95
Raob $ff_{925\,mb}$	-0.06	3.37	0.06	3.77
Geopotential Height (m)				
$Ht_{500\,mb}$	-29	36	-41	50
$Ht_{1000\,mb}$	-5.4	28	-6.6	33
Air Temperature (K)				
$T_{500\,mb}$	-0.4	1.5	-1.0	2.0
$T_{2\,m}$	-3.1	5.1	-3.0	5.4
Pressure (mb)				
Sea Level Pressure	-1.5	3.7	-1.9	4.5

Table 4.2. COAMPS Southwest Asia model forecast errors for 1 February, 2003 through 30 April, 2003. (From: FNMOC 2004).

cyclones is well documented on their model characteristics and tendencies web page (https://www.fnmoc.navy.mil/).

No tabulated data, similar to that of Tables 4.1 or 4.2, of GFS performance relative to its own analyses is provided in the report. However, FNMOC (2004) does verify GFS 10-meter wind speed forecasts against station observations to assess the GFS wind speed biases and compares them to NOGAPS. This comparison is graphically illustrated in Figure 4.1, taken from the FNMOC (2004) report. Over the entire 3 month period, the GFS wind speed forecast tends towards a bias of approximately 1.5 knots too fast at 12 hours, with a general slight increase in the bias out to 120 hours (FNMOC 2004). By comparison, the NOGAPS tendency is for wind speeds approximately 0.5 knots too slow, with the bias remaining constant from tau-0 to tau-120 (FNMOC 2004).

For additional comparison, the 10 meter wind speed bias for COAMPS at 18 km resolution, averaged over the entire period, is shown in Figure 4.2. This figure, also from FNMOC (2004), shows a bias of approximately 1.5 knots too fast, remaining relatively constant throughout the time domain. The saw-tooth pattern in Figure 4.2 can be attributed to systematic biases associated with the diurnal cycle (FNMOC 2004). These biases tend to cancel each other out at 0000 and 1200 GMT and tend to be additive at 0600 and 1800 GMT (FNMOC 2004). Figure 4.3 shows the wind speed bias for the 6 km COAMPS data (FNMOC 2004). This figure shows a similar saw-tooth pattern, but with an improved average wind speed bias of approximately 0.75 knots too fast.

When the shamal criteria are applied to the data, which limits the sample size to the three shamal events listed above, FNMOC (2004) finds that the biases increase in magnitude dramatically. They state that NOGAPS tends to under-forecast winds by 14-16 knots and GFS under-forecasts them by 12-14 knots. COAMPS exhibits the widest spread, under-forecasting winds by 12-18 knots (FNMOC 2004). These results are shown graphically in Figures 4.4 and 4.5 and represent averaged values over all three shamal events.

The tendency for slow wind speed forecasts during shamal events will be verified against METAR observations in the central Arabian Peninsula at 1200 GMT, 25 March in the subjective analysis of section C of this chapter. In general, we shall see that the subjective analysis for the particular date chosen agrees well, at least qualitatively, with the assertions made by FNMOC. The agreement is especially good near the cold frontal region of the passing synoptic cyclone.

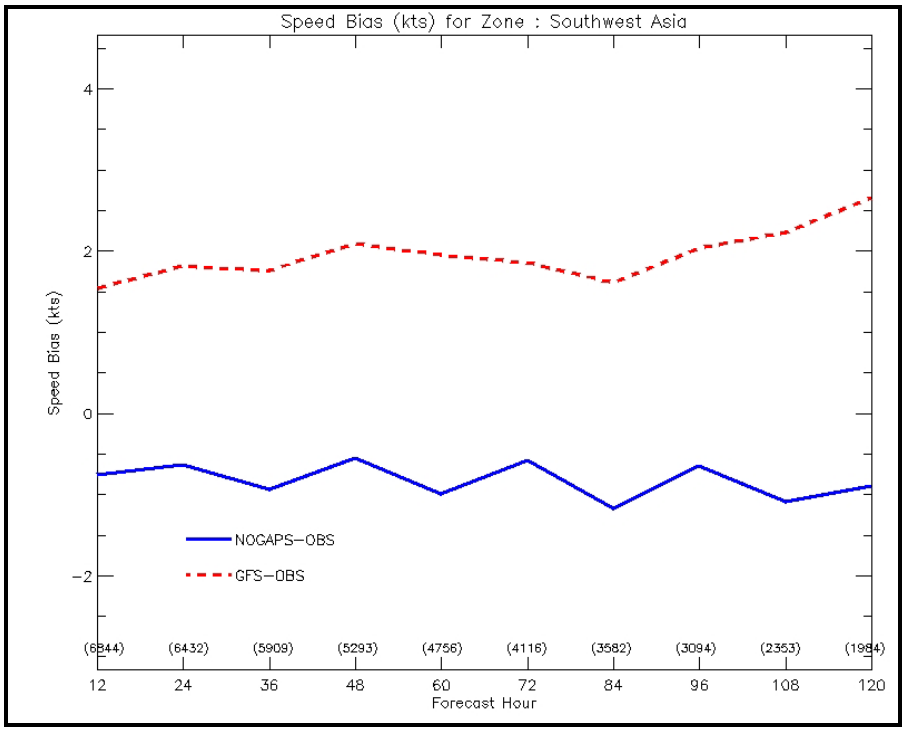

Figure 4.1. NOGAPS and GFS wind speed biases averaged over period from 1 February, 2003 to 30 April, 2003. (From: FNMOC 2004)

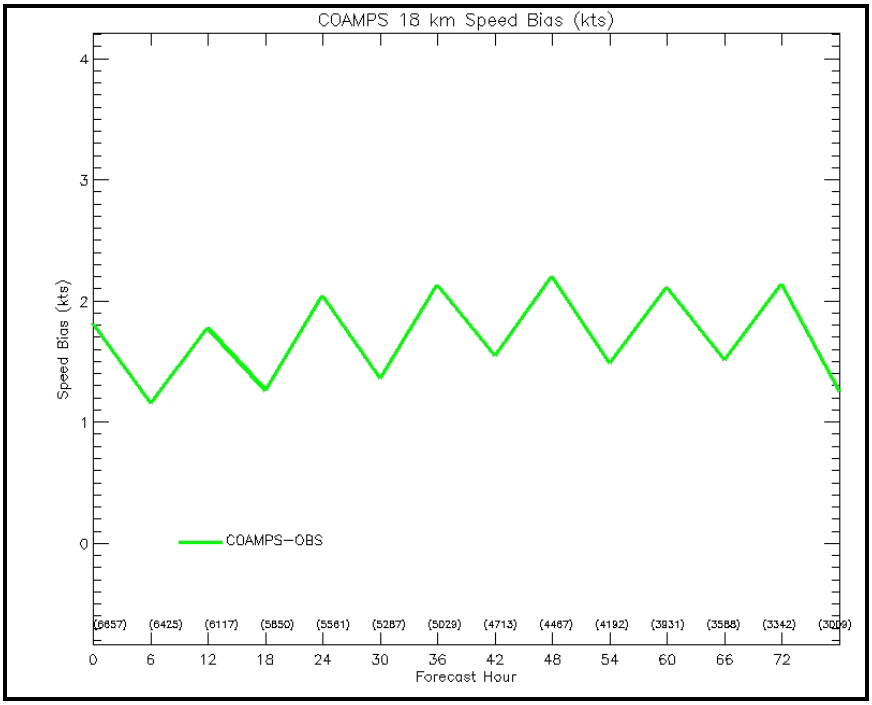

Figure 4.2. COAMPS 18 km wind speed biases averaged over period from 1 February, 2003 to 30 April, 2003. (From: FNMOC 2004)

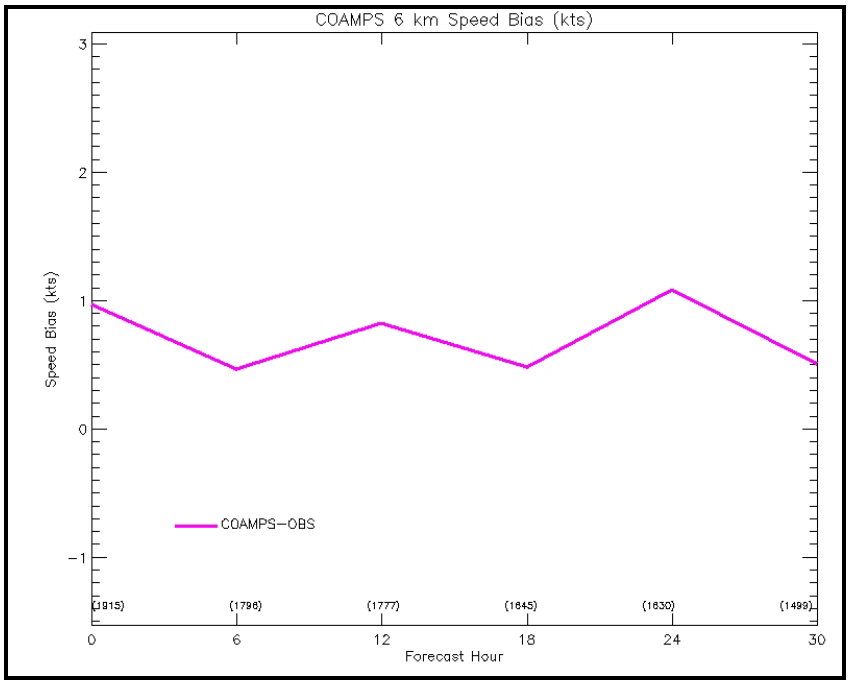

Figure 4.3. COAMPS 6 km wind speed biases averaged over period from 1 February, 2003 to 30 April, 2003. (From: FNMOC 2004)

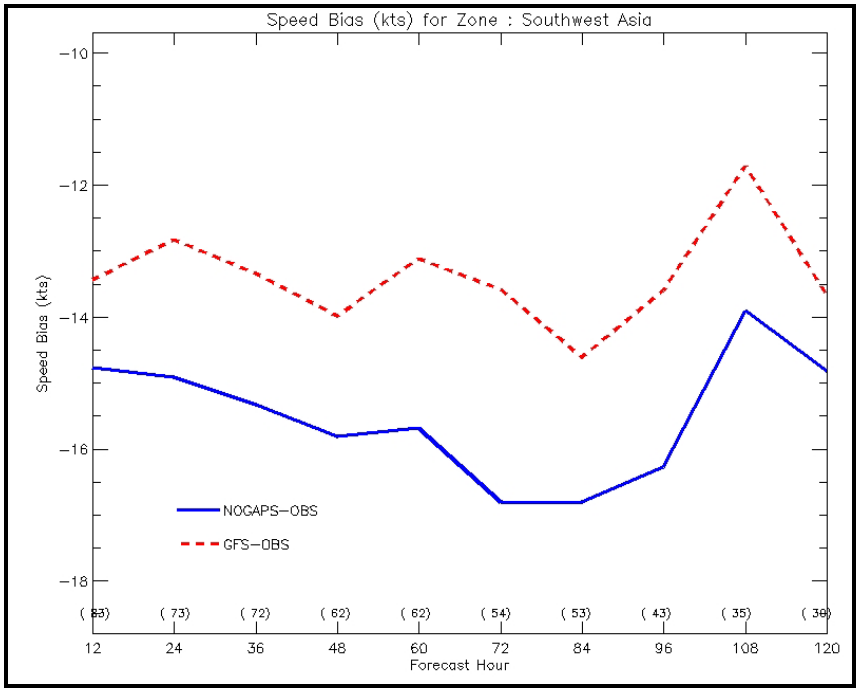

Figure 4.4. NOGAPS and GFS wind speed biases for data limited to the three shamal cases studied. (From: FNMOC 2004)

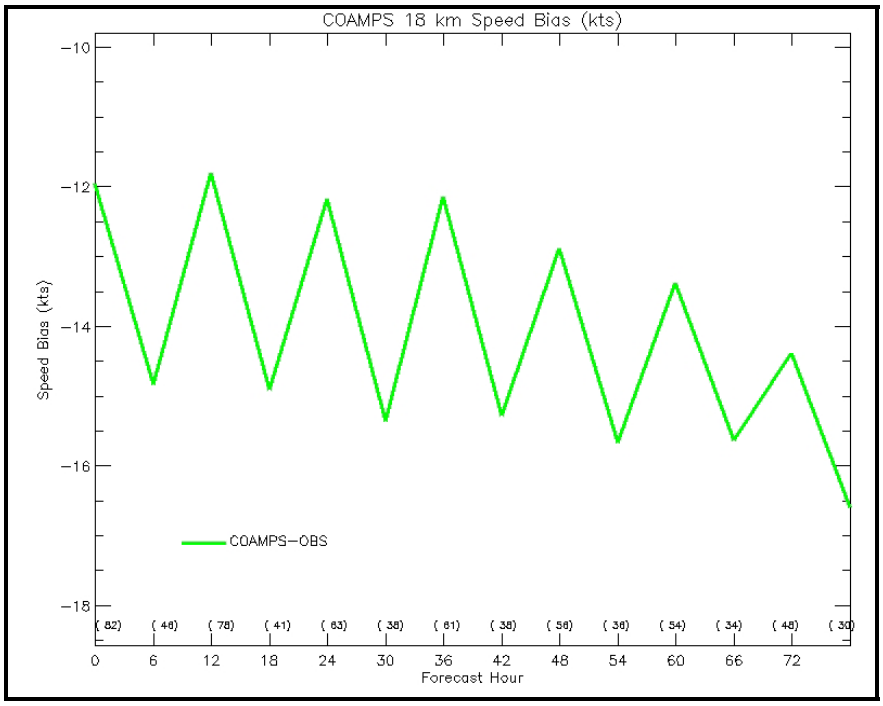

(A)

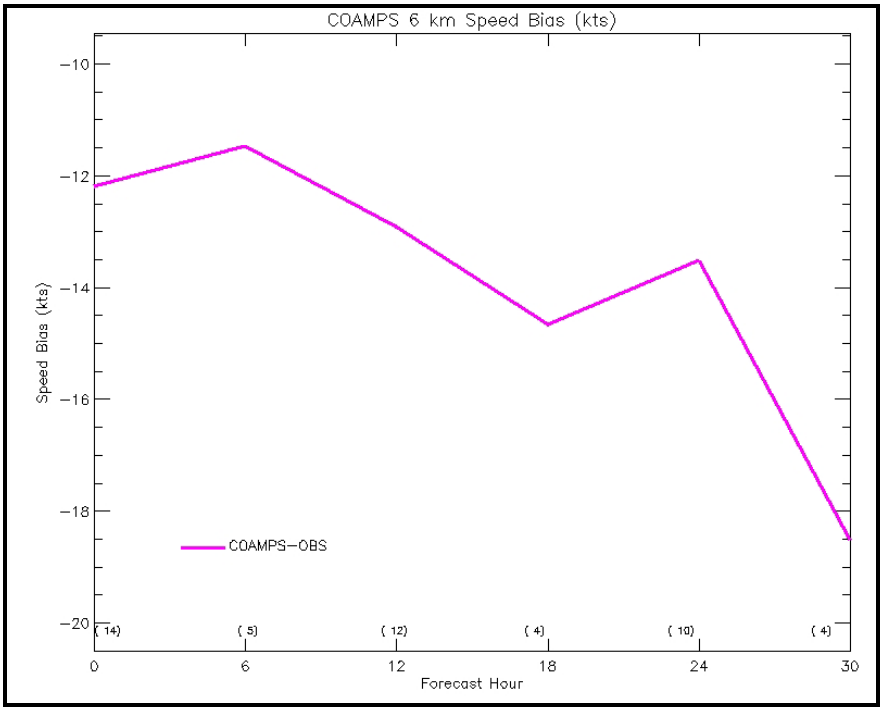

(B)

Figure 4.5. COAMPS wind speed biases for data limited to the 3 shamal cases studied. (A) 18 km resolution and (B) 6 km resolution. (From: FNMOC 2004)

2. Subjective Case Study: 25-27 MARCH 2003

For the 25-27 March, 2003 shamal event analyzed in this thesis, the FNMOC (2004) paper also performs a qualitative/subjective analysis of the numerical weather prediction model performance. As a more detailed subjective analysis will follow in the next section, the results obtained by FNMOC will only be summarized here.

The FNMOC (2004) verification is conducted by overlaying the forecast and analysis fields for 500 mb height, 1000 mb winds and METAR observations for the 1200 GMT, 25 March 2003 verifying time of the forecast. The verification is carried out to the 72-hour forecast for GFS and NOGAPS, and the 48-hour forecast for COAMPS.

According to FNMOC (2004), GFS exhibits the best skill in placement of the 500 mb trough center, and subsequently provides the best guidance as to the onset of wind-induced dust and sand storms. They also state that NOGAPS is fast, placing the 500 mb trough approximately 200 km to the southeast of the verifying position at 1200 GMT, 25 March 2003 (FNMOC 2004).

Their analysis also indicates wind speeds at 1000 mb vary from model to model. GFS is stated to exhibit a tendency to over-forecast winds by 5 knots over large parts of the AOR at both 48 and 72 hours (FNMOC 2004). They also find that NOGAPS is weak by approximately 5-10 knots over the same area at 72 hours.

The COAMPS 24 and 48 hour forecasts for 1200 GMT, 25 March 2003 are said to provide very good guidance to forecasters (FNMOC 2004). FNMOC (2004) states that the intensity of the COAMPS 500 mb trough and 925 mb wind

strengths are well forecast out 48 hours. They state that the model has a slightly fast displacement of the 500 mb trough, and 925 mb winds are slightly weak in northeastern Saudi Arabia/southern Iraq (FNMOC 2004).

B. VERIFICATION OF 500 MB HEIGHT FIELD FORECASTS

In studying the forecast details of the dust storm that hits the AOR on 25-27 March 2003, a qualitative look at the 500 mb trough reveals how the models performed in forecasting the upper level features. For purposes of this case study, the forecast verification time is chosen to be 1200 GMT, 25 March 2003. This verification time represents well the approximate time that dust storms began or were already underway in much of the AOR, and it correlates with the verification time used in the FNMOC study.

For purposes of comparing analysis differences, Figure 4.6 shows the 500 mb analysis height field at the forecast verification time for NOGAPS (shown in light blue), GFS (shown in yellow), and COAMPS (shown in green). Of note is the fact that all three models' analyses qualitatively capture the same features. All three show a 5340 m low center located approximately 100 km off the coast of Israel and Lebanon in the eastern Mediterranean Sea. The main difference lies in the structure of the center of the low. Away from the center, however, the height gradients generally agree between the three models. Because the model analysis fields generally agree with one another, each model can be compared to its own analysis, and in the process be qualitatively compared against the other two. NOGAPS is evaluated out to 84 hours, GFS out to 72 hours,

and COAMPS out to 48 hours, which represents the forecast limits of the data set used in this verification.

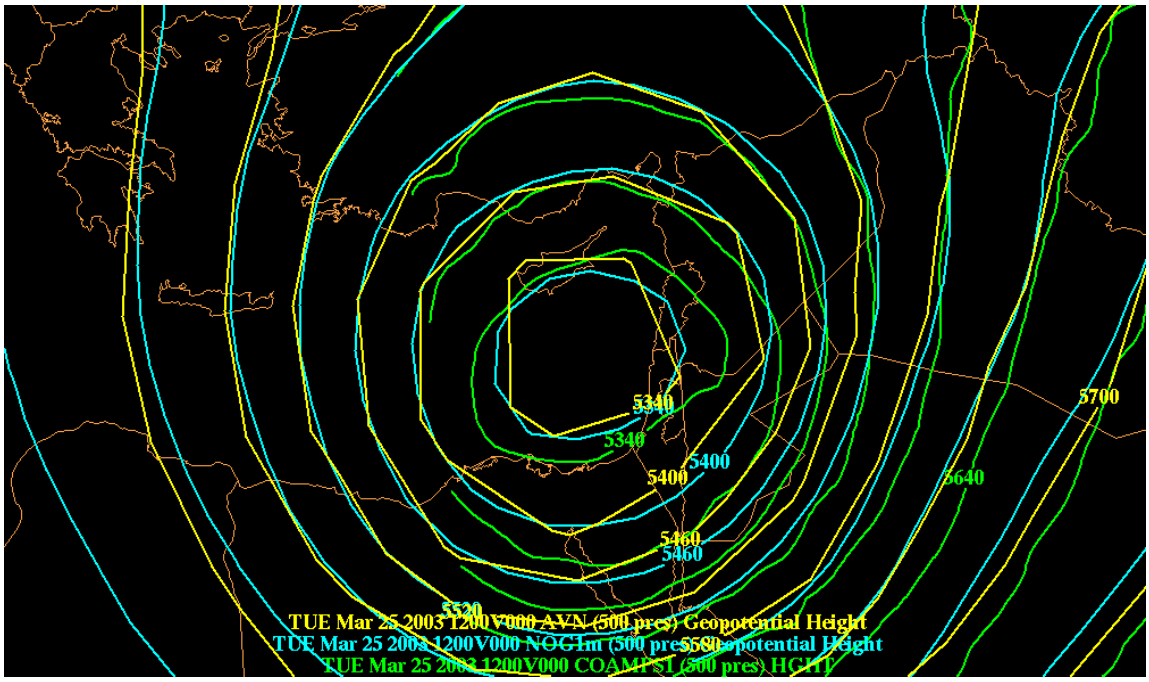

Figure 4.6. 500 mb height analysis fields for GFS (yellow), NOGAPS (light blue), COAMPS (green): 1200 GMT, 25 March 2003.

1. NOGAPS 500 mb Verification

Figures 4.7-4.11 show 500 mb forecasts (blue dashed lines) for the verification time overlaid on the NOGAPS analysis field (solid green lines). This sequence of figures steps through the model forecasts from tau-84 to tau-36 in 12 hour increments.

Figure 4.7 shows that at 84 hours out, NOGAPS is relatively slow, placing the center of the low almost 300 km to the northwest of the analysis field that verified. Although NOGAPS is slow, it does provide good overall guidance on the depth of the trough and associated height gradient. At tau-72, this error decreases to approximately

240 km northwest, and continues to decrease with each successive forecast until tau-36, when the error is qualitatively very small. Figures 4.8-4.11 capture this gradual decrease in position error with time.

That NOGAPS seems to be slow relative to the analysis is in direct contrast to the findings in the FNMOC paper. As previously stated, the FNMOC (2004) paper placed the 500 mb trough at tau-72 approximately 200 km southeast of the verifying analysis. This discrepancy is possibly the result of a misinterpreted chart. It is possible that the analysis field and the forecast field were inadvertently confused for each other in the FNMOC paper. Regardless, FNMOC's own Figure 20 (FNMOC 2004) is virtually identical to Figure 4.8, which clearly shows the forecast field lagging the analysis field.

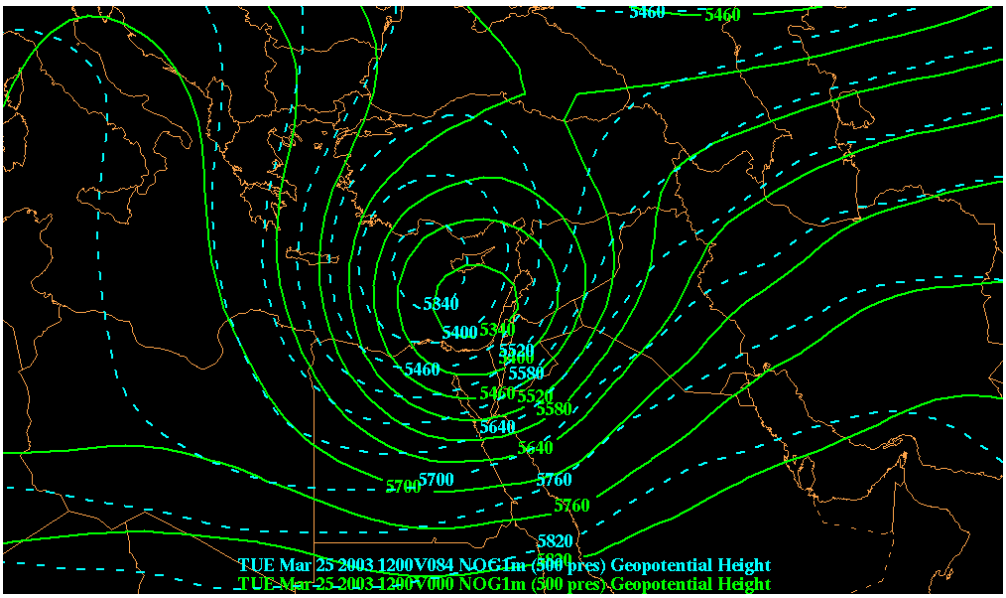

Figure 4.7. NOGAPS 500 mb 84-hour forecast (blue dashed lines) relative to model analysis (solid green lines) for 1200 GMT, 25 March 2003.

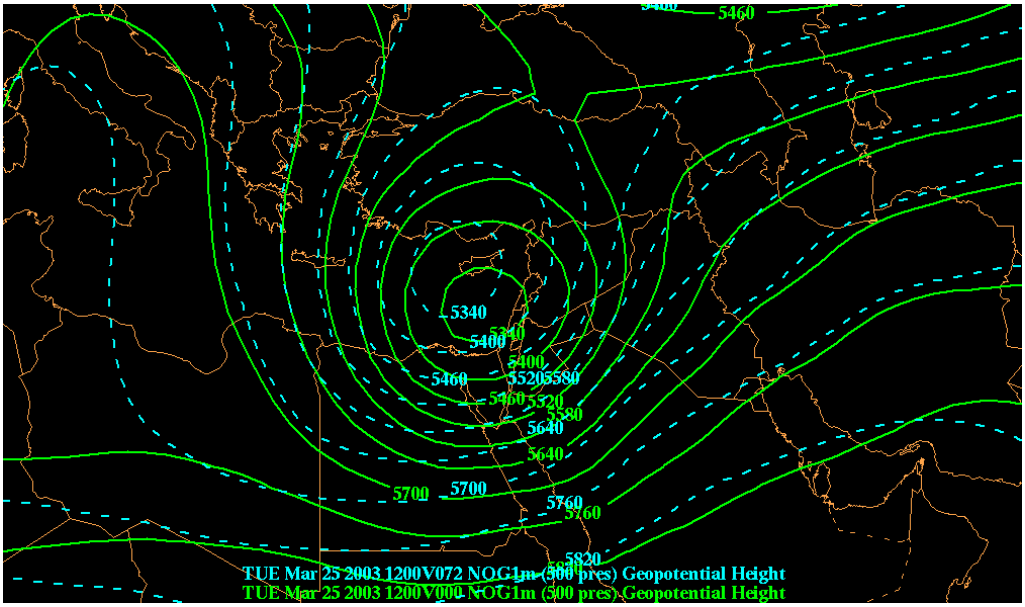

Figure 4.8. Same as Figure 4.7 for the NOGAPS 72-hour 500 mb height forecast.

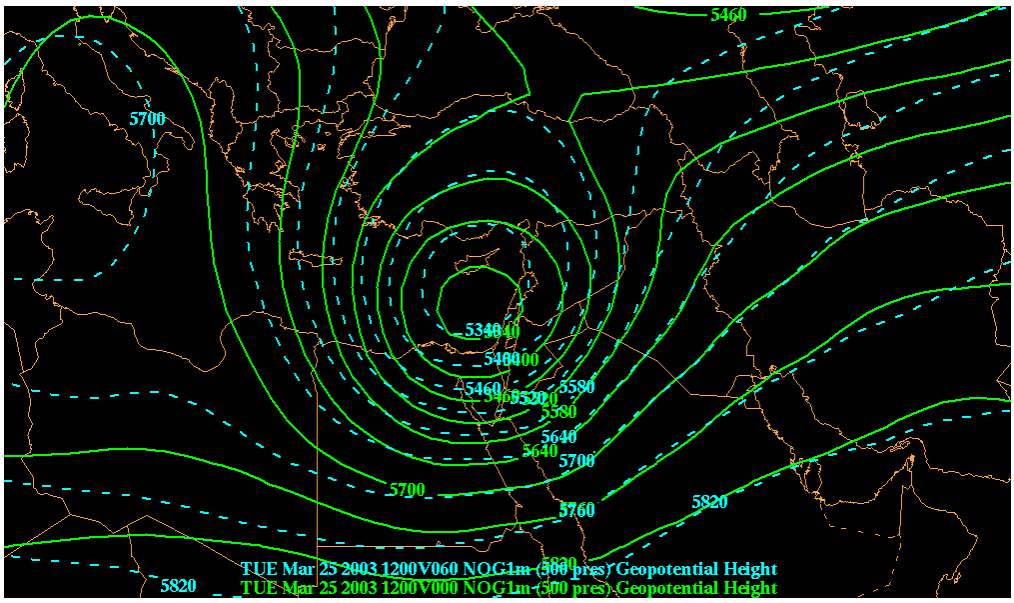

Figure 4.9. Same as Figure 4.7 for the NOGAPS 60-hour 500 mb height forecast.

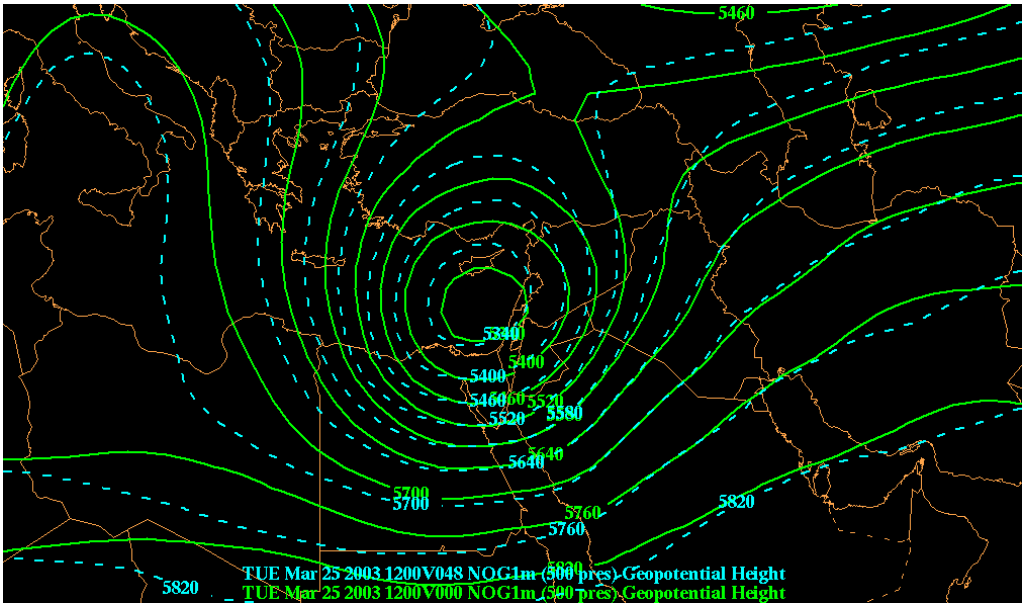

Figure 4.10. Same as Figure 4.7 for the NOGAPS 48-hour 500 mb height forecast.

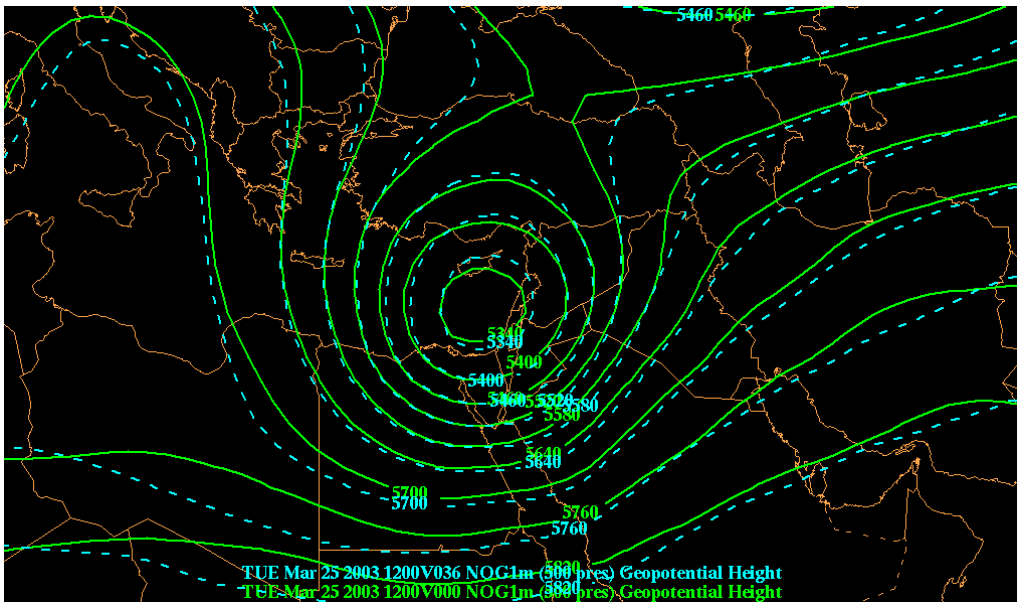

Figure 4.11. Same as Figure 4.7 for the NOGAPS 36-hour 500 mb height forecast.

2. GFS 500 mb Verification

Following the same type of verification procedures, the GFS 500 mb height forecast (blue dashed lines) is overlaid on its analysis fields (solid green lines) in

Figures 4.12-4.14. Once again, this sequence of figures steps the verification through the forecasts from tau-72 to tau-36 in 12-hour increments, with the exception that the data for tau-60 is missing.

Figure 4.12 shows that at 72-hours, GFS has the best placement of the upper level low center, with respect to the analysis field. The center is located approximately 120 km west/southwest of the notional position of the verifying low center. This result agrees well with the findings in the FNMOC (2004) study. The main drawback to GFS at tau-72 is the fact that it does not depict the overall depth of the trough very precisely, particularly in the center. The area of the forecast 5340 m low center is substantially smaller than the analysis, by a factor of approximately one sixth. However, the height gradient on the upwind and downwind sides of the trough is generally very good as distance from the low center increases.

Figures 4.13 and 4.14 show the forecast verifications for tau-48 and tau-36 respectively. Theses figures clearly show that by the 48 hour forecast, the discrepancy between the forecast and the analysis low center is resolved, giving even better guidance to the forecaster.

3. COAMPS 500 mb Verification

The higher resolution COAMPS model verification is graphically depicted in Figures 4.15-4.17. Using the same color conventions (forecast = blue dashed lines, analysis = green solid lines), the verification starts at the maximum forecast tau, in this case 48 hours, and steps through the analysis in 12-hour increments to the 24-hour forecast.

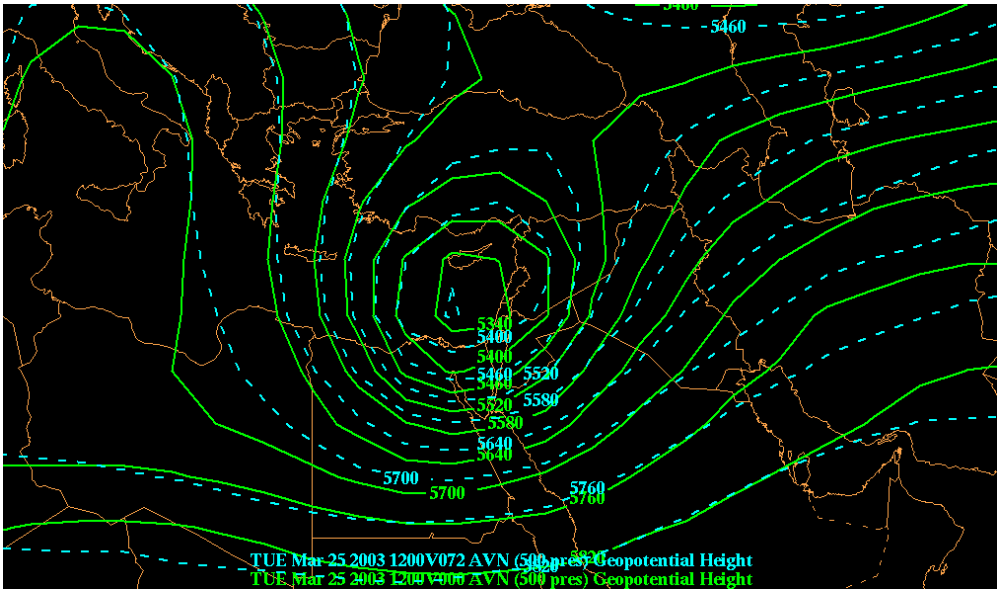

Figure 4.12. GFS 500 mb 72-hour forecast (blue dashed lines) relative to model analysis (solid green lines) for 1200 GMT, 25 March 2003.

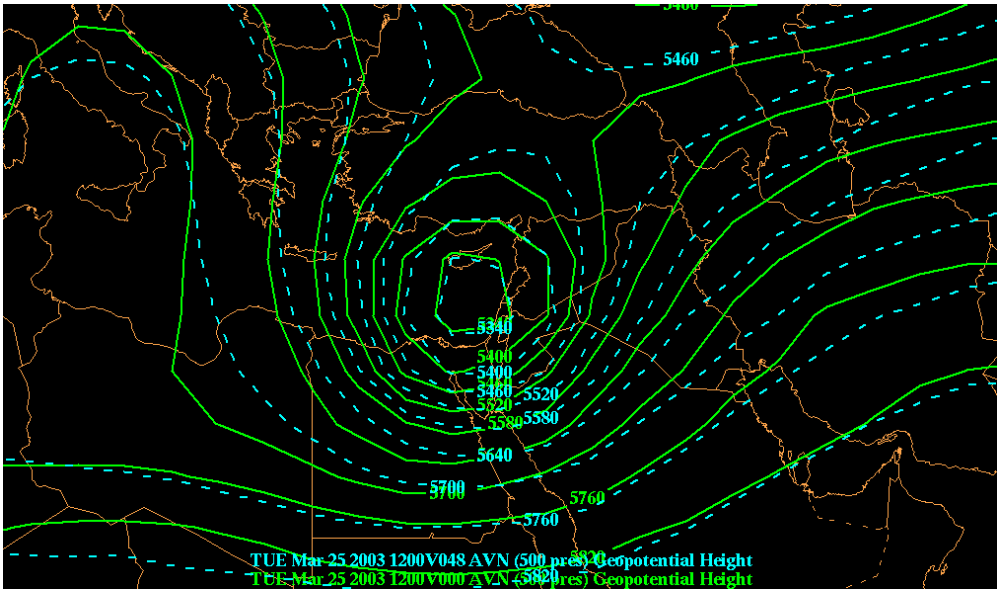

Figure 4.13. Same as Figure 4.12 for the GFS 48-hour 500 mb height forecast.

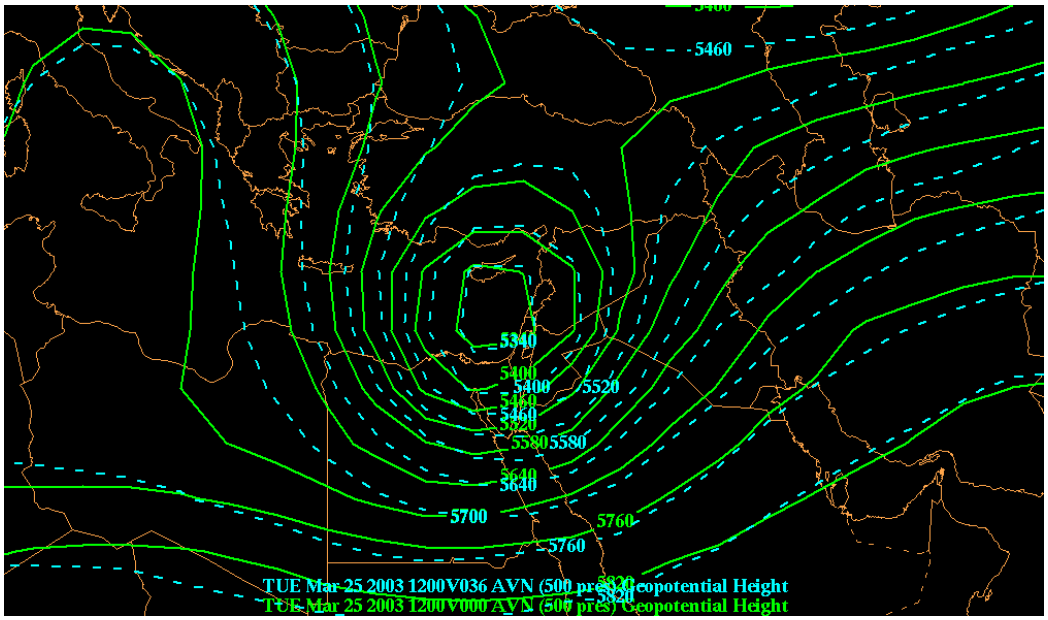

Figure 4.14. Same as Figure 4.12 for the GFS 36-hour 500 mb height forecast.

Figure 4.15 shows that the model at 48-hours has the center of the low pressure approximately 220 km to the east/northeast of the verifying analysis field location. The low pressure center also covers too broad a region, covering the entire eastern Mediterranean and large portions of Syria and southern Turkey,. The trough itself is forecast approximately 60 m too deep. The height gradient is well forecast, but shifted to the east slightly, due to the eastward displacement of the low center.

For the 36-hour forecast, verified in Figure 4.16, COAMPS exhibits better placement of the low center, however the region of low pressure is still too broad. Moving out from the center, the height field on the downwind side of the trough starts to match the analysis field much better. Over central Iraq, the forecast trough is approximately 40

m too deep, and the height gradient is once again well forecast.

At tau-24, the model forecast is over-taking the analysis field, as graphically depicted in Figure 4.17. The low center is approximately 150 km southeast of the verifying analysis. The downwind side of the trough once again starts to deepen relative to the analysis field. The eastward displacement of the forecast trough center illustrates a slightly fast tendency that agrees with the verification done by FNMOC (2004). However, COAMPS in general provides relatively good information to forecasters out to 48 hours.

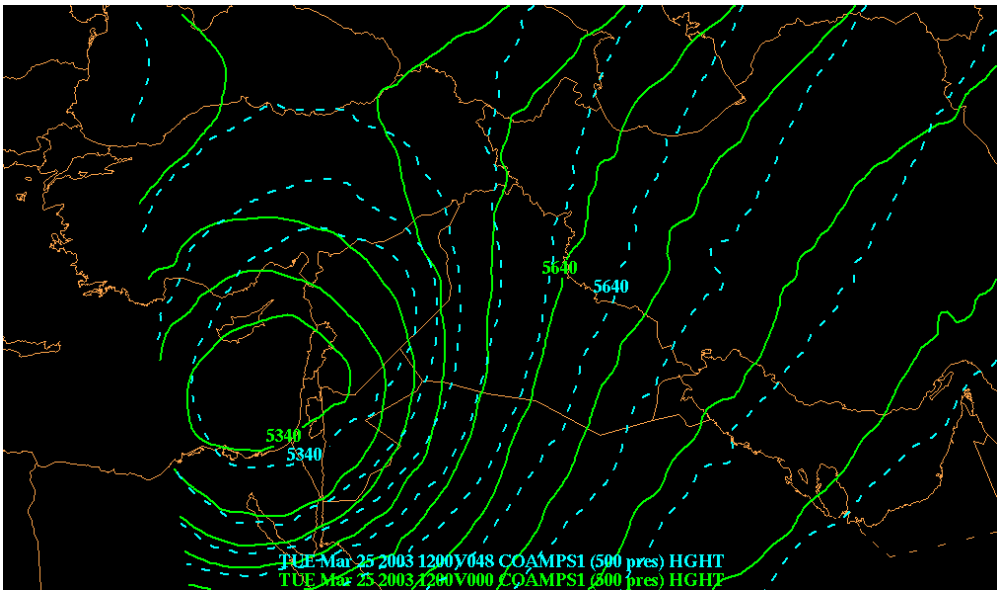

Figure 4.15. COAMPS 500 mb 48-hour forecast (blue dashed lines) relative to model analysis (solid green lines) for 1200 GMT, 25 March 2003.

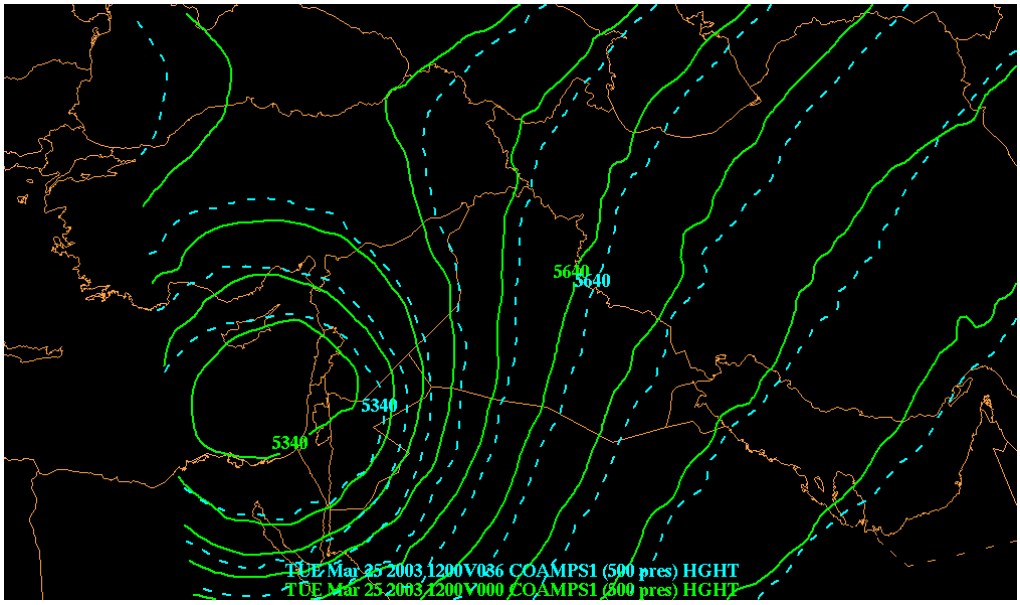

Figure 4.16. Same as Figure 4.15 for the COAMPS 36-hour 500 mb height forecast.

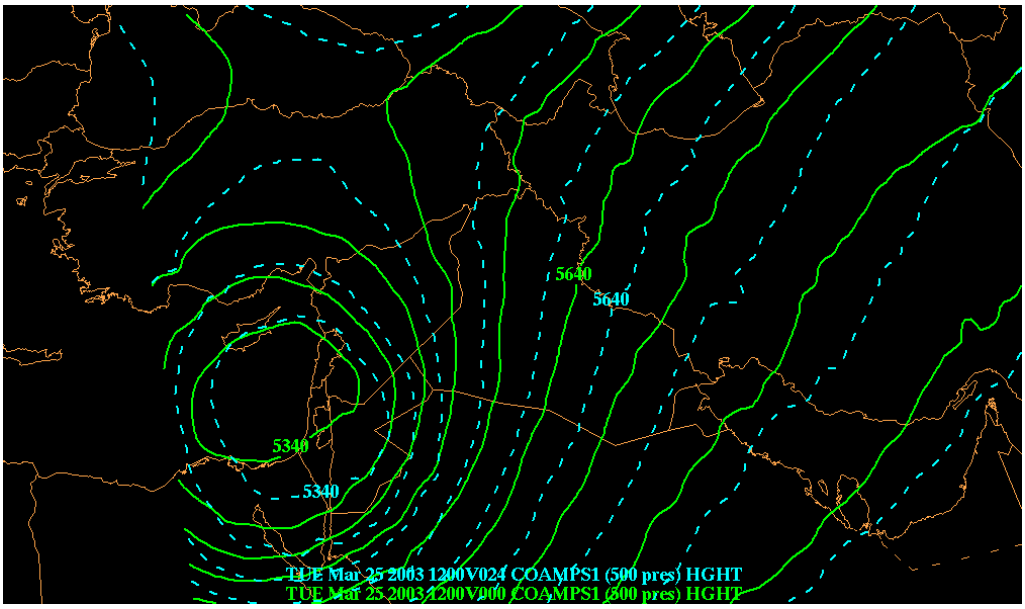

Figure 4.17. Same as Figure 4.15 for the COAMPS 24-hour 500 mb height forecast.

C. VERIFICATION OF THE SLP FIELD AND 1000 MB WINDS

In verifying the forecasts of the surface winds which produced the dust storm studied in this thesis, a similar approach is taken. For each of the three models, the

forecast sea-level pressure (SLP) field and 1000 mb winds are overlaid on the SLP analysis field and METAR observations for 1200 GMT, 25 March 2003. Each model is compared against its own analysis, and the observations to determine its qualitative accuracy. Once again, to establish a basis for comparison, Figure 4.18 shows the verifying SLP analysis field of each model overlaid with each other. From Figure 4.18, it is easily seen that the models are generally in good agreement on the SLP field. All models capture a kidney bean-shaped pressure field, which is the result of the merger between the main low center to the north and the short-wave disturbance that transited northern Africa along the cold front of the main system. The resultant system shows an approximate 992 mb low pressure center over western Iraq. Moving away from the center, the pressure gradients for each model's analysis field are also generally in agreement. With this figure forming the foundation for the verification, it is now possible to look at each model's performance.

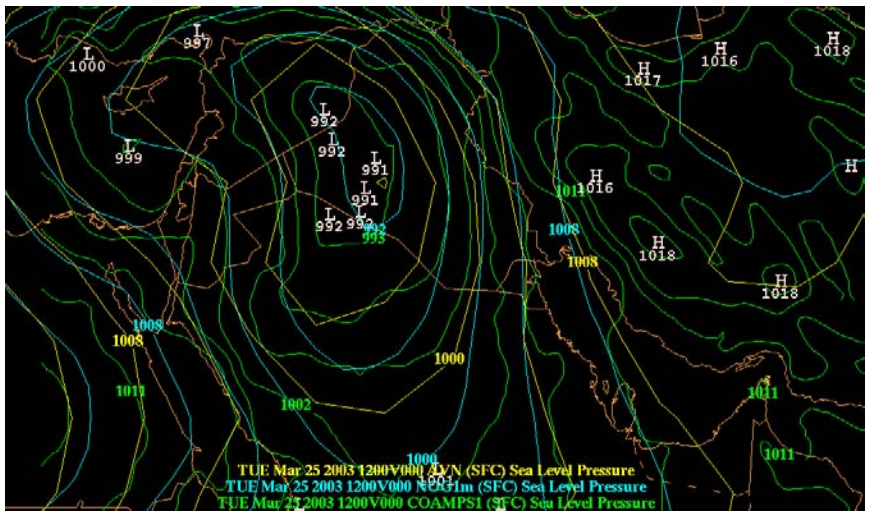

Figure 4.18. SLP analysis field for GFS (yellow), NOGAPS (blue), and COAMPS (green): 1200 GMT, 25 March 2003.

1. NOGAPS SLP Verification

Similar to the 500 mb case study of the previous section, the verification of the NOGAPS SLP forecast begins at 84 hours and steps to 72 hours for comparison to the GFS. Figure 4.19 shows the 84-hour NOGAPS forecast SLP field (shown in dashed yellow) and 1000 mb surface winds (shown in red barbs) overlaid on the verifying analysis (shown in blue) and hourly METAR reports (shown in green) for 1200 GMT, 25 March 2003. Figure 4.20 shows the same information, but for the 72-hour forecast.

From Figure 4.19, it is easily seen that the 84-hour forecast does not quite capture the 991 mb low center that verified over western Iraq in the analysis field. The forecast is for a 999 mb low approximately 300 km to the south, with a secondary 998 mb low over Turkey. While the forecast low pressure system is not as deep and does not have the same kidney bean shape, it does capture, at least qualitatively, the ridging over Lebanon, Jordan and Israel that verified in the wake of the frontal passage.

The 1000 mb winds verify extremely well against the METAR observations for eastern Saudi Arabia. Wind directions are generally in agreement and within 10-15 degrees of the METAR observations. Wind speeds are also in good agreement away from the southern low. Over much of eastern Saudi Arabia, well ahead of the front, the forecast winds speeds are either exact or within 5 knots too fast. However, in northern Saudi Arabia near the western side of the southern low pressure center, the wind speeds lag the observations by approximately 5-10 knots. This performance analysis agrees well with the findings in the FNMOC study.

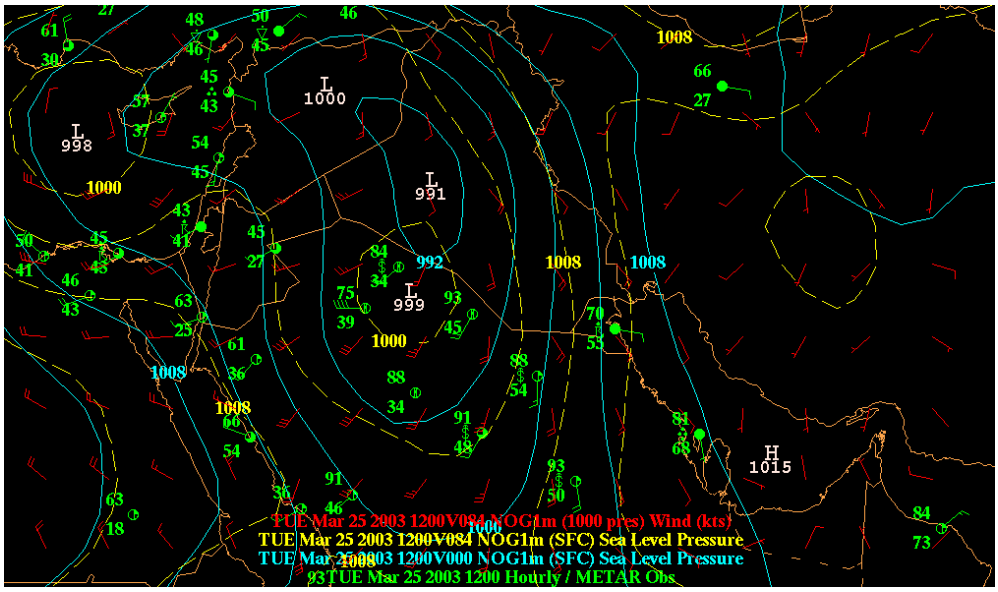

Figure 4.19. NOGAPS 84-hour forecast of SLP pressure (yellow dashed lines), 1000 mb winds (red barbs), analysis pressure field (blue solid lines), and METAR Observations (green): 1200 GMT, 25 March 2003.

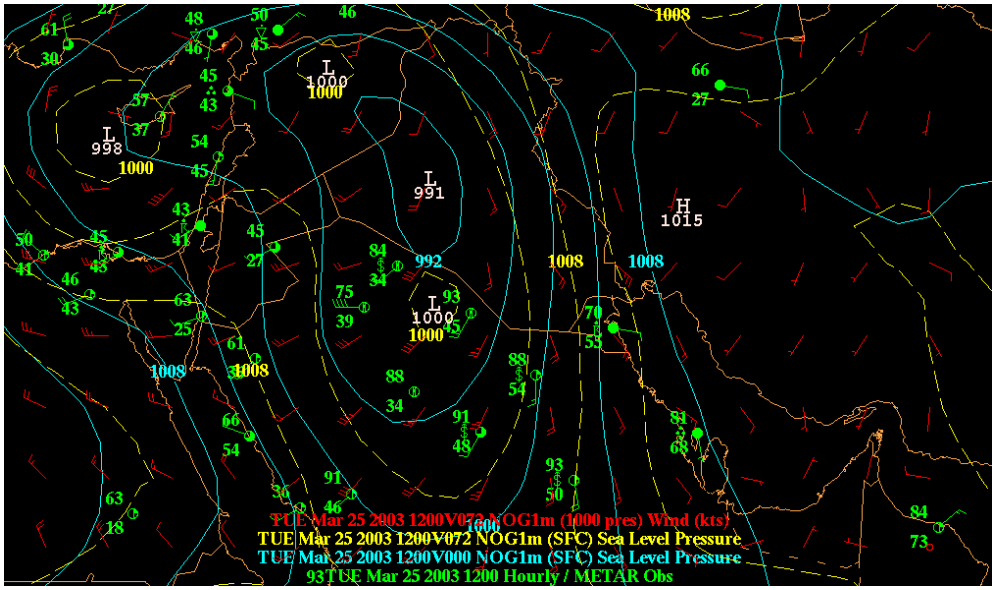

Figure 4.20. Same as Figure 4.19 for the NOGAPS 72-hour SLP forecast.

Comparing Figure 4.19 with Figure 4.20, the 72-hour forecast shows little change qualitatively in the overall pressure field, while maintaining a similar high quality

wind forecast. Of interest to note in both Figures 4.19 and 4.20, is the fact that in the frontal region near the southern low, which is known to cut across central/eastern Iraq and Saudi Arabia at this time, stations with wind speeds of 15 knots or greater are reporting some degree of blowing dust or sand in the verifying hourly METAR report.

2. GFS SLP Verification

Figure 4.21 shows a similar verifying analysis for the GFS 72-hour forecast with color conventions similar to Figures 4.19 and 4.20. At 72 hours, GFS places the southern low pressure approximately 100 km east of the verifying position over central/western Iraq. The forecast low, like NOGAPS, is also not as deep as the analysis field, with the low center reaching only 997 mb, vice the 991 mb low center in the analysis field. Overall, the GFS forecast provides better guidance than NOGAPS on the shape of the low pressure system, relative to the model's own analysis, but misses some of the details such as the post-frontal ridging over Lebanon, Jordan, and Israel, which is captured by NOGAPS.

The 1000 mb wind directions vary far more than NOGAPS compared to the 1200 GMT hourly METAR for 25 March 2003, although the forecast does capture the correct quadrant. Wind speeds are generally forecast 5-10 knots too fast in northeastern Saudi Arabia and Kuwait, away from the frontal system, and approximately 20 knots too slow in north/central Saudi Arabia near and behind the southern low center. This result generally agrees with the FNMOC (2004) study.

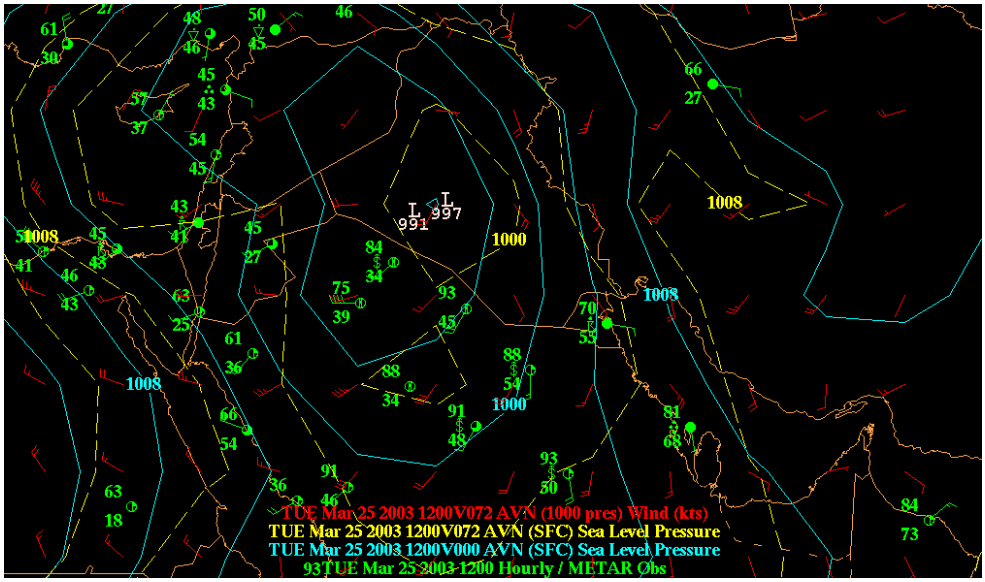

Figure 4.21. GFS 72-hour forecast of SLP pressure (yellow dashed lines), 1000 mb winds (red barbs), analysis pressure field (blue solid lines), and METAR Observations (green): 1200 GMT, 25 March 2003.

3. COAMPS SLP Verification

Verification of the COAMPS SLP and 1000 mb wind forecasts is carried out for the 48-hour forecast and compared against the 24-hour forecast, as graphically depicted in Figures 4.22 and 4.23. The color conventions used in these figures are once again similar to those used in the NOGAPS and GFS verifications.

As shown in Figure 4.22, at tau-48, the COAMPS forecast SLP field is not as deep as the analysis field. The central low pressure is forecast to be 996 mb, compared to a 992 mb central pressure in the verifying analysis. The model also places the central low pressure system approximately 100 km to the east. The pressure gradient on the eastern side of the low pressure center is not captured as well as the previous two models. In fact, the gradient is weaker, which we shall soon see results in an under forecast 1000 mb wind field over northern Saudi Arabia and

eastern and central Iraq At 48-hours out, COAMPS does perform better on the post-frontal ridging occurring over the western portion of the AOR when compared to the 72-hour forecast for GFS. This result is not surprising given that it is a much higher resolution model (18 km vice 50 km), run much closer to the verifying time (48 hours vice 72 hours).

As previously stated, the 1000 mb wind field is generally under forecast in strength. As graphically depicted in Figure 4.22, the winds in the northern and eastern Arabian Peninsula are on average 5-10 knots too slow. In one particular case in northern Saudi Arabia, just south of the Iraq/Jordan border, the model under forecasts the wind speed by approximately by 35 knots, compared to the verifying METAR report. In fairness to COAMPS, all of the models have at least some degree of difficulty with under forecasting the verifying wind speeds in this region. It is possible, given the location of that particular wind speed aberration, that there are some terrain effects from the Jordanian, Syrian, and northern end of the Al Hijaz mountain ranges that are not well accounted for in the models. If there is an error in accounting for these terrain effects, the resultant error in COAMPS would be greatest, given the higher resolution of the model. NOGAPS and GFS, being global models probably smooth these errors out a bit more. The weak wind strengths are also noted by FNMOC (2004).

The 24-hour forecast, shown in Figure 4.23, clearly improves upon the forecast pressure field relative to the analysis. The central low pressure is well forecast at 24-hours, matching nearly identically to the analysis field.

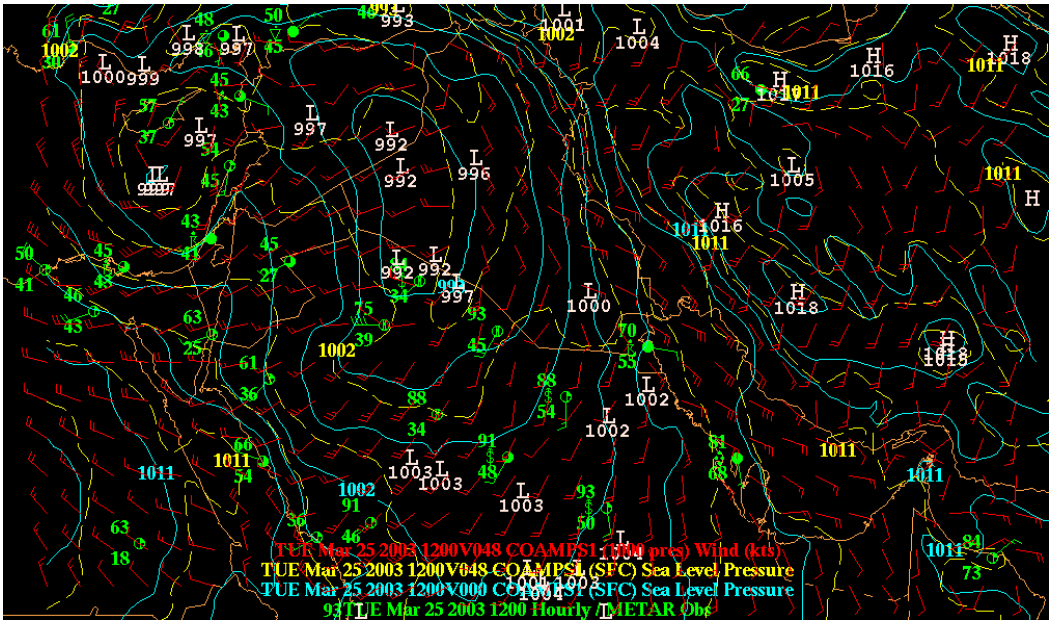

Figure 4.22. COMPS 48-hour forecast of SLP pressure (yellow dashed lines), 1000 mb winds (red barbs), analysis pressure field (blue solid lines), and METAR Observations (green): 1200 GMT, 25 March 2003.

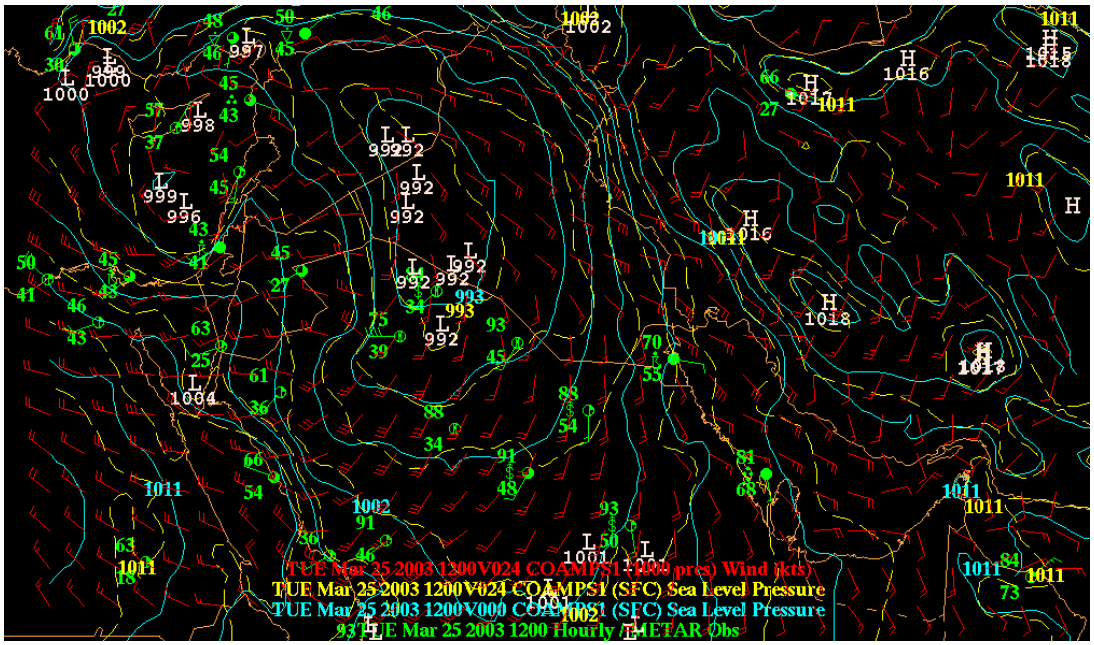

Figure 4.23. Same as Figure 4.22 for COAMPS 24-hour SLP forecast.

The pressure gradient on the eastern side of the low is much improved, which results in much better wind speed forecasts across most of the AOR. In both the 24 and 48-hour forecasts, COAMPS generally provided very good wind direction information, which would be expected with a higher resolution model.

D. VERIFICATION CONCLUSIONS

In general, all three models provide excellent guidance to forecasters as to the conditions leading to a strong dust event. For timing of the synoptic scale cyclone, the GFS performs best, which explains why 28th Operational Weather Squadron forecasters almost exclusively choose it as their model of consistency in their forecast discussions for this event (Finta 2004). However, NOGAPS and COAMPS also perform very well in this particular case.

The southern low pressure associated with the short-wave disturbance that transited across north Africa along the cold front was generally forecast by all models to be about 5-10 mb too shallow, especially at longer forecast times. Moving away from the low pressure center, however, the pressure gradient was generally well forecast in all models. This presents a possible explanation for the under-forecast winds in and near the cold frontal region of the cyclone, and better forecasts far ahead of the front.

Given the composition of dust source regions in the AOR, an average surface wind speed of 13-15 knots over a wide area of the northern Arabian Peninsula should be enough to generate a large scale dust storm. In all three models, these conditions are revealed and verified. For NOGAPS, these conditions verify out to 84-hours, for GFS

out to 72-hours. Given their solid performance, with a data set encompassing a larger time domain, it is reasonable to estimate that they would verify well maybe out to as long as 120 hours.

COAMPS, even with the slightly under forecast wind strengths, still gives good guidance out to 48 hours. It also gives the forecasters a higher resolution look at the surface features close to the verifying time of the forecast.

In any case, claims that this shamal event is well forecast far enough in advance to provide mission planners with critical information on blowing dust and restrictions to visibility, do seem to verify on the basis of this information. The only drawback to these models performance is that they tend to under-forecast winds near the frontal boundary, which if not understood and accounted for by the forecaster, could lead to under-forecast intensities for the dust storm itself.

THIS PAGE INTENTIONALLY LEFT BLANK

V. IMPACTS TO OPERATIONS

A. BRIEF HISTORICAL PERSPECTIVE

Throughout the history of modern airpower, weather has proven to be a major influence on combat operations. In his recently published book, Air Force historian Richard Davis (2003), in reviewing the Operation DESERT STORM air campaign, states that weather has "prevented or spoiled more combat operations than any other single factor." Even in this day of highly sophisticated numerical models, weather continues to be a major issue and the most uncontrollable element in mission planning (Brown 2003).

The weather patterns in the Middle East and Southwest Asia are at times difficult to forecast, which can compound mission planning problems in currently one of the most important theaters of operations in the world. According to Brown (2003), many war planners for Operation DESERT STORM may have been given a false sense of optimism regarding meteorological conditions in the region due to the prevailing favorable weather patterns in the long period of build up to the first Gulf War.

Based upon regional climatology data for Southwest Asia available in 1990-1991, it was estimated that the ceilings and visibilities over Baghdad would be greater that 10,000 feet and 5 miles at least 60 percent of the time in January, and 70 percent of the time in February (Brown 2003). This proved not to be the case, as ceilings and visibilities were considerably lower much more frequently than expected (Brown 2003).

As an example of how this impacted operations, Brown (2003) states that in the middle of February, 1991, which

was arguably one of the worst weather periods during the first Gulf War air campaign, over 300 sorties in the Kuwaiti Theater of Operations were cancelled in a single day. He also states that, based on statistics from the 37th Tactical Fighter Wing, nearly 25 percent of all F-117 strike missions were aborted due to bad weather in the early days of DESERT STORM.

The decision to cancel scheduled sorties in Operation DESERT STORM was most often not safety of flight related. According to Grant (2004), the dust storms and clouds that frequented the AOR during the winter and spring of 1991 interfered with infrared targeting pods that guide laser-guided bombs to their targets. As a result, only approximately 8.8 percent of munitions dropped in the first Gulf War were precision weapons (Brown 2003).

At that time, mission planning personnel needed constant weather updates to decide whether to press on with scheduled sorties, cancel them, or change weapons allocations around for a different type of attack (Grant 2004). As a historical note, the Joint Direct Attack Munition (JDAM), which is a Global Positioning System (GPS)-guided bomb, was not available to DESERT STORM planners. The JDAM was developed after the first Gulf War to address the short-comings of laser-guided weapons, particularly in low-optical visibility conditions that dust storms in Southwest Asia bring.

Brown (2003) suggests that once the ground war started, Lt Gen. Charles Horner, the Joint Forces Air Component Commander (JFACC) for DESERT STORM committed his air forces more aggressively to support troops on the ground in contact with the enemy, regardless of the weather

conditions. Brown (2003) quotes Lt Gen. Horner as saying, following the start of the ground campaign, "The weather considerations that were valid last week, are no longer valid. [There are] people's lives depending on our ability to help them, if help is required over the battlefield, then it's time to go to work."

Even after the ground combat operations commenced, prompting a decision to fly missions in less than optimal conditions, weather was still a crucial factor in determining how to mitigate collateral damage, ensure the survivability of air crews, and choose weapons load-outs to maximize the delivery of lethal combat power to the enemy. Air Force weather personnel employed during the first Gulf War still managed to help find gaps in cloud cover and optimized times to schedule strike packages, with the impressive results realized in the air campaign (Grant 2004).

Twelve years later, additional upgrades to weapon systems, and improved weaponry, such as the JDAM, have not mitigated the need for accurate weather information. Forecasting resources are still essential for mission planning operations (Grant 2004). Weather data is now part and parcel of the operations tempo, with Combined Air Operations Center (CAOC) staff members being briefed twice a day on current and future conditions around the AOR (Grant 2004). Five day forecasts are essential to keeping Air Tasking Order (ATO) planners informed on future conditions at major bases and key target areas (Grant 2004). This is a direct result of lessons learned in the first Gulf War.

Based on statistics provided by Maj. Christopher Finta, USAF (2004b), of the 28th Operational Weather Squadron and the work of Lt CDR Jacob Hinz, USN (2004), of the Naval Postgraduate School, we shall now look at some of the impacts of the Joint METOC forecasts on scheduling for the major storm period from 21 to 28 March 2003.

B. 28TH OWS AFTER ACTION STATISTICS

The statistics, as compiled by the 28th OWS, for Operation IRAQI FREEDOM (OIF) provided by Maj. Finta (2004b) detail some of the effects of weather on air operations for the time period from 19 March to 18 April, 2003. This time frame encompasses the shamal event described in this thesis, plus an additional storm which hit Iraq the first week of April, 2003.

The data shown in Figure 5.1 (Finta 2004b) graphically depict the break down of Air Tasking Orders (ATOs) affected by weather. According to Finta (2004b), during the time period from 19 March to 18 April, 31 daily ATOs were executed in the air campaign. He states that over 75 percent of these ATOs were adversely affected by weather. 20 percent of the ATOs are described as having had "major" weather effects, implying over 6 percent of their sorties non-effective or cancelled (NE/CANX). No precise definition of NE/CANX is given, but one can assume a non-effective sortie as one in which the primary or secondary objectives were not met. A cancelled sortie most probably implies that the cancellation occurred within 72-hours of ATO execution. Finta (2004b)defines "modest" weather effects as ATOs with 1-5 percent of their sorties listed as NE/CANX.

In total, the OIF after action statistics (Finta 2004b) list 1650 sorties as NE/CANX due to weather during this time period. This number represents approximately 4 percent of the roughly 40,000 sorties flown between 19 March and 18 April, 2003 (Finta 2004b).

Figure 5.2, also taken from Finta (2004b), breaks down by percentage those NE/CANX sorties by cause. Of note is the fact that low ceilings and visibility account for 94 percent of NE/CANX sorties, while thunderstorms and other weather hazards account for only 6 percent. This result is not surprising given the intensity of the frequent dust storms in the region, which often drop visibilities to zero in a matter of hours.

Figure 5.3 (Finta 2004b) shows the break down of the same 1650 NE/CANX sorties; this time by mission type. Assuming the preponderance of sortie losses came during the two dust storms, which we shall later see is a valid assumption, it is easy to see that the dust events had a profound impact across the full spectrum of air operations.

From Figure 5.3, we see that the dust storms had approximately equal impacts on Close Air Support (CAS), Airlift and Strike operations. They had much less impact on Intelligence, Surveillance, and Reconnaissance (ISR) missions, as well as other operations including Defensive Counter Air (DCA) and Electronic Attack (EA).

According to Finta (2004b), in 95 percent of the cases involving weather-related NE/CANX missions, the forecast was accurate to at least 12 hours prior to ATO execution, and in some cases accurate at far greater taus. As an

example of a forecast verifying at a longer tau, a post-deployment report from the USS Kitty Hawk reported:

> 25 MAR Some aircraft diverted to Bahrain upon return from missions due to onset of sandstorm and reduced visibility to less than 200 yards on ship. Forecast from 4 days prior to event verified. (FNMOC 2004)

By the time the 25-27 March storm had passed, the aircraft carriers Kitty Hawk, Abraham Lincoln, and Constellation had cancelled two complete take-off and landing cycles, which reduced their carrier air wings' sortie productivity by 20 percent (Clemetson 2003).

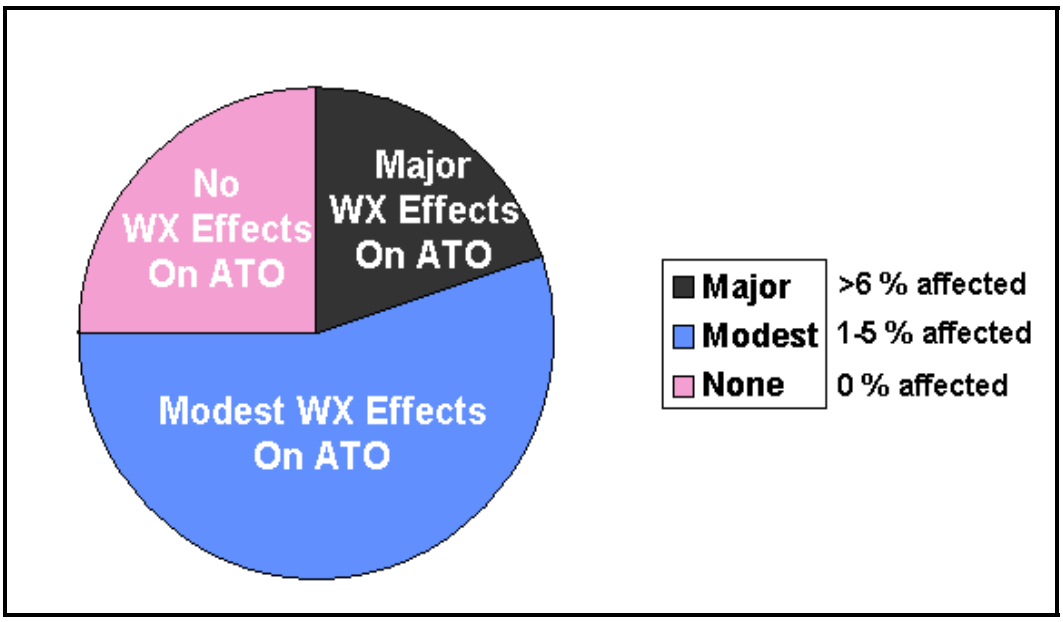

Figure 5.1. Breakdown of weather effects on Air Tasking Orders for period from 19 March to 18 April, 2003. Classifications are by percentage of scheduled sorties affected by weather. Major weather effects implies ATO had greater than 6 percent of its sorties effected. (After: Finta 2004)

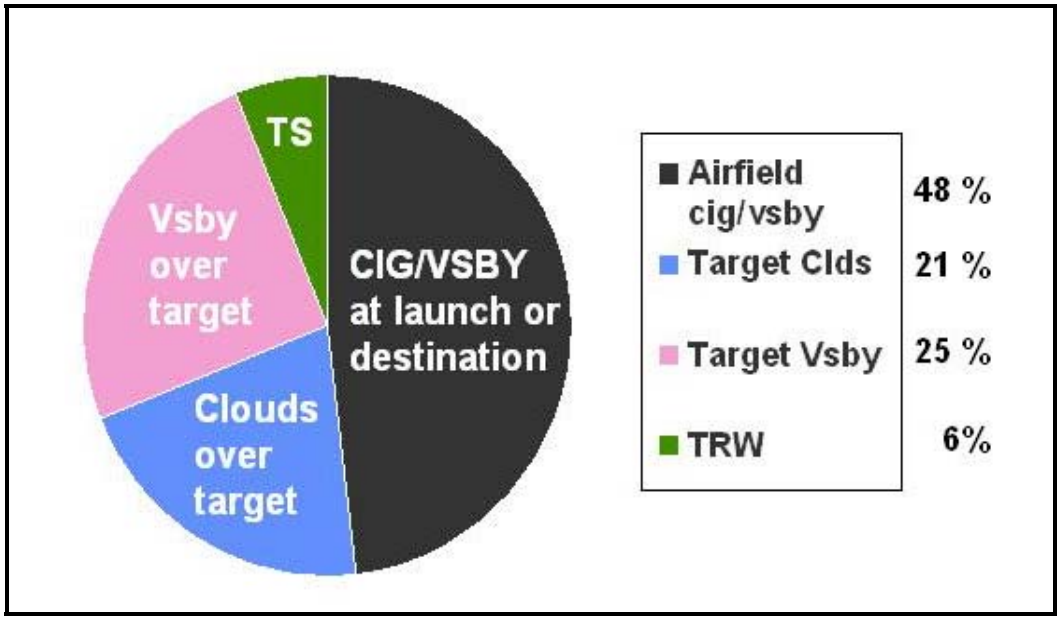

Figure 5.2. Breakdown of weather related sortie losses by percentage of cause from 19 March to 18 April, 2003, by cause. (After: Finta 2004)

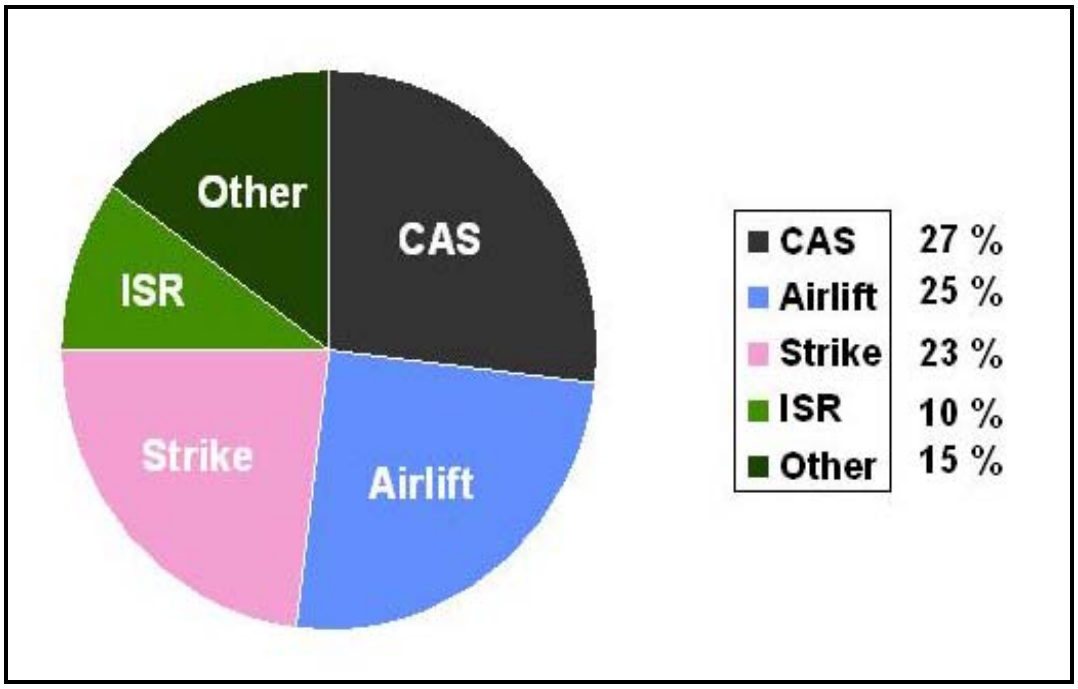

Figure 5.3. Breakdown of weather related sortie losses by percentage of mission type from 19 March to 18 April, 2003, by mission type. (After: Finta 2004)

The statistics provided by Finta (2004b) point to some key conclusions about weather support for the 25-27 March shamal impacting the AOR. These statistics also validate the assumption that the preponderance of the NE/CANX sorties came during the two dust events.

First, a power-point slide show detailing the after action report (Finta 2004b) states that on 19 March there were 130 sorties cancelled for various weather reasons. Finta (2004b) asserts that none of these cancellations were a surprise to mission planners and CAOC staff. No further explanation of this assertion is given, possibly for classified reasons. In general, the weather was good during the first few days of the air campaign.

Secondly, the report also states that as early as 21 March, the Combined Forces Air Component Commander (CFACC) was mandating ATO changes on the basis of the 3-5 day forecasts (Finta 2004b). Between 21 March and 23 March, no NE/CANX sorties due to weather were officially declared, but changes to the ATO continued to be driven by the outlook for 25 March (Finta 2004b). By 24 March, with the storm system rapidly approaching as expected, the mission planners began calling for JDAM-only aircraft to be launched, in an effort to minimize the effects of the expected dust storm (Finta 2004b). From the time the dust storm hit the AOR on 25 March until the time it lifted out of the region on 27 March, a total of 817 sorties were listed as NE/CANX due to weather (Finta 2004b).

In the period between the storms, from 28 March to 6 April, far fewer sorties were affected by the weather. From the time the second storm hit on 7 April until its passing on 19 April, another 411 sorties were listed as

NE/CANX due to weather (Finta 2004b). The 1228 sorties lost due to weather during the two dust storms represent approximately 75 percent of the 1650 sorties lost during the entire 31 day period. This validates the previous assumption that the preponderance of sortie losses due to weather came during the two dust events.

The final point made by the after action report provided by Finta (2004b) is that during the study period, no sorties were cancelled needlessly on the basis of a forecast that predicted bad weather when good weather ended up verifying. This differs from the findings of Hinz (2004).

C. METOC IMPACT ON SCHEDULING (21-28 MARCH 2003)

The study conducted by LCDR Jacob Hinz, USN, (2004) takes an in depth look at the impacts on scheduling of meteorology and oceanography (METOC) information provided to mission planners . In his work, Hinz suggests that there is a direct indication that METOC forecasts played a direct role in influencing the scheduling of sorties, particularly in the 21-28 March time frame.

Hinz (2004) states that due to CAOC scheduling data that did not break out sorties by mission type, he operated under the assumption that three types of missions dominated the ATOs in the early phases of OIF. In particular he states that due to the ground forces advancing along the southern front in the early stages of the war, he assumed that the dominant mission types would be Kill-Box Interdiction/Close Air Support (KI/CAS), High Altitude Reconnaissance (U2), and Laser-Guided Bomb strikes (LGB) (Hinz 2004). He reasons that KI/CAS would be used heavily

to support friendly forces in contact with the enemy; LGB would be used to strike and surgically remove critical nodes, and U2 would be used to survey and assess the battle space (Hinz 2004). Hinz (2004) further groups LGB and KI/CAS mission types on the basis of overall similarities in the missions and categorizes them under the term LGB. ATO planning for U2 and LGB missions can typically begin as far out as 5 days prior to mission execution. With this fact in mind, Hinz begins his study by looking specifically at the time period from 21 March to 27 March.

Figure 5.4, taken from Hinz (2004), shows in the upper panel the total number of sorties scheduled by day from 17 March to 12 April 2003, and percentages of sorties cancelled (by cause) in the lower panel. It should be noted that the source Hinz (2004) uses for the number of scheduled sorties is still classified, therefore the graphic in the upper panel of Figure 5.4 has the actual numbers of sorties removed. However, this graphic can still be analyzed qualitatively to establish trends and relationships.

Of note in Figure 5.4 is the dramatic rise in the number of sorties scheduled between 22 March and half-way through 24 March, followed by a dramatic decline in the number of sorties through noon on 25 March. Hinz (2004) asserts, quite reasonably, that this dramatic rise is the result of mission planners hoping to strike as many targets as possible before the forecasted dust storm hit the region. This assertion agrees well with the information provided by Finta (2004) that showed the CFACC dictating ATO changes on the basis of the forecasts between 22 March and 25 March. Recall that Finta (2004b) stated that GPS-

only weapons were scheduled to be dropped on 24 March. Furthermore, the drop off in scheduled sorties after noon on 24 March depicted in Figure 5.4 also lends credibility to the claim that mission planners believed forecasts that stated the frontal system would impact the area on or around 25 March.

Further strengthening this argument is Figure 5.5 (Hinz 2004), which shows the percent deviation from a 5-day running mean of scheduled sorties. The period between 22 March and 25 March is characterized by a strong positive deviation from the mean schedule. The schedule was increased on 21 March and 24 March by as much as 20 percent and 10 percent, respectively. Hinz (2004) once again asserts that this deviation from the mean coincides with forecasts of green conditions (i.e., forecasts of minimal METOC impacts on operations) as far out as 72 hours.

The lower panel of Figure 5.4 (Hinz 2004) shows the numbers of cancelled sorties, by percentage, and the cause of the cancellation. The greatest percentage of cancellations occurs in the time period from 25 March to 28 March, with the vast majority of those being due to weather.

Figure 5.5 (Hinz 2004) shows that the period from 25 March to 28 March is characterized by as much as a 5 percent decrease in scheduled sorties. It would appear that the mission planners believed the forecast for the dust storm to hit on 25 March and decreased the schedule accordingly, but perhaps not enough to mitigate the resultant spike in sortie cancellations. Hinz (2004) suggests that the increase in cancelled sorties could be

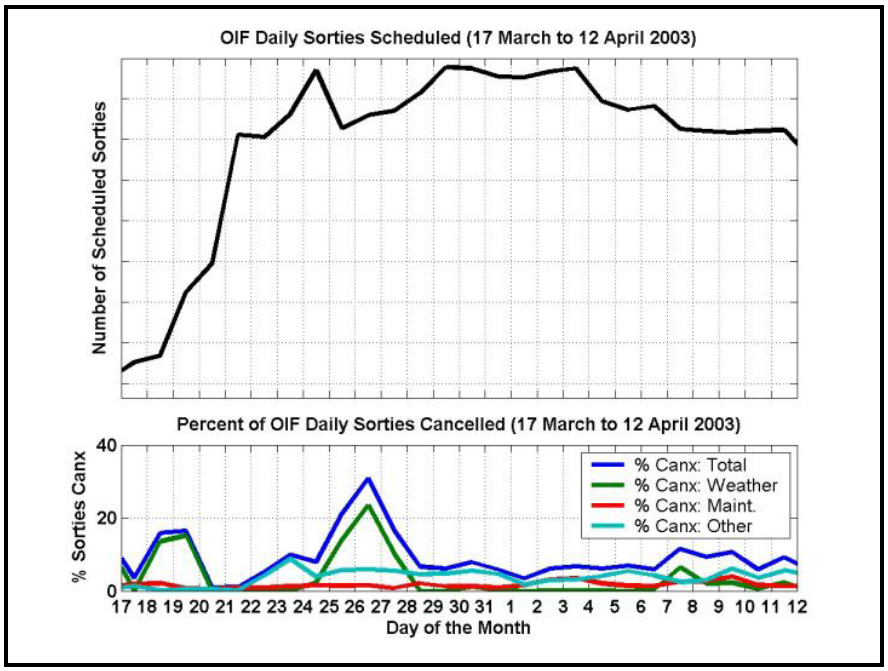

Figure 5.4. Upper panel: number of scheduled sorties; Lower panel: percentage of sorties cancelled. (From: Hinz 2004)

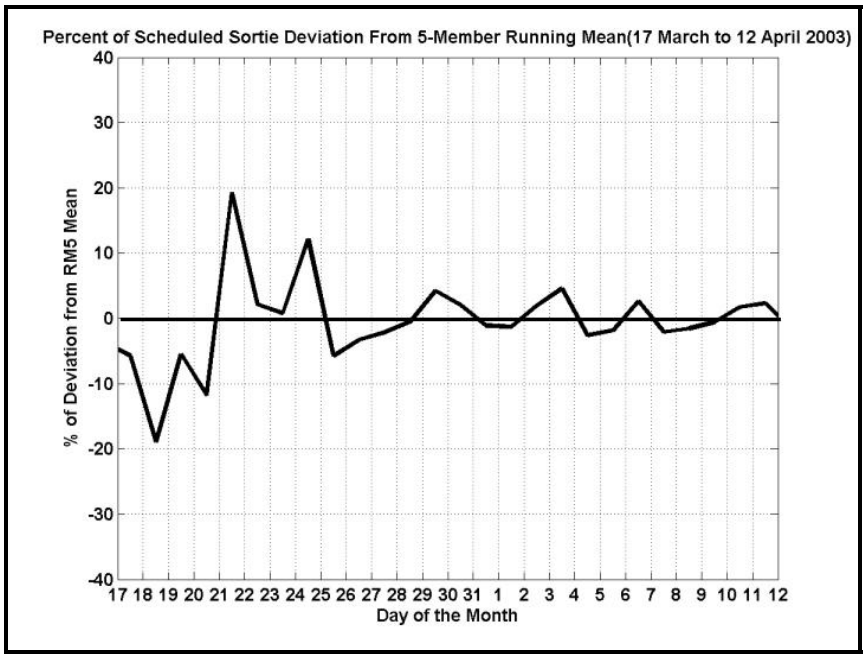

Figure 5.5. Percent schedule deviation from 5-day running mean. (From: Hinz 2004)

the result of overly optimistic forecasts indicating the storm would clear out of the area more quickly than actually verified. Hinz (2004) also proposes that sorties were scheduled and flown despite accurate forecasts of major negative METOC impacts because of the need to support ground troops in contact with the enemy, thus leading to a spike in the number of NE/CANX sorties.

The gradual rise in number of scheduled sorties after approximately noon on 25 March, graphically depicted in Figure 5.4, could also indicate a belief on the part of the mission planners that the conditions would gradually improve throughout the 26th and 27th, adding support to Hinz's discussion of overly optimistic forecasts causing a spike in sortie cancellations. This belief is loosely supported by anecdotal evidence uncovered by the author in the writing of this thesis that suggests the forecasters may have believed the frontal passage would occur on 24 March instead of 25 March. Once again, the decision to use only GPS-guided weaponry on 24 March, as stated by Finta (2004), could be used to suggest that the general consensus was for large scale dust storm generation as early as the 24th.

Without analyzing the actual forecasts given to the mission planners, it is difficult to say what the mission planners held as fact. However, the preponderance of the model data examined in this thesis, suggests that the information available to forecasters should have enabled them to provide good information to the mission planning cell. In the end, the air campaign was successful, and that is all that counts.

THIS PAGE INTENTIONALLY LEFT BLANK

VI. CONCLUSIONS AND RECOMMENDATIONS

Southwest Asia is currently one of the most significant theaters of operations for the U.S. Military, and will conceivably remain so for the foreseeable future. The climate of the region is highly conducive to the production of severe dust storms, particularly on the synoptic scale, which can have a profound effect on military operations there. The dust storms driven by transiting extra-tropical cyclones are especially intense. Such was the case with the storm that hit the AOR between 25 and 27 March, 2003.

At the outset of combat operations in Operation IRAQI FREEDOM, the coalition forces were achieving unprecedented rapid advances in territory, even compared to the first Gulf War. On day five of the campaign, the advances came to a screeching halt within 100 miles of Baghdad. A dust storm, initiated by the passage of a cold front that intensified with the merger of a passing short-wave trough from north Africa, brought visibilities down to almost zero within a matter of hours. This storm impacted air operations across the entire AOR, including Naval Air operations far out into the Arabian Gulf. It also delayed an impending ground attack on the Iraqi capital. In spite of these effects, military meteorologists were able to assist military planners in mitigating at least some of the impact of this storm.

All three models examined in this thesis captured well the features of the upper level trough, as it dug south out of the Ukraine, across the Black Sea and Turkey, and tracked east across the AOR. They also performed well in

tracking the 850 mb low pressure system progression eastward, along with its merger with the short-wave disturbance which intensified the cold front.

Metrics provided by Finta (2004b) and the work of Hinz (2004) further indicate that the METOC community performed well in providing useful forecasts on the March storm to the mission planners. As a result of these forecasts, mission planners were able to front load ATOs with extra sorties prior to the onset of the dust storm. Additionally, they were able to make changes to planned weapons loads, favoring GPS-guided munitions. These changes were made far enough in advance to maintain constant pressure on the enemy despite the severe dust storm. This ability to make rapid changes to mission plans, in response to changes in environmental predictions could arguably be a major factor in preventing any enemy counter-strikes during storm periods in future conflicts.

While the numerical models performed well in forecasting this particular event, other types of tactical decision aids are also aiding forecasters in predicting dust events. Due to time constraints, the performance of the U.S. Air Force's Dust Transport Application (DTA) and the U.S. Navy's Navy Aerosol Analysis and Prediction System (NAAPS) was not evaluated. A thorough case study of how these dust models perform in providing guidance as to this particular case would be useful in analyzing and predicting future storms, particularly in Southwest Asia.

Future work should also compare model output to actual forecasts, including the generation of forecasts based only on model output to assess the value added by human forecasters. This work would be very important in

assessing the most significant sources of error, as numerical models continue to improve.

A continued emphasis on numerical model validation and improvement, coupled with further studies of metrics to track METOC impacts on operations scheduling will ensure that military planners in future conflicts will be able to exploit the weather conditions for battle, and ensure success for our troops.

THIS PAGE INTENTIONALLY LEFT BLANK

LIST OF REFERENCES

Bartlett, K.S., 2004: Dust storm forecasting for Al Udeid AB, Qatar: an empirical analysis, Air Force Inst. of Tech., Wright-Patterson AFB, OH., pgs 6-11

Brown, M., 2003: A look back: big role, major weather, Air Force Weather Agency, On-line article retrieved from: https://afweather.afwa.af.mil/observer/JUN 2003/a look back.html, (Last accessed on 26 November 2003)

Byers, D.J., 1995: Synoptic and mesoscale influences on refraction during SHAREM 110, Naval Postgraduate School, Monterey, CA, pgs 22-23

Clements, T., J.F Mann, R.O. Stone, and J.A. Eymann, , 1963: A study of windborne sand and dust in desert areas, U.S. Army Tech. Rep. ES-8, 61 pgs

Clemetson, L., 2003: In and F-18, 5 seconds from a deck veiled by a sandstorm, New York Times, On-line article retrieved from: http://www.nytimes.com/2003/03/27/international/worldspecial/27CARR.html, (Last accessed on 21 November 2004)

CNN.com, 2004: Special report: war in Iraq: war tracker, CNN, On-line article retrieved from: http://www.cnn.com/SPECIALS/2003/iraq/war.tracker/index.html, (Last accessed on 14 July 2004)

CNN Student News, 2003:'Shock and awe' campaign underway in Iraq, CNN, On-line article retrieved from: http://www.cnn.com/2003/fyi/news/03/22/iraq.war/, (Last accessed on 14 July 2004)

COMET Program , 2003: Forecasting dust storms, Univ. Corp. for Atmos. Research, On-line training program retrieved from: http://meted.ucar.edu/mesoprim/dust/, (Last accessed on 14 July 2004)

Davis, R.G., 2003: On target: Organizing and executing the strategic air campaign against Iraq, Air Force History Support Office, Bolling AFB, 385 pgs

Evans, J.P and R.B. Smith, 2001: Modeling the climate of southwest Asia, Department of Geology and Geophysics, Yale University, On-line article retrieved from: http://www.yale.edu/ceo/Projects/swap/pubs/evans&smith2001.pdf (Last accessed on 6 August 2004)

Fleet Numerical Meteorology and Oceanography Center (FNMOC) Model Validation and Verification Team, 2004: Operation IRAQI FREEDOM (OIF) Numerical Model Verification, FNMOC, Monterey, CA, 51 pgs

Finta, C., 2004a: Personal communication between Maj. Christopher Finta, 28 OWS Chief, USCENTAF Operations Center, 28th Operational Weather Squadron, Shaw AFB, SC, and the author 6 June 2004

Finta, C., 2004b: Operation IRAQI FREEDOM (OIF): weather support after action report and lessons learned, 28th Operational Weather Squadron, Shaw AFB, SC, Power-point slide presentation e-mailed to the author 6 June 2004

Franklin, D., 2004: Climate of Iraq, National Climatic Data Center, On-line article retrieved from: http://www.ncdc.noaa.gov/oa/climate/afghan/iraqnarrative.Html, (Last accessed on 3 November 2004)

Glickman, T.S., 2000: Glossary of meteorology, 2nd ed., American Meteorological Society, pg 316

Grant, R., 2004: Storms of war, Air Force Magazine On-line, On-line article retrieved from: htts://www.afa.org/magazine/july2004/0704storm.asp, (Last accessed on 26 November 2004)

Grossman, E.M., 2003: Marine General: Iraq war pause 'could not have come at worse time', Inside the Pentagon, On-line article retrieved from: http://ebird.afis.osd.mil/ebfiles/e20031002221316.html (Last accessed on 2 October 2003)

Heidorn, K.C., 2002: Dust in the wind, Weather Almanac: June 2002, On-line article retrieved from: http://www.islandnet.com/~see/weather/almanac/arc2002/alm02jun.htm, (Last accessed on 12 November 2004)

Higdon, M., 2002: Dust Up, Air Force Combat Climatology Center, Ashville, NC, On-line article retrieved from:

https://afweather.afwa.af.mil/observer/MAR_APR_2002/dust_up.html, (Last accessed on 6 August 2004)

Hinz, J.C., 2004: Developing and applying METOC metrics to sea strike operations: a case study of Operation IRAQI FREEDOM, Naval Postgraduate School, Monterey, CA, 201 pgs.

Israeli Science and Technology Home Page, 2004: website: http://www.science.co.il/images/satellite/f/Middle-East-day.jpg (Last accessed on 14 September 2004)

Lee, R., 2003: The third Persian Gulf war, The History Guy, On-line article retrieved from: http://www.historyguy.com/GulfWar2.html (Last accessed on 13 July 2004)

National Oceanic and Atmospheric Administration (NOAA), 2004: website: http://www.osei.noaa.gov/Events/Iraq/2003/ (Last Accessed on 15 October 2004)

NERC Satellite Receiving Station, Dundee University, Scotland, 2004: website: http://www.sat.dundee.ac.uk/, (Last Accessed on 30 November 2004)

Perrone, T.J., 1979: Winter shamal in the Persian Gulf, NAVENVPREDRSCHFAC, TR 70-06, 172 pgs.

Pike, J., 2004: Operation IRAQI FREEDOM, Global Security, On-line article retrieved from: http://www.globalsecurity.org/military/ops/iraqi_freedom.htm, (Last accessed on 7 July 2004)

Revkin, A.C., 2003: A formidable enemy: dust, New York Times, On-line article retrieved from: http://www.nytimes.com/2003/04/01/science/earth/01DUST.html?pagewanted=2, (Last accessed on 15 July 2004)

Westphal, D.L., O.B. Toon, and T.N. Carlson, 1988: A case study of mobilization and transport of Saharan dust, Journal of the Atmospheric Sciences, **45**, pgs. 2152-2154

Wilkerson, W.D., 1991: Dust and sand forecasting in Iraq and adjoining countries, Air Weather Service TN-91/001, 63 pgs

THIS PAGE INTENTIONALLY LEFT BLANK

INITIAL DISTRIBUTION LIST

1. Defense Technical Information Center
   Ft. Belvoir, Virginia

2. Dudley Knox Library
   Naval Postgraduate School
   Monterey, California

3. Carlyle H. Wash
   Naval Postgraduate School
   Monterey, California

4. Tom Murphree
   Naval Postgraduate School
   Monterey, California

5. Christopher Finta
   28th Operational Weather Squadron
   Shaw AFB, South Carolina

6. Jacob Hinz
   USS Nimitz
   San Diego, California

7. Douglas L. Westphal
   Naval Research Laboratory
   Monterey, California

8. John W. Anderson
   26th Operational Weather Squadron
   Barksdale AFB, Louisiana